UNIVERSITÀ
DEGLI STUDI
FIRENZE

DOCTORAL PROGRAMME IN INDUSTRIAL ENGINEERING
DOTTORATO DI RICERCA IN INGEGNERIA INDUSTRIALE

XXXII

Modeling and optimization of turning process for thin-walled parts and slender tools

ING/IND-16

Doctoral Candidate
Lisa Croppi

Supervisors
Prof. Gianni Campatelli

Dott. Ing. Antonio Scippa

External Referees
Prof. Paolo Albertelli

Dean of the Doctoral Programme
Prof. Maurizio De Lucia

Prof. Naoki Uchiyama

Years 2016/2019

Dedicated to my family, my friends and to all the people I met during my Ph.D activity

Summary

In the last decades, the effort of several researches was focused on the study and improvement of chip removal process in order to achieve an optimal compromise between accuracy and manufacturing costs. Despite several progress were made in that field, some machining process are still critic. Two of them are deep boring process and thin wall components turning. The presence of high compliance elements in the cutting system (i.e. tool in case of boring process and workpiece in case of thin wall components turning) lead to static deflection, responsible of geometrical errors, and unstable vibrations (i.e. chatter) that dramatically compromises workpiece surface quality and decrease tool life. In both of cases, the employment of suitable cutting parameters may mitigate the issue, but, at the same time, is correlated to a consistent decreasing of the productivity. For this reason, approaches that aim at modify cutting system response were developed in order to guarantee tolerance required and chatter stability.

In this research three different solutions have been evaluated and developed.

An active boring bar was designed in order to effectively damp vibrations in deep boring process. The focus of the research was focused on the strategy of integration of the actuator on the tool body, found to be crucial even if not yet addressed in literature. Designed active boring bar was realized and testes in order to demonstrate its effectiveness in chatter mitigation.

For what concerns thin wall components turning, a strategy to detect the optimal support configuration, in order to guarantee tolerance required and chatter stability, was implemented and numerically evaluated.

Finally, the effectiveness of passive devices (i.e. Tuned Mass Dampers) on chatter mitigation was evaluated. In the first part of the activity, an experimental procedure was followed in order to correctly design Tuned Mass Dampers (TMDs). Once their effectiveness was experimentally demonstrated, a model able to predict TMDs effect on workpiece dynamic response was developed in order to provide a support tool for Tuned Mass Damper design. This model was validated according with the experimental results collected in the first part of the activity.

Preface

Parts of the activities reported in this thesis have been conducted in collaboration with Professor Yutaka Nakano of the Tokyo Institute of Technology (Japan).

Parts of the activities reported in this thesis have been conducted within the DAMP IT project founded by Regione Toscana and are described in the related project reports and deliverables. The work package partners, TECMA – S.r.l., D.Electron – S.r.l., Meccanica Ceccarelli & Rossi S.r.l. and VENTURAPLUS S.r.l. contributed to the development of the prototype and partially to some of the achievements reported in this work.

In addition, parts of this thesis have been published in peer reviewed journals and conference proceedings. The cited publications reported the research work carried out during my Ph.D. under the supervision of Dr. Gianni Campatelli and with the support of the co-authors. More in detail, parts of this research activity have been submitted for publication on international peer reviewed journal as:

- N. Grossi, L. Croppi, A. Scippa, G. Campatelli, A Dedicated Design Strategy for Active Boring Bar, Applied Science 2019, 9(17), 3541;
- Y. Nakano, T. Kishi, H. Takahara, L.Croppi and A.Scippa, Experimental Investigation on the Effect of Tuned Mass Damper on Mode Coupling Chatter in Turning Process of Thin-Walled Cylindrical Workpiece, APVC2019 - The 18th Asian Pacific Vibration Conference
- L. Croppi, N. Grossi, A. Scippa, G. Campatelli, Fixture design and optimization for turning thin wall components, Machines 2019, 7 (4), 68

Table of contents

List of figures

List of tables

Acronyms List

FRFs	Frequency Response Functions
TF	Transfer Function
SS	State Space
TMD	Tuned Mass Dampers
CAFD	Computer Aided Fixture design
FEM	Finite Element Method
FEA	Finite Element Analysis
SLD	Stability Lobe Dyagram
MRR	Material Removal Rate
RBR	Ruled Based reasoning
CBR	Case based reasoning
GA	Genetic Algorithm
NN	Neural Network

Introduction

Turning process is one of the main technologies for axisymmetric component thanks to machining accuracy, manufacturing costs and versatility. Despite over the years, scientific literature supported manufacturing industries by developing predictive models and dedicated techniques in order to achieve the best compromise between workpiece quality and costs, some machining process are still critical. One of the main issues is due to the high compliance of the components that constitute the cutting system. In particular this is the case of machining with slender tools, like deep boring bar process, and thin wall components turning. In both of cases deflection under cutting forces are responsible for machining errors, while the onset unstable vibrations (i.e. chatter) that compromises workpiece surface quality and tool life, limits productivity. The main difference between these two cases is that, while in case of deep boring bar the response of the most critical element (i.e. the tool) is constant, in case of thin wall components turning, static and dynamic stiffness varies during machining, due to both local effects and material removed. Due to the low stiffness of boring bar and thin wall components, techniques that act by properly selecting cutting parameters may be ineffective or imply an inacceptable drop in productivity. For this reason, approaches that aim at improve static and/or dynamic response of the most critical component in the cutting system, were evaluated. From the analysis of the state of the art, three different approaches with different pros and cons were detected, analyzed and adapted.

Focusing on deep boring process, active damping techniques are one of the most promising approaches. These systems, including at least a sensor, a controller and actuators are able to monitor the chatter onset and to actively act in order to mitigate vibrations. Besides their good effectiveness in chatter mitigation, their main advantage is they are retrofittable to different configurations (i.e. tool overhang). Even if several active approaches were proposed in literature, the majority of the efforts were focused on the implementation of an effective control logic. However, the whole active system effectiveness also depends on the integration of actuators on the active boring bar. Therefore, the first part of Ph.D. activity was focused on the design of an active boring bar evaluating the most effective integration of piezo electric actuators on the tool body. The activity was carried out within DampIT project, founded by Tuscany Region, with the aim of design an active boring bar starting from a standard boring bar. Proposed solution is able to guarantee: i) the protection of the actuators, ii) a correct preload of the actuators during machining, iii) dynamic equivalence between standard and active boring bar, iv) the possibility of actuate in two direction. The active boring bar was manufactured and tested in order to prove its effectiveness on chatter mitigations. Results testify to an increasing of chatter stability field, that allows an increase of productivity in stable conditions. Moreover, the possibility of measure and actuate in two

perpendicular direction allowed to compare different strategy for detection and actuation that will be more in depth analyzed in the future.

Focusing on thin wall components turning, one of the most used approaches for static and dynamic stiffness increasing is by adding system that supports the workpiece during machining. In the industrial field, additional supports number and positions are usually chosen basing on the experience. To aid supports design and placing, Computer Aided Fixture Design (CAFD) techniques were developed with the aim of integrate prediction models and optimization algorithms in order to detect the optimal solution according with different aims (workpiece deflection minimization, vibration suppression, etc.). Despite several approaches were presented in literature, the majority of them is focused on milling process. Therefore a new approach, tailored for thin wall components turning was developed. The algorithm, implemented in Matlab® is able to read workpiece 2D section geometry, toolpath and tool geometry as inputs, and to create and perform a static and a dynamic simulation of the process. Indeed, the workpiece model is automatically created and simulations results are read and elaborated in order to predict geometrical errors and chatter stability varying tool position and supports configuration. The employment of 2D elements for workpiece modelling and a two-step strategy for optimal supports number and position guarantees reasonable computational time. As result, all the possible supports configurations (in terms of supports number and position) that allow to guarantee tolerance required and stable machining are detected. The final choice of the optimal solution, that can take into account several additional aspects including mounting easiness and cost, is then demanded to the supports designer. The procedure was implemented and numerically validated on a test case (baffle combustor).

The last part of the activity was focused on passive techniques for chatter mitigation in thin walled components turning. The choice of a passive technique, for this specific case, is due to the difficulty of installing active devices on a rotating component. Tuned Mass Dampers (TMDs) are one of the simplest passive devices and, if properly designed, are able to switch the dominant mode of a component into two smaller peaks. However, their effectiveness is limited to a short frequency range and, then, they cannot be used on component with different dynamics. TMDs design is crucial for their effectiveness and require the knowledge of the dynamic response of the component on which they will be installed. In the first part of the work an experimental approach was followed to measure workpiece dynamic, chatter frequency and to evaluate the effect of TMDs on cutting dynamics. Once their effectiveness was demonstrated, in the second part a dedicated model was developed to predict workpiece response, chatter onset and the effect of TMDs on chatter stability.

1. Thesis structure and goals

The research activity carried out during the PhD course concerned modelling and optimization of chip removal process, focusing on deep boring and thin walled components turning. The thesis is structured in 6 chapters, Chapter 1 is the introduction where the aim of the research is presented, Chapter 2-3-4-5 are the core of the thesis and describe the state of the art and the research activities carried out, while Chapter 6 is dedicated to the conclusions that include a summary of all achieved goals and potential future developments. More in detail:

- In the **Chapter 2**, the review of the state of the art is presented to provide a general framework of the issues related to these processes and discuss modelling techniques and improvement strategies presented in literature. Each strategy is analyzed in order to point out limits and possible application fields.
- **Chapter 3** presents proposed approach for chatter mitigation in deep boring process. The state of the art concerning active damping techniques is presented in order to highlights the main lacks that proposed approach aims to cover. The whole design proposed strategy is presented in detail together with numerical and experimental results that confirms the goodness of the integration strategy.
- **Chapter 4** deals with the proposed approach for fixturing optimization strategy that aims to aid support design in order to guarantee tolerance required and stable machining in thin walled components turning. The whole structure of the algorithm and each block are presented and discussed in detail. At the conclusion of this chapter, numerical results for a test case are shown.
- **Chapter 5** concerns the application of passive techniques (i.e. Tuned Mass Dampers) on thin wall components turning in order to increase machining stability. The first part of the chapter is focused on TMDs design an tests using experimental approach. Once TMDs effectiveness is demonstrated, in the second part a model to predict TMDs effect on chatter stability is presented.
- In **Chapter 6** the conclusions and the future developments of the Ph.D. activity are presented and discussed

2. Static and dynamic issues in chip removal process: state of the art

Turning process represent one of the most suitable machining for axisymmetric components, thanks to their capability of combine a high versatility, good accuracy and competitive manufacturing costs. In this process, workpiece is mounted on a machine tool and the final component is obtained by removing material by means of a cutting tool moving with respect of the workpiece. The workpiece rotates along its axis, while the tool moves along workpiece axis direction and radial direction. The cutting system is usually identified with the whole of machine tool, tool and workpiece. Programming a turning cycle means find the most suitable cutting tool, clamping conditions and toolpath in order to satisfy workpiece requirements (i.e. tolerances and surface quality) while maximizing productivity. If the whole cutting system is considered rigid and thermal aspects are neglected, final component quality and productivity are completely defined by tool geometry and toolpath (i.e. all the position of the tool during machining).

Among the years, the research supported manufacturing industries by studying these process and providing solution to increase productivity and final components quality. However, some machining process are still critic. Two examples are deep boring process where, due to the necessity of create deep holes with small diameters, the employ of slender tools may be unavoidable, and thin walled components turning. In both of cases, due to the presence of an high compliant element in the cutting system, static and dynamic issues influence workpiece quality and limits the productivity. Among this, tool and/or workpiece static deflection is recognized as the one of the main sources of dimensional and geometric error in precision machining [1], while unstable vibrations [2] onset causes a drastic worsening of workpiece surface quality. These two phenomena have been deeply studied in literature and tailored solution were proposed in order to reduce geometrical error and mitigate chatter. A more in depth discussion concerning these issues and solutions presented in literature is reported in the Section 2.1 and 2.2.

2.1. Geometrical error prediction and limitation

During cutting operations tool and workpiece exchanges a cutting force by which material can be removed. In case of high compliance workpiece, cutting force may cause non negligible workpiece deformations (in case of compliant workpiece) or tool deflections (in case of slender tools). As a consequence, in both of cases, the true depth of cut is different from the nominal one and a lower quantity of material is removed causing geometrical errors that can be incompatible with requirements. While in case of slender tool the stiffness of the

most compliant element (i.e. the tool) in correspondence of the cutting point is constant, in case of thin walled component, workpiece stiffness varies with the tool position, due to local effects and to material removed. Moreover, in case of thin wall components turning, clamping conditions may significantly contribute to the geometrical errors. In the most common clamping configuration, indeed, workpiece is fixed by means of jaws, that causes a radial clamping force distributed in a small area. Since thin wall components are highly compliant along radial direction, deformation due to clamping forces may be relevant and contribute to increase geometrical errors [3,4].

It is then clear, that thin walled components turning process are more critical and more difficult to predict compared with deep boring bar process. Schematically the effect of local deflection on diametral error is schematized in Figure 2.1. While considering component and tool infinitely rigid, material removed is totally defined by radial depth of cut b (Figure 2.1a), in case of high compliance workpiece, local static deflection δ_{wr} changes workpiece–tool relative position, modifying final component diameters of ΔD (Figure 2.1b)

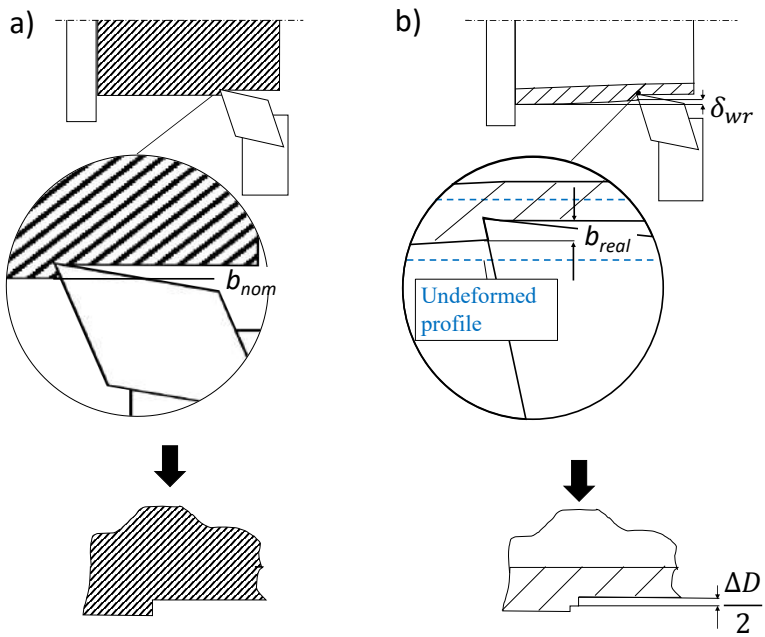

Figure 2.1. a) Rigid workpiece case b) Compliant workpiece case and geometrical error source

2.1.1. Geometrical error prediction

In order to predict the entity of geometrical errors in turning, several models were developed. Most of them are based on the integration of a cutting force model and a workpiece deflection model, while in some cases Artificial Neural Networks (ANNs) approaches were employed [5,6]. The first approach is more general but it requires a more deep knowledge of the phenomena and is based on simplifications. In the second one a set of model input is selected and correspondent outputs are evaluated by means of experimental

tests. The group of data is used to train a neural network able to learn the underline correlations between inputs and outputs. Once the neural network is trained, it is able to give output estimation, but it's affordability is limited to the considered test case. For this reason, despite the complexity of creating a model able to easy take into account all the variables of the phenomenon, modelling approach are the most used.

As widely demonstrated in literature [7–9], cutting forces entity is strictly correlated to cutting parameters, in particular to the radial depth of cut. Since, as shown in Figure 2.1, real radial depth of cut depends on workpiece deflection, an iterative approach (Figure 2.2) is usually employed to estimate both cutting force and workpiece deflection in case of high compliance components.

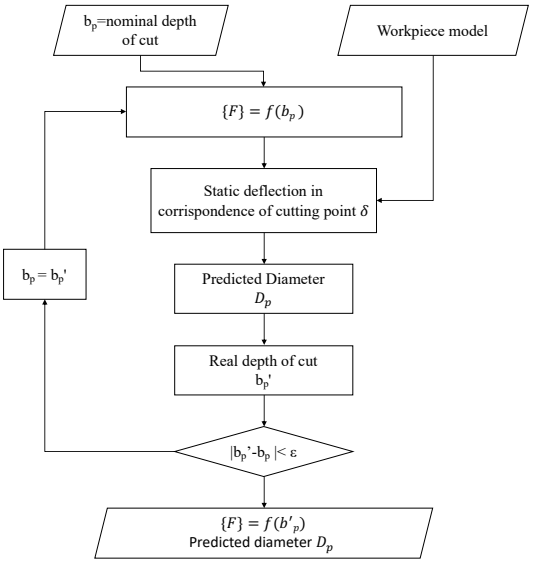

Figure 2.2. Iterative approach for geometrical error estimation

Carrino et al. [10] expressed the correlation between workpiece deflection and cutting forces by means of a system of six equation and six unknown starting from: i) tool position, ii) tool geometry, iii) nominal depth of cut, iv) chip deformation and friction parameters, v) workpiece material, vi) cutting speed, vii) workpiece geometry, viii) fixturing. Due to non-linearity of proposed equation system, an iterative approach is used.

The main difference between available geometrical errors prediction models regards the implemented cutting force and workpiece model. In the first models, tailored for slender cylinder with uniform section, workpiece was modeled by means of analytical approaches [11] in which workpiece was modeled with beam models. Some of them also included the loss of stiffness due to material removal [12], but their main limit is related to cylindrical shape workpiece. In order to extend prediction models to component with varying diameter, finite difference models [13] and Finite Elements (FE) approaches [14] were proposed. Compared with analytical models, numerical ones allows to estimate geometrical error for a larger variety of component, but computational costs is increased.

To overcome this issue Mayer [15] proposed a geometric analysis for diameter errors predicting in bar turning able to take into account also machine tool and tool deflection (experimentally evaluable) and considering all the three cutting force components.

Moreover, expressing workpiece deflection, varying axis position, in a closed form (obtained from a workpiece FE model [16]), it allows a computational time reduction while guaranteeing accuracy and generality.

As mentioned in the previous section, in case of thin wall components turning, clamping and cutting forces creates two deformation states that interfere with each other. In case of ring shaped components, numerical models [3,17] that allows to reduce computational time may be employed.

2.1.2. Geometrical error reducing strategies

According with Zhu et al. [18] strategies to reduce errors may be divided into two categories: real time compensation and pre–compensation by modifying toolpath.

For what concerns turning process, one of the first real time cutting force induced error compensation approach was presented by Yang et al. [14]. Method proposed by Topal and Cogun [19] is able to compensate error even in case of complex geometries. Toolpath pre-compensation techniques are widely used in case of thin wall component milling.

Since, as mentioned, clamping conditions deeply influences machining accuracy, errors may be reduced by carefully design clamping system. Kurnadi and Morehouse [20] presented a systematic approach to obtain the optimal combination of the number of jaws and range of acceptability of clamping forces for ring shaped components mounted on CNC lathe machine. Thanks to Computer Aided Fixture Design [21] techniques it is possible to combine predictive models for machining process with optimization strategies in order to detect the most suitable configuration in order to minimize geometrical errors. However these approach were focused on milling process.

In conclusion, few solutions were proposed in literature for geometrical error reducing

2.2. Chatter prediction models and mitigation strategies

During machining, due to the cutting system dynamic stiffness, vibrations arises. In particular, three types of vibrations can be originated in metal cutting:

- **Free vibrations** occur when the mechanical system is displaced from its equilibrium and is allowed to vibrate freely and may occur, for example, in case of collision between cutting tool and the workpiece.
- **Forced vibrations** appear due to external harmonic excitations. In milling process, for example, the principal source of forced vibrations is due to the periodic behavior of the cutting force. However, forced vibrations are also associated, for example, with unbalanced bearings or cutting tools, or it can be transmitted by other machine tools through the workshop floor.

- **Self-excited vibrations** extract energy to start and grow from the interaction between the cutting tool and the workpiece during the machining process. These vibrations are originated by the closed-loop interaction between the cutting process and the dynamics the machine tool structure, as formalized by

Merritt [22]. This interaction can become unstable due to the fact that the oscillating movements of the structure themselves are sustaining the periodic excitation forces leading to an exponential increase of vibration amplitudes. This phenomenon is generally called "chatter" and is regarded as the most detrimental effect for the cut. This type of vibration brings the system to instability with several consequence on machining process including:

- Poor surface quality
- Unacceptable inaccuracy.
- Excessive noise.
- Disproportionate tool wear.
- Machine tool damage.
- Reduced material removal rate (MRR).
- Increased costs in terms of production time.
- Waste of materials.
- Waste of energy.
- Environmental impact in terms of materials and energy.
- Costs of recycling, reprocessing or dumping non-valid final parts to recycling points

Excited vibrations in machining process are distinguished between primary and secondary chatter. In the first case, chatter can be caused by the cutting process itself (i.e. by friction between the tool and the workpiece, by thermo-mechanical effects on the chip formation or by mode coupling). Mode coupling chatter [23,24] occurs in case of relative vibrations between the tool and the workpiece simultaneously in two perpendicular directions with the same frequency and phase shift. In this case an elliptical motion occurs and, moving the tool on this elliptical path, the motion receives more and more energy, vibrations are intensified and the elliptic motion is grown (Figure 2.3).

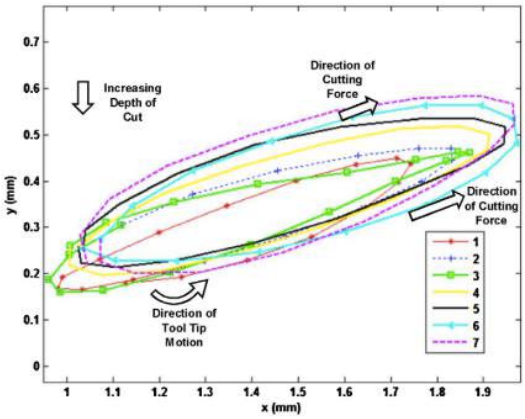

Figure 2.3: Trajectory of tool tip motion in xy-plane in the selected part of the process, numbers indicate vibration cycles [23]

Regenerative chatter occurs at the frequency close to the most dominant mode of the machine tool structure. Once dominant mode is excited, at each revolution a wavy surface is generated. Depending on the phase shift between the two successive waves, the maximum

chip thickness may grow exponentially while oscillating at a chatter frequency that is close to, but not equal to, a dominant structural mode in the system (Figure 2.4). As result, cutting forces exponentially increase, cutting tool life is reduced and a poor wavy surface is created.

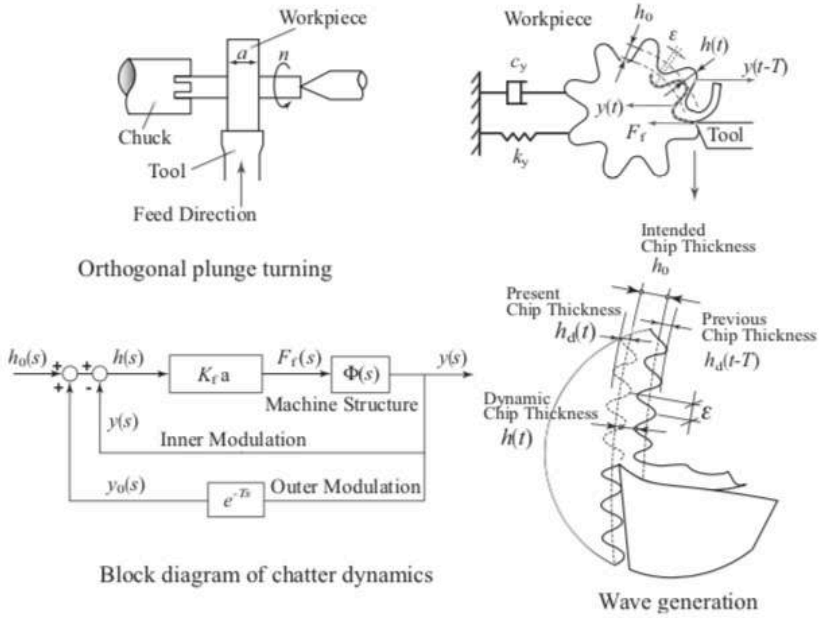

Figure 2.4: regenerative chatter mechanism

As stated by Quintana [25] "nowadays, authors still refer to vibrations as a limiting factor, one of the most important machining challenges and, of course, an aspect to be improved". This statement is confirmed by several studies concerning both chatter prediction and techniques able to mitigate chatter.

2.2.1. Techniques for chatter identification and prediction

Because the great interest, several identification and prediction approach were proposed in literature. A first distinction is made between analytical and experimental approaches.

Analytical approaches are based on chatter prediction models able to evaluate process stability given dynamic system behavior (i.e. relative Frequency Response Functions – FRFs), cutting parameters and tool geometry [26]. They usually include a cutting system dynamic model and a dynamic cutting force prediction models. Since the cutting system is usually approximated with the most compliant element in the cutting system, in case of slender tool, the entire system can be approximated with the tool tip FRFs [27,28], while in case of thin wall components, workpiece dynamic response has to be considered [29,30]. Since workpiece response varies during machining due to different local stiffness and material removed, the most suitable approach for workpiece dynamic response prediction is the use of Finite Element Analysis (FEA). Depending on the approach, results may be

expressed in terms of Stability Lobe Diagrams [31], Nyquist plot [32], force trend in the time domain [33,34]. SLD represents stability field as a function of spindle speed and depth of cut: the edge between this two area has a typical lobate trend and identifies the critic stability limits, in correspondence of whom vibration amplitude is constant in the time (Figure 2.5).

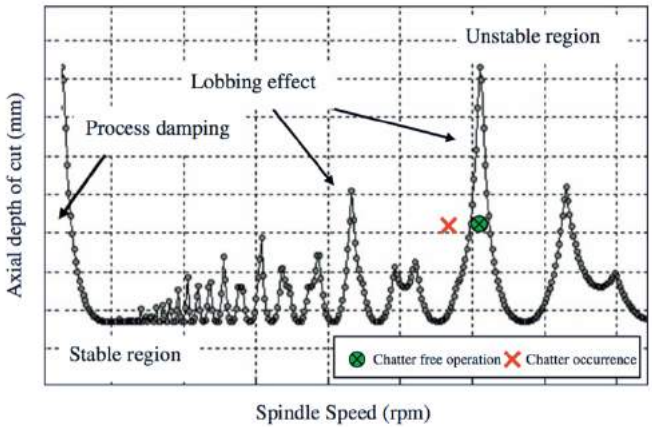

Figure 2.5: Example of SLD [25]

Due to its simplicity and clarity, it is the most popular technique among researches in particular because it offers a valid instrument for cutting parameter selection in order to maximize Material Removal Rate (MRR) while guarantying a stable machining. However, since these techniques are based on simplified models, their accuracy may be not enough. On the other hand Nyquist plot and time domain approaches do not provide a wide view of the stability field but can be applied to more accurate models. Indeed, these approaches are mainly used to estimate if given a specific tern of cutting parameters (cutting velocity, depth of cut and feed per tooth) the machining is stable. Since workpiece local response varies during machining, stability field changes during machines.

Experimental approaches include signal acquisition and processing techniques. These approaches differ both for the acquired signal (forces, displacements…) and for processing techniques (time-domain, frequency domain and time–frequency domain analysis). Compared with analytical approaches, these techniques allow to take into account all the non-linearities, and to more accurately describe the chatter phenomena without requiring specific competence. However specific sensors and devices are required.

2.2.2 **Chatter suppression techniques**

According with Quintana and Ciurana [25], a first high level distinction between chatter suppression techniques is between strategies that uses the lobbing effect and approaches that acts on the system dynamic behavior. The first category includes all methods that ensure chatter stability by properly choosing cutting parameters, while the second includes all methods that act changing the system response, by means of active or passive devices. The first group is then divided in out-of-process and in–of-process techniques. Out–of–process strategies aim at find the stability field limits, by means of chatter prediction models [35], and select cutting parameters in the stable zone. However, these approaches required an accurate cutting process modelling (including system dynamic characterization) that could be incompatible with the operator's competences. In the in–process approaches, a

signal (such as vibrations, sound, power…) is continuously monitored and, once chatter is detected, cutting parameters (usually spindle speed [36]) are properly changes in order to suppress chatter. However, the improvement that techniques that uses the lobbing effect can provide can be limited in case of high compliance component machining. In such cases, stability field, and then stable cutting parameters range, is very limited. For this reason the employment of devices able to modify the cutting system response is widespread in case of thin walled component machining.

By changing cutting system dynamics, is possible to enlarge the stability field of machining. However, additional devices, that need to be properly designed, are required.

Passive strategies for chatter mitigation changes cutting system dynamics by means of devices, able to dissipate energy, that do not require external power. According with several models for chatter prediction [37], chatter stability field is correlated to relative FRF between tool and workpiece in correspondence of the cutting point. By reducing dominant mode peak amplitude, is then possible to extend chatter stability field and increase MRR in stable conditions. Several passive auxiliary systems, summarized in Figure 2.6, can be attached to a component in order to improve its dynamic response.

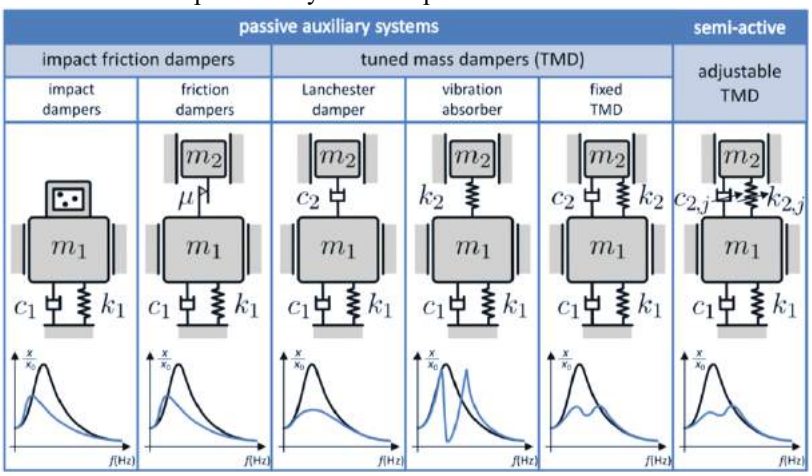

Figure 2.6: Auxiliary systems to change dynamic response at the critical vibration mode[38]

Friction dampers [39,40] use the frictional force that results from the relative movement between the vibrating element and the added mass or the different parts of the damper. However, since friction is difficult to simulate, in many cases these systems are set up based on a trial and error procedure.

Among passive techniques, Tuned Mass Dampers are the most common devices for chatter mitigation. Even if the effectiveness of this approach for chatter suppression was demonstrate in literature [41–45], the main limit of these strategies is that the damping effect is limited to a short frequency range. As a consequence TMDs must be carefully designed (tuned) according with a specific cutting system and, then, they are not retrofittable. In industrial field, their employment is limited to high compliance tools, were the TMDs are tuned on tool natural frequency that does not change during machining. Moreover each tool can be used in different component machining. In case of thin walled component machining, TMDs design is more complicated, due to the necessity of design different TMDs for each component. Moreover material removed may significantly change chatter frequency [29].

Active techniques for chatter suppression allows to measure and detect chatter onset and to act with specific counteracting in order to interfere with the mechanism that generate chatter and suppress it. As a consequence, they need at least a sensor (to measure the phenomenon), a controller (to detect chatter onset and program the counteracting) and an actuator (to realize the counteracting). Despite the complexity, once the control logic is implemented, they do not require any expertise in dynamic modelling and they can be retrofitted to different combination of tools and components. Due to the complexity of active systems, these devices are usually mounted on the non-rotating element, that is tool in case of turning/boring [46–49] and workpiece in case of milling [50].

Lastly, in case of thin walled component machining, component stiffness (i.e. most compliant element in the cutting system) may be increased by means of fixtures and stiffeners able to support the flexible parts in the most critical points. Strategies for their optimal placing were proposed mainly in milling in order to reduce forced vibration and increase dynamic machinability [51,52]. However, as in case of CAFD techniques for geometrical error minimization, approaches similar to the ones developed for milling process may be adapted for thin walled components turning.

2.3. Conclusion on techniques to improve workpiece quality

In order to summarize, thin wall component machining is complicated due to both static and dynamic workpiece issues. From one hand low static stiffness causes workpiece deformations that alter the nominal distance between tool and surface to be machined, causing geometrical errors. In addition, low dynamic stiffness produces a limited chatter stability field, drastically reducing productivity.

For what concern geometrical errors reduction in thin wall components machining, two main approaches were detected: tool path compensation and supports employment. In case of high compliant components, however, toolpath compensation leads to an unacceptable decreasing of the MRR. On the other hand, support design may be complicated and time consuming and approaches that aid supports design are mainly focused on workpiece positioning and simple geometries for milling machining.

Research concerning geometrical error reducing, and chatter mitigation was mainly focused on slender tools (both in turning and in milling) and on thin wall components milling process. However, these solutions may be adapted, with some considerations to thin walled components turning. In particular:

- Since active system requires external power, they cannot easily installed on rotating components. Then they cannot be used to change workpiece dynamic response. However, they can be installed on the cutting tool in order to effectively counter act chatter onset.
- Support design techniques developed for thin walled component milling, may be adapted to axisymmetric components in order to evaluate optimal support number and position able to both guaranteeing tolerance required and chatter stability.
- TMDs may be attached to a thin wall component to provide a damping effect. A dedicated tuning strategy must be developed

The aim of this activity is to develop this strategy in order to offer solutions that can be easily applied in an industrial context. For this reason the first step was the design of an

active boring bar for chatter mitigation. In the second step, focus was shifted to the workpiece static and dynamic behavior developing a strategy for support position able to guarantee tolerance required and stability and a strategy for TMDs design able to increase chatter stability field.

3. Active boring bar design

This part of the thesis have been conducted within the DAMP IT project founded by Regione Toscana, which aim is to improve deep boring bar process thanks to an active device able to mitigate chatter vibrations that limit process productivity and compromise workpiece quality. In detail, the main project aims were:

1. Guide lines definition for active devices design and components selection
2. Study and development of a Cyber Physical System (CPS) for turning process able to monitoring vibrations in real time and interface with the IT infrastructure of the company, by means of the development and the integration of specific sensors
3. Extension of the CPS by means of actuator integration in order to act to mitigate vibrations
4. Realization and experimental verification of a prototypal active boring bar for turning process, configurated as a CPS

In particular, presented work of thesis was focused on the design of the prototypal active boring bar, the implementation of a chatter prediction model able to numerically verify the effectiveness of the system on chatter mitigation and the analysis of experimental results.

At first, a deep analysis of the state of the art was carried out in order to analyze active systems developed for chatter mitigation and detect the most promising solutions and control logic.

As mentioned in section 2.2.2 active approaches, compared with passive one, require a more complex architecture able to monitor, diagnose and act on the process in order to suppress chatter vibration. Vibration is continuously acquired by sensors, and the signal is processed in real time to detect chatter onset. Control logic, properly design and implemented, receives the signal and drives the actuators in order to contrast chatter. Despite the complexity, these approaches are more suitable for industrial application, since they are able to mitigate chatter in different configurations (e.g., different tool set-up, different cutting parameters). Design of an active boring bar involves the design of monitoring system (sensors), actuation system and control logic.

Since now, research works were mainly focused on development and implementation of different control logics, such as optimal control [47], direct position feedback [53] and direct velocity feedback (DVF)[48][54]. Among all, DVF is the most common and mature control logic, since it was demonstrated to be a robust approach [49] and its effectiveness

was proved in several applications for chatter mitigation [55][56]. Beside control logic, active strategies effectiveness is strongly related to the inertia of the applied sensors and actuators. However, no work was dedicated to the design of the structure of such devices. Indeed, few design solutions were presented in literature focusing only on building prototypes to demonstrate control logic effectiveness. As result some critical aspects in actuation system design has not yet been addressed and a systematic approach for active boring bar design has not been presented.

The aim of the presented work is to develop a structured approach for active boring bar design based on DVF control system, focused on actuation system and its integration on the cutting tool. Starting from a commercial boring bar, the method supports actuators selection, positioning and housing in order to increase the damping effectiveness for chatter suppression, while respecting technological limits. The proposed approach covers aspects that has not yet addressed in literature, that are crucial for a correct active system functioning. In particular this approach includes: i) an effective model for preload estimation in order to protect actuators from traction stress even during machining, ii) a design strategy for preload system, iii) a design strategy for protective covers (necessary to protect actuators) that guarantees static and dynamic equivalence between original boring bar and active boring bar. Following the proposed method, an active boring bar was designed and manufactured. Using the developed prototype, experimental tests were carried out in order to validate the method and assess the prototype performances.

3.1. Proposed Method

An active boring bar is composed of at least a sensor, capable of detecting the onset of the vibration to be mitigated, an actuator that generates counteracting forces based on a tailored control logic embedded in a real-time controller, as schematized in Figure 3.1.

In particular, in case of DVF control logic, the controller receives, as input, vibration velocity and determines a counteracting force proportional to the velocity. As result, DVF acts as a pure damping strategy, reducing vibration amplitude around natural frequencies, which are the most critical for chatter onset.

However, damping effectiveness depends not only on the control logic, but on the entire actuation system that, therefore, needs to be carefully designed. In particular actuators choice and their integration.

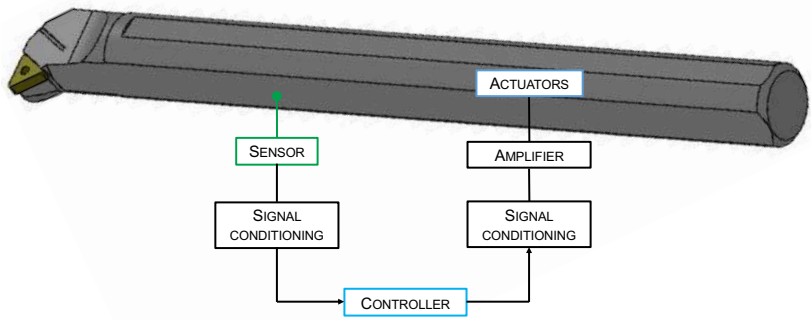

Figure 3.1: Active boring bar framework

In order to effectively contrast chatter both frequency and direction of the unstable vibration must be considered. Indeed, the first aspect defines the frequency range of vibrations that must be damped (crucial for sensors and actuators choice), while the second one is related to actuation directions (crucial for actuators optimal placing). Chatter frequency can be estimated by means of chatter prediction models or experimentally measured and it is related to system dynamics. Actuators and sensors resonance frequency should be at least 5 times greater than chatter frequency in order to guarantee sufficiently low inertia and an effective response time of the active system. Direction along which chatter arises depends both on chatter type and on boring bar dynamic behavior. In particular, in case of primary chatter, unstable vibrations occur in the cutting velocity direction (Figure 3.2a), while in case of regenerative chatter, instability is related to vibrations along radial depth of cut direction (Figure 3.2b).

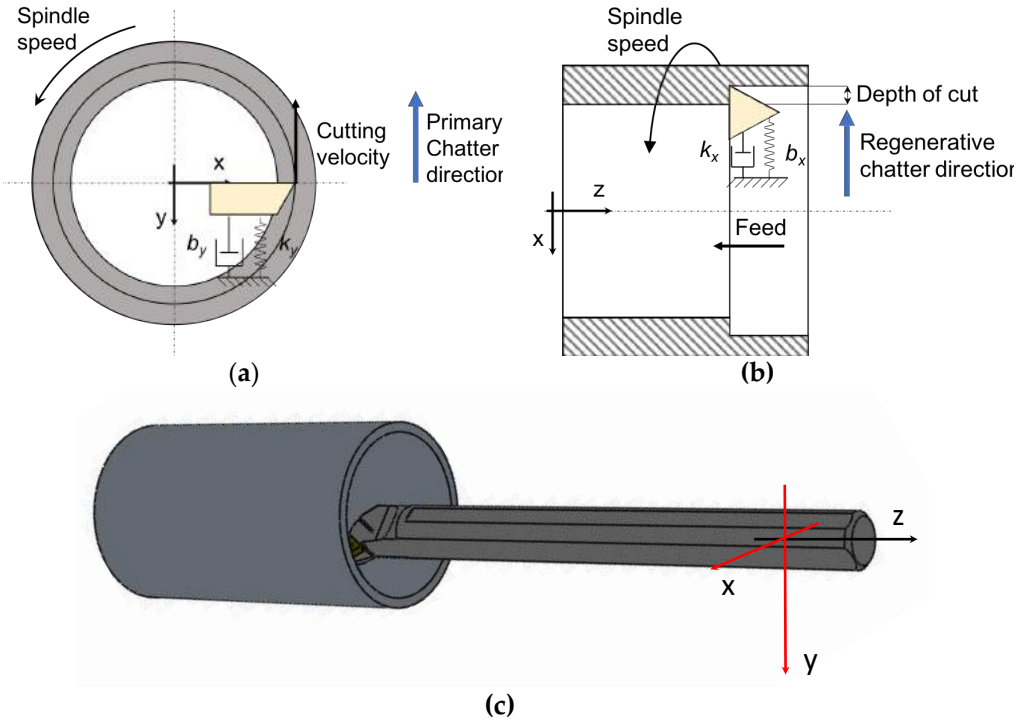

Figure 3.2: a) primary chatter b) regenerative chatter c) boring bar most flexible directions (red lines)

Therefore, in the first case, optimal actuation direction is along cutting velocity, while in the second case it is necessary to actuate in the radial depth of cut direction. As observed by Pratt and Nayfeh [57], chatter passes from primary to regenerative varying radial depth of cut, due to the presence of tool nose, that determines cutting force direction. In deep boring process, tools, due to the high aspect ratio, are highly flexible in both these direction (Figure 3.2c). Then, in order to ensure a damping effect independently of depth of cut, active boring bar must be able to reduce vibrations both along cutting velocity and feed direction.

In addition to these requirements, since DVF control logic acts only on frequency range close to the system natural frequency, the active boring bar design should consider static behavior as a constraint: standard and active boring should share the same static behavior and adding the actuation system should not worsen the static and dynamic response of the structure with control off.

Lastly, technological limits must be considered. In particular, since tool overhang is selected based on the maximum hole depth that can be manufactured, while radial size is constrained by the minimum hole radius, final solution can not imply a significant overhang reduction or radial size increase.

Summarizing, five requirements are identified:

1. The damping system should be capable of generating counteracting forces in the frequency range of the unwanted vibrations to be mitigated.
2. The active boring bar should be capable of damping vibrations along two directions.
3. The dynamic and static behavior of the active boring bar, with control off, should be as close as possible to the ones of the standard system.
4. The housing of the actuators should not reduce the actual exploiting overhang of the standard boring bar.
5. The housing of the actuators should not exceed a given radial dimension.

3.1.1. Most effective actuation strategy selection

In this section, the chosen actuation strategy is presented and motivated. Different actuation solutions were presented in literature for active boring bars. Chen et al. [58] proposed a solution using magnetic actuators, mounted on a tailored system. Even if this kind of actuators are found to be effective, due to their capability of giving high loads, in the proposed solution the presence of the actuator, mounted on the external surface of the tool, reduces its overhang. In [59] a tool adaptor with an integrated active system is designed and numerically tested. The main drawback of this solution is the required actuation forces, significantly higher compared to other solutions due to inertia, since actuation is applied on a heavy and stiff region (holder). Therefore, in the most common applications [60,61] (Figure 3.3), actuators are integrated in the tool body and actuation direction is parallel to the tool axis. In this scheme, motion normal to the tool axis is achieved by exploiting the moment (M_{act}) generated by applying the actuator forces (F_{act}) with a specific arm respect to the tool axis.

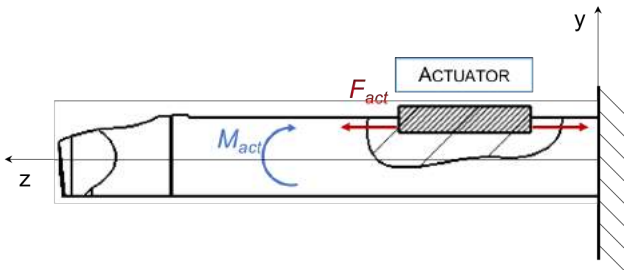

Figure 3.3: Chosen actuation strategy

Although the solution is the most feasible (applying the actuation force directly on the most flexible directions is complicated), it shows limitations due to the need of balancing two opposite needs. From one hand, the actuation effectiveness increases with the distance between actuator and tool axis, on the other hand this distance is limited by technological requirements.

Since actuation system effectiveness is limited by the maximal radial dimensions, actuators with high energy density (i.e., force/volume ratio) and capable of providing an adequate actuation force in the required frequency range (e.g., 0-1kHz) are required. Based on these requirements, piezoelectric actuators represent a preference choice. Two types of actuators may be employed: patches (or layer) or stack (or multilayer). Thanks to their flexible structure, the first ones can be mounted also on curved surface and they do not required preload, their size is reduced, and they do not require dedicated housing slots on the bar. However, their application to active boring bar is very limited, since they cannot provide adequate actuation forces.

On the contrary, multilayer actuators are able to generate higher loads and are suitable for dynamic applications, but, due to necessity to protect them from shear and tensile stresses, their integration on the boring bar is more complicated. Even if solutions with piezoelectric actuators were presented in literature [48], a systematic approach for active boring bar design, that covers all the most crucial aspects, has not yet been developed. In particular the following open issues were highlighted:

1. Solution for actuators integration and placing to optimize the system effectiveness considering the inertia of the system and electronics, two actuations directions and available space.
2. Solution for actuators housing protecting them shearing stress, positive tensile stress and from chip and debris.
3. A strategy that guarantees the dynamic and static equivalence between active boring bar and standard boring bar.

Proposed approach supports active boring bar design considering all these aspects. In particular, the first goal was achieved and presented in section 3.1.2. Proposed solution to protect actuators form shear and traction stress is presented in section 3.1.3. The needs of protection system for actuators, while guarantee static and dynamic equivalence between standard and active boring bar are combined by means of the employment of protective cover properly designed, as presented in section 3.1.4.

3.1.2. Proposed approach for actuators positioning

Starting from the actuation solution in Figure 3.3, a strategy for actuators placing, in order to maximize effectiveness, while satisfying requirements, was developed.

As mentioned, one of the main advantages of active damping techniques is their versatility. Using these approaches, it is possible to improve chatter stability in different tool configurations (i.e. overhangs). Since in the proposed approach, actuators are integrated on the boring bar, in order to maximize range of available overhangs, the configuration with one actuation section, placed as close as possible to the tooltip, is selected.

According with requirements presented in section 2.1, the integration strategy of the actuators on the boring bar body must guarantee: i) the actuation in both radial and cutting

velocity direction ii) maximum effectiveness (i.e. maximize the harm of the forces generated by the actuators iii) limited radial size iv) dynamic and static equivalence. In the proposed strategy, requirements i), ii) and iii) are achieved by means of a section optimization (presented in this section) while the last requirement is achieved by properly dimensioning protective covers in order to compensate the loss of stiffness due to material removed (section 2.5).

In order to find the optimal actuator position, different configurations were evaluated. In Figure 3.4a the most effective configuration in case of one actuation direction is presented, however this design provides low actuation forces and a single actuation direction (y). To increase the effectiveness, multiple actuators can be used, either in parallel (Figure 3.4b), or rather on two sides with opposite actuation forces (Figure 3.4c), optimal placement to reduce the required space. To achieve a multidirectional actuation, solution showed in Figure 3.4d involves the employment of two actuators for each damping direction. In particular, actuators named X1 and X2 acts to damp vibration along x direction, while Y1 and Y2 damp vibration along y direction. Since this solution exploits two actuators at time, effectiveness can be further increase by activating all the four actuators, as presented in the selected configuration (Figure 3.4e) that includes the 4 actuators on 45° position respect to the two directions. Using this configuration actuation in x direction is achieved by A and B working with opposite signal of C and D, while actuation in y direction, is achieved by A and D working with opposite signal of B and C. As result, even if actuators distance from the tool axis is reduced, using double actuation forces increases the resultant moment.

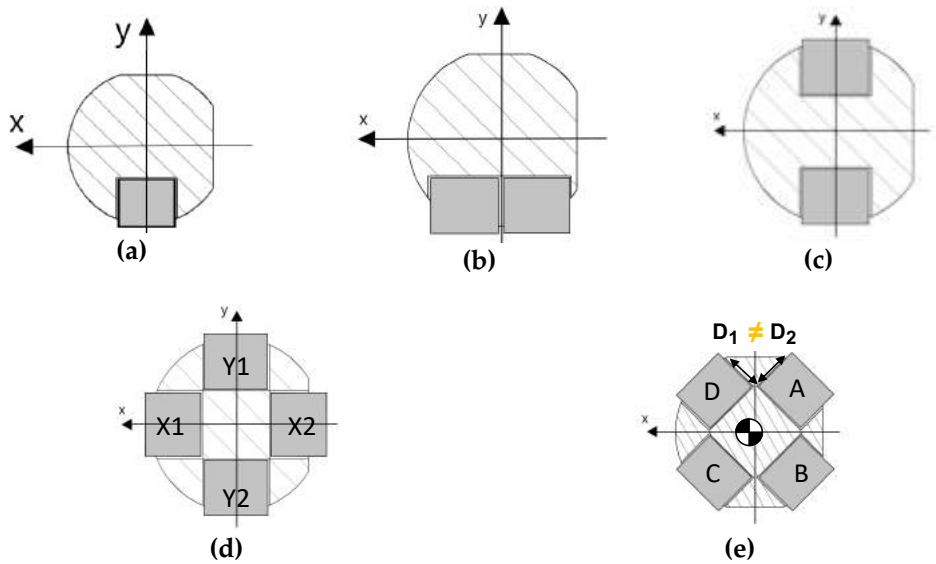

Figure 3.4: Evaluated solutions a) one actuator b) two parallels actuators c) two side actuators d) four actuators along x and y direction e) selected configuration where D1 and D2 are the distances of the slots from the boring bar external surface

Optimal radial position (i.e., radial distance of actuators from tool axis) is the one that allows to maximize the arm of the force while respecting radial imposed size. Moreover, the centroid of modified boring bar section should be aligned with the one of the original

sections, in order to avoid different preferential direction of inflection among the different section. This implies that, in case of boring bar section not symmetric within x and y direction, actuators radial position has to be different. (Figure 3.4e).

Actuators are then placed at the minimum distance from tool axis that allows to reduce stress concentration due to the shape of the edge, and thickness of each slot was calculated in a way that the inertial centroid of modified section is the same of the one of original section.

In order to guarantee the same static and dynamic behavior of the original boring bar, the loss of stiffness due to material removed must be compensate. Since the presence of actuators does not provide enough stiffness to compensate material removal, additional components are required. In order to reduce the number of components, protective covers, required to avoid inclusion of chip and debris on the housing slot, can be properly dimensioned to achieve this goal. The methodology for optimal protection cover dimension is presented in section 3.1.4.

3.1.3. Actuators housing strategy and preload estimation

To protect the actuators against lateral forces, spherical end-tips are adopted (Figure 3.5a). The main advantage of this configuration are: i) since the joint between actuator and slot can be schematized by a hinge, shear stress are not transferred to the actuators (Figure 3.5b) ii) thanks to the spherical shape of the components, the contact between actuators and boring bar is guaranteed even in case of tool deflection (Figure 3.5c) iii) the correct alignment of actuators, after tool deflection, is guaranteed.

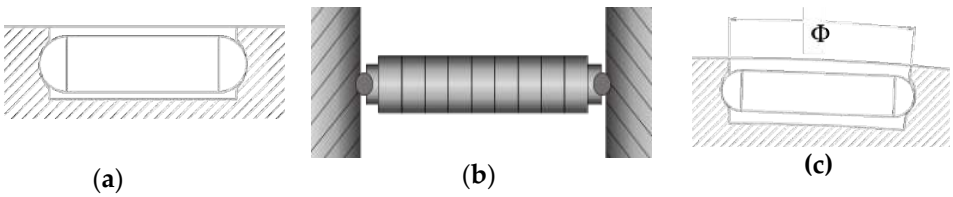

Figure 3.5: a) housing strategy b) schematized configuration c) contact between actuators and boring bar in case of tool deflection

In order to protect piezo electric actuators from tensile stress, actuators must be preloaded [62]. Manufacturers suggest a value for basic preload that is the minimum preload in case of no additional forces act on the actuator.

In our case, due to tool deflection, the preload required is the sum of basic preload and an additional preload able to compensate the distancing of the hemispherical slots, in which actuators are installed. The most critical condition is identified by chatter, where cutting forces, as well as distancing of the two sections, are maximum. Cutting forces in chatter condition may be measured or estimated, while relative displacement between interface sections can be computed using a FE approach: exploiting the condition of dynamic equivalence between original and modified boring bar, the model of the original boring bar can be used to estimate the maximum distancing of the section in correspondence of the contact surface with actuators. An impulsive force with the same amplitude and direction of the maximum cutting force in chatter condition should be applied at the tool tip (i.e., where cutting forces are exchanged) in order to estimate frequency spectra of displacement in

correspondence of the interfaces between tool and actuator. Then minimum additional preload should be calculated as the force able to compensate maximum displacement. In case of the boring bar section is not symmetric within x and y axis, global preload must be adjusted in order to obtain a null resultant moment on the section.

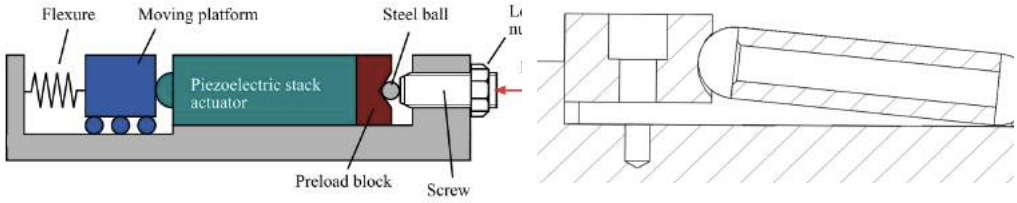

(**a**) **(b)**

Figure 3.6: Preload mechanism a) mechanical [62] **b) by interference (selected solution)**

Once preload is estimated, the most effective and easy to apply preload system was detected. The most adopted solution in literature is a mechanical mechanism composed by flexure, moving platform and screw [62] (Figure 3.6a). This solution ensures the adjustment of the preload, but the presence of different moving components affects the effectiveness of the actuator, since part of the motion of the actuator is reduced by the flexibility of the additional components. Considering the importance of the effectiveness in the defined application, a different mechanism that exploits mechanical interference is proposed. In the proposed design, the actuator is forced inside the housing with a defined interference that preloads the actuator inside the slot. This solution allows to reduce the number of components required, hence increasing the actuator effectiveness. In the proposed design, preload is applied using a threaded insert with a spherical housing, as presented in Figure 3.6b. The advantages of this solution are that it is easy to assemble, and the required preload can be easily obtained properly dimensioning insert. However, interference must be accurately identified, since preload cannot be adjusted or changed.

The correct interference must compensate the deformations, due to preload, of actuators and slots also considering local deformations in the contact area between actuators and slots. In the proposed approach (schematized in Figure 3.7), each actuator is modeled as a single lumped stiffness (KP), while each slot is modeled as a three lumped stiffness in parallel, in order to consider both boring bar (KB) and contact stiffness (KH).

KH can be computed based on Hertzian theory. In particular, given compression force, material property of the two bodies in contact and their geometry, it is possible to estimate contact circle radius and depth of penetration and then equivalent stiffness. KP can be experimentally measured, while boing bar stiffness (KB) is evaluated by means of a FE approach estimating the slots elongation due to computed preload applied in correspondence of estimated contact area.

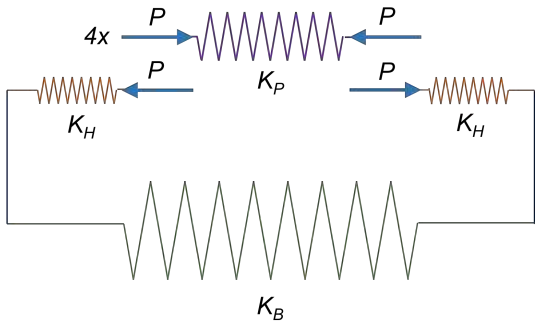

Figure 3.7: Proposed model for interference estimation

To guarantee the contact between actuator and boring bar, slot length must be equal to actuator length. Due to preload P, actuator length decreases of x_P, while the distance between the wall of the slot increase as a result of both the elastic yielding due to contact between them (x_H) and of the boring bar deformation (x_B). Then, assuming a slot of nominal length L_0 and an actuator of length L_p, the following equation must be respected

$$L_o + x_B + 2x_H = L_P - x_P + i \tag{3.1}$$

In order to guarantee the contact between slot and actuator, interference should be able to compensate the relative displacement between them.

$$i = x_B + 2x_H + x_P \tag{3.2}$$

According with model proposed in Figure 3.7, interference (i) may be expressed as

$$i = {}^{2P}/_{K_H} + {}^{4P}/_{K_B} + {}^{P}/_{K_P} \tag{3.3}$$

3.1.4. Protective covers proposed design approach

As mentioned before, the role of the protective covers is twofold: from one hand they protect the actuators from chip debris and cutting fluids, from the other hand they may be used to compensate the loss of stiffness on the section due to the presence of slots. The protective cover should be designed to fulfill these objectives, while not exceeding radial encumbrance. The most suitable solution was found to be a single cover for each actuator screwed on the boring bar body. Moreover, to reduce dimensions and decrease the number of components, covers can be integrated with the insert used to provide preload (Figure 3.8).

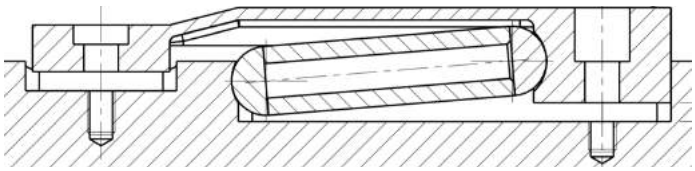

Figure 3.8: Proposed solution for covers

A FE approach is proposed to find the dimensions that allow to compensate the loss of stiffness due to material removed. By means of active boring bar model, that includes both the actuators and the covers, it is possible to predict its response including inertial effect of all components. Varying covers dimensions and detect the dimension that gives, in case of control off, a static and dynamic behavior as close as possible to the original boring bar.

In Table 3.1, a summary of issues, requirements and solutions that proposed method is able to achieve is presented.

Table 3.1: Issues, requirements and proposed solution for the design of an active boring bar.

	Issues	Req.	Proposed solution
State of the art	How to damp vibration		By means of a moment (i.e. a force applied at a given distance from tool axis)
	How to provide force		By means of multilayer piezo electric actuators
Proposed methodology	How to integrate actuators	4,5	By means of slots on boring bar body
	How to protect actuators form shear stress		Hemispherical tips
	How to protect actuators from positive tensile stress		Preload
	How to protect actuators form chip and debris		Protection Covers
	How to compensate the loss of stiffness due to slots	3	Properly designed covers to compensate the loss of stiffness due to the presence of slots
	How to optimize actuation effectiveness	1	By properly choosing actuators (hard-doped ceramic)
		2,3,4,5	By properly placing actuators - Axial position optimization - Actuation section optimization (four actuators within 45° within x and y direction)
	How to estimate preload	3	As the sum of basic preload and an additional preload that compensate interface section distancing due to tool deflection. Preload is then adjusted in order to balance the moment
	How to realize required preload		Interference
	How to estimate interference		By means a simplified model
	How to realize interference	4,5	By means of an insert

3.2. Case study

Once control logic effectiveness was numerically tested, presented approach was applied to a case study. Active boring bar is designed starting from a commercial boring bar made by Sandvik (S32U-PTFNL16W) equipped with a TNMG160508PM-4325 cutting insert, presented in Figure 3.9.

Figure 3.9: Original boring bar

Boring bar is used to machine holes of 50 mm minimum diameter and 160 mm maximum depth on a CN lathe (Mori Seiki SL-2500Y). Maximum radial size was then set to 40 mmm and minimum overhang was set to 163 mm. Preliminary cutting tests on K100 (DIN 1.2080) steel material, which chemical composition and hardness are reported in Table 3.2, were carried out to measure maximum cutting force and chatter frequency (section 3.1).

Table 3.2: K100 (DIN 1.2080) properties

Workpiece	Chemical composition				Hardness
Material	C%	Si%	Mn%	Cr%	(HB)
NCE46	2.00	0.25	0.35	11.5	240

3.2.1. Chatter force and frequency measurement

Experimental cutting tests were carried out in order to experimentally measure dynamic forces and detect critical depth of cut in order to validate proposed model.

Using the framework shown inFigure 3.10, where the boring bar is mounted with 163 mm of overhang, cutting forces and accelerations were measured by means of a Kistler 9257A dynamometer and a PCB 356A32 tri-axial accelerometer, acquired by LMS SCADAS SCM202V acquisition system.

Figure 3.10: Experimental setup for chatter tests

Spindle speed and feed per revolution were set at 700 rpm and 0.2 mm/rev respectively, while radial depth of cut was gradually increased until chatter condition was detected. For given values of spindle speed and feed per revolution, the machining was found to be unstable with a radial depth of cut of 1.5 mm. Measured cutting force along the three directions in the time and in frequency are shown in Figure 3.11a and Figure 3.11b respectively. Maximum force amplitude is around 3800 N along cutting velocity direction. Chatter frequency is around 463 Hz, while correspondent cutting force amplitude on cutting force direction is 430 N (Figure 3.11b).

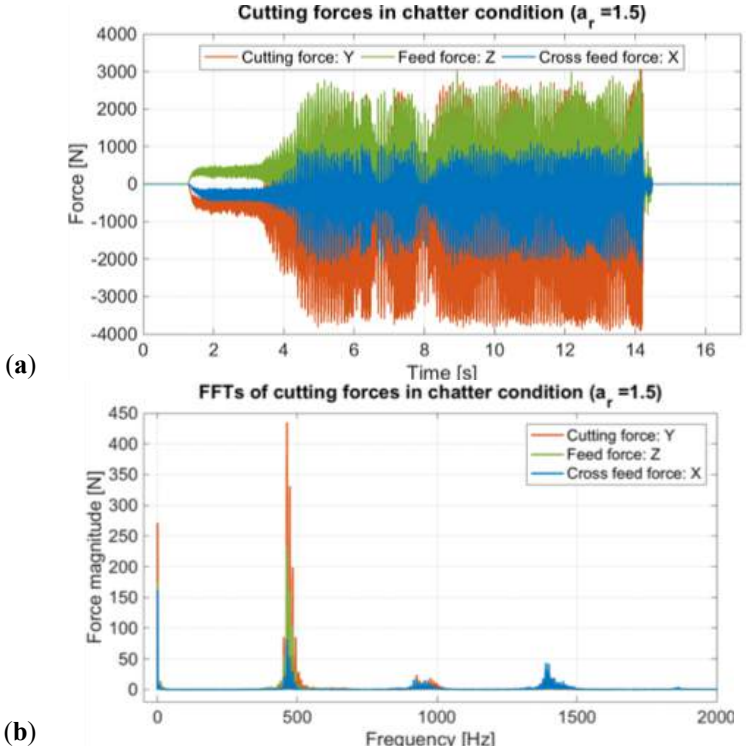

Figure 3.11: Cutting forces a) time history b) frequency spectrum

3.2.2. Active boring bar design

Once chatter conditions were detected, and maximum cutting forces were measured, the active boring bar was design according with the proposed methodology.

NOLIAC SCMAP-NCE46-10-10-2-200-H36-C01 was found to be the best compromise between force that can be provided, dimensions and response time. In particular, since it is not provided with preload mechanism and case, its size is reduced to 10x10x36 mm, compliant with the available space. Moreover, the selected actuator is made of hard-doped ceramic that reduces self-heating issues arising at high frequencies. Its characteristics are reported in Table 3.3.

Table 3.3: Selected actuator characteristics

Piezoelectric material	Dimensions			Free stroke [μm]	Estimated blocking force [N]	Unloaded resonant frequency [kHz]
	Length [mm]	Width [mm]	Height [mm]			
NCE46	10	10	36	32.3	3200	30

Actuation section was placed near the tool tip in order to allow the use of the tool with different overhangs. Considering the selected configuration (section 2.2) maximum slots depth along radial direction, that respect the radial size limit, was found to be 6.5 mm.

The difference in terms of thickness between slots on tool insert side and the opposite one, that guarantees section centroid alignment, was found to be 1 mm (Figure 3.12).

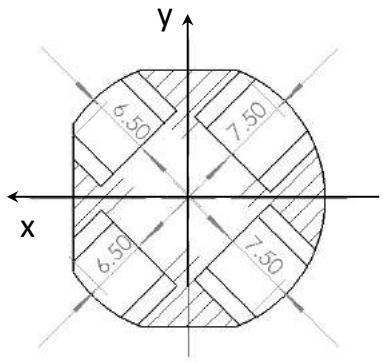

Figure 3.12: Slot radial dimensions

Preload required was calculated following the approach presented in section 3.1.3, using MSC Nastran® FE solver. The boring bar FE model is showed in Figure 3.13.

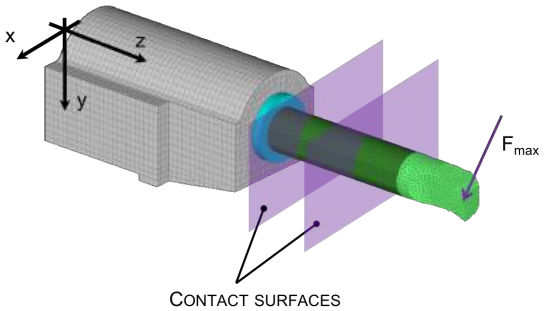

Figure 3.13: Boring bar model for slots surface distancing estimation

According with Table 3.4, maximum relative displacement between slot section was predicted to be 6 μm at the measured chatter frequency (463 Hz). Preload that allows to compensate this distancing was estimated in 4 kN. Global required preload is then 5 kN.

Table 3.4: Maximum distancing of slots section

Force direction	Displacement direction	Maximum displacement [mm]	Correspondent frequency [Hz]
X	Z	0.024	463
Y	Z	0.008	463

Covers are supposed to be jointed to the tool body by means of hexagon socket head cap screws able to provide an adequate force for placing. Hole position was chosen spaced enough from the contact area, where contact stress is less than 0.1% of maximum contact stress. As result, slot length is obtained as the sum of insert length and actuators length (Figure 3.14).

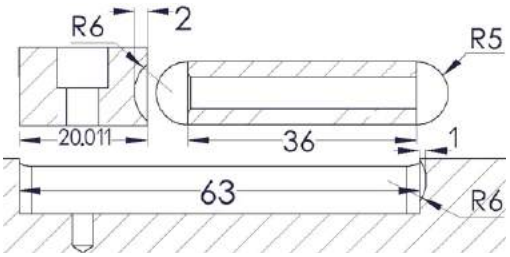

Figure 3.14: Slots dimensions

Using the model presented in section 3.1.3, interference was estimated for selected preload, based on the equivalent stiffness. Boring bar FE model is shown in Figure 3.15.

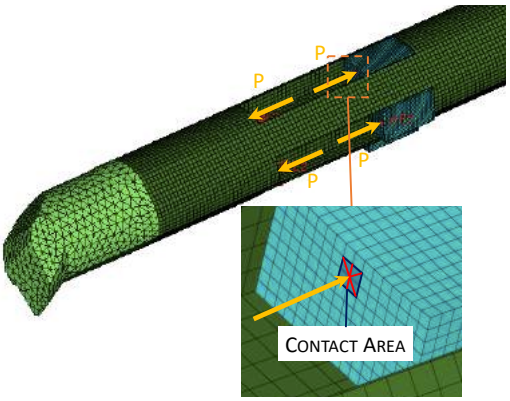

Figure 3.15: Boring Bar FE model for stiffness estimation

In Table 3.5, measured stiffness of actuator and estimated contact stiffness and boring bar stiffness are reported.

Table 3.5: Actuators, contact and boring bar equivalent stiffness

K_P [N/mm]	K_H [N/mm]	K_B [N/mm]
7.20e4	2.39e05	6.39e05

Resulting interference was found to be 0.133 mm.

By means of FE model shown in Figure 3.16, according with approach presented in section 3.1.4, cover thickness, that guarantees the compensation of material removed for actuators housing, was found to be 1.5 mm (for the two covers on insert side) and 1.8 mm (for the other two covers).

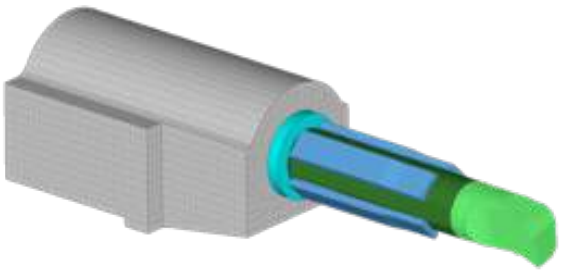

Figure 3.16: Active boring bar FE model for protective covers design

In Table 3.6 properties of the section, in correspondence of actuators, of the different models are reported in terms of cross sectional area (A) and second moment of area with respect to central axis of inertia x and y (J_x and J_y respectively).

Table 3.6: Comparison between original boring bar, boring bar with slots and active boring bar with covers

Configuration	A [mm²]	J_x [mm⁴]	J_y [mm⁴]
Original boring bar	760.38	45042.61	47493.32
Boring bar with slots	373.08	16074.55	17581.10
Boring bar with covers	514.32	42032.73	43644.03

The employment of designed covers compensates the loss of area due to material removed in correspondence of the slots and allows to obtain almost the same inertial properties of original boring bar ensuring a similar static response.

The comparison between the dynamic responses of the different models is shown, in terms of tooltip Frequency Response Function (FRF), in Figure 3.17.

a)

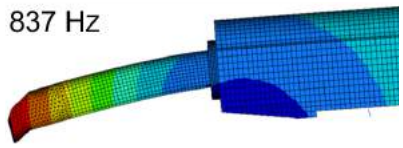

b)

c)

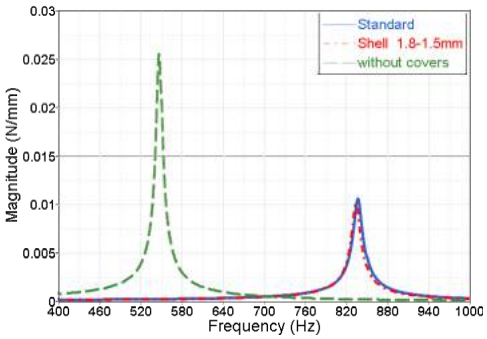

Figure 3.17: a) original boring bar dominant mode b) active boring bar dominant mode c) comparison between original (i.e, standard) and active boring bar in terms of FRF

Due to material removal, the dynamic response of the boring bar significantly changes, both in terms of natural frequency and peak amplitude. The employment of

designed covers allows to obtain a dynamic response almost identical to the original boring bar. In particular, the difference in terms of natural frequency is less than 1%.

3.2.3. Active boring bar manufacturing

The designed active boring bar was realized and assembled (Figure 3.18). The standard bar from Sandvik Coromant (S32U-PTFNL-16W) was machined to obtain the four slots and protective covers were directly milled starting from bar made of 1.2738 steel (40CrMnNiMo8). In order to guarantee the designed interference, manufacturing process for the protective covers was carefully organized. In particular, length of each actuator was measured and the distance between the center of the sphere and the cover back plane of the covers was corrected according to the measured value.

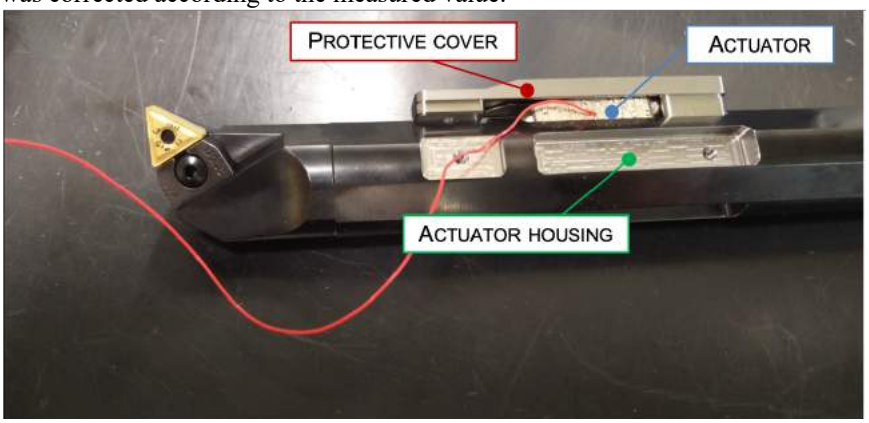

Figure 3.18: Designed active boring bar

3.3. Active boring bar experimental validation

3.3.1. Comparison between original and modified boring bars

At first, experimental tests were carried out in order to compare the standard boring bar with the realized active boring bar in case of control off. The aim of this validation is to verify that designed active boring bar presents an equivalent static and dynamic behavior of the standard one (req. 3). Experimental modal analysis was carried out on both boring bars in free-free (Figure 3.19a) and constrained (fixed-free) conditions (Figure 3.19b).

a) 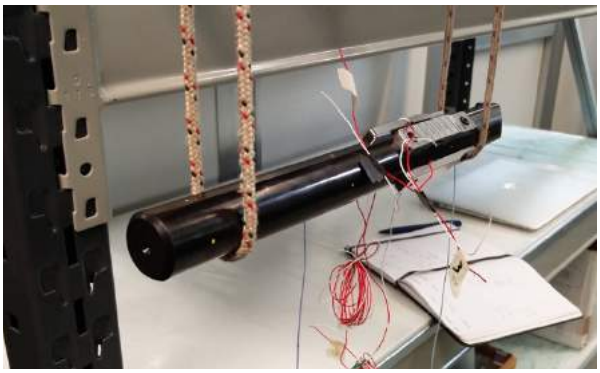 b) 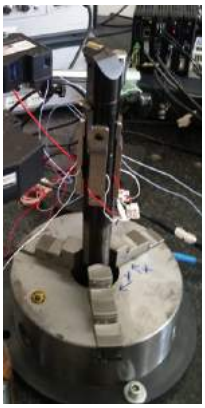

Figure 3.19: Setup for active boring bar experimental modal analysis a) Free-free condition b) Fixed-free condition

Experiments were performed by means of impact testing using a PCB 08C03 impact hammer and two mono-axial accelerometers (PCB 352C22), roving hammer strategy was adopted, and required FRFs were computed by means of the dedicated acquisition system (SCADAS SCM202V). Using LMS software, FRFs were analyzed and dominant modes characteristics (mode shapes, natural frequencies) were extracted by means of Polymax algorithm [21].

Results in terms of dominant mode natural frequencies are reported in Table 3.7. The difference in terms of natural frequency between original and active boring bar (less than 5%) indicates a good match between the two systems. As a consequence, the effectiveness of design approach to achieve dynamic equivalence was demonstrated.

Table 3.7: Comparison between original boring bar and active boring bar

Condition	Standard - natural frequency (Hz)		Active - natural frequency (Hz)	
	X	Y	X (error)	Y (error)
Free-free	1190	1218	1134 (-4.7%)	1169 (-4.0%)
Fixed-free (overhang 245 mm)	329	276	317(-3.7%)	263 (-4.7%)

3.3.2. Damping system effectiveness: dynamic behaviour of active boring bar when control is on

In order to test the designed active system effectiveness, experimental tests were carried out to compare standard and active boring bar dynamic behavior with control on.

DVF control logic was implemented in Matlab® Simulink v14 and integrated using VeriStand 2014 in a National Instruments PXIe 1071 controller equipped with a BNC-2110. Velocity signal is acquired by the controller, and the actuation signal is generated by multiplying the velocity of a defined control gain. In order to protect the actuator by

overvoltage (±100V that corresponds to ±3V on the command signal), a saturation block (set at ±2.5 V) was added before the PXI output.

Control logic input signal (i.e., velocity) was obtained by integrating the acceleration signal measured using piezoelectric accelerometers (PCB JM357B11, Brüel & Kjær 4393), by means of an external conditioner (Brüel & Kjær 2635). Employment of such accelerometers, characterized by a resonance frequency of 50 kHz, ensures a sufficient synchronism between excitation and response. To make the actuation system able to act in both directions (x and y) two sensors were placed on the boring bar (Figure 3.20a). Sensor position was chosen in order to realize a "collocated" positioning, so that sensor and actuator act on the same point, as suggested for the application of DVF control logic.

In order to evaluate the effect of the actuation system, the prototype was tested with different dynamic forces applied by means of a shaker (Brüel & Kjær 4809), controlled by the LMS SCADAS SCM202V acquisition system. The experimental setup is shown in Figure 3.20b. The active boring bar was fixed by means of a three-jaws chuck and displacement were measured by means of a laser sensor (Keyence LK-H085) and the sensors installed on the boring bar.

(a)

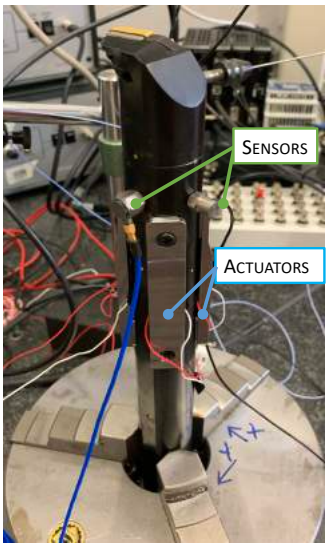

(b)

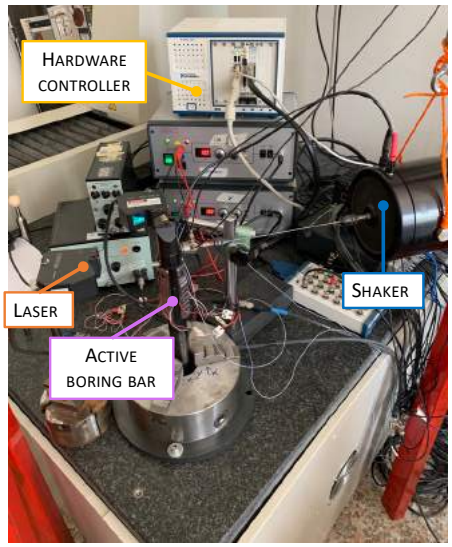

Figure 3.20: a) Active boring bar b) Experimental setup

At first, the system was excited by single frequency force (pure sine) at 240 Hz (close to the resonance frequency of the system). Results in case of control on and off (Figure 3.21) show how the active damping system is able to significantly mitigate vibration (reduction of about 85%).

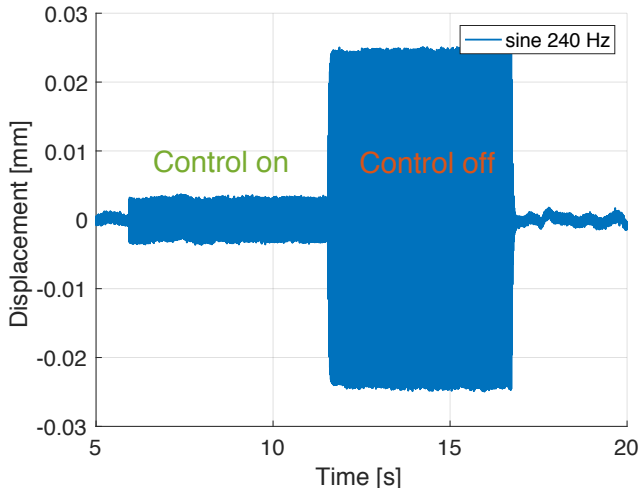

Figure 3.21: Measured displacement in case of control on and off in case of single frequency force applied

Then the system was tested by exciting the active boring bar with a multifrequency force (chirp sine between 0-500 Hz). Results in case of control off and on (Figure 3.22) highlight the effectiveness of the active system in adding damping to the system: vibrations in the frequency range close to the natural frequencies are significantly reduced. Outside these frequency ranges the control does not affect the vibrations level, as expected, and no distortions are found.

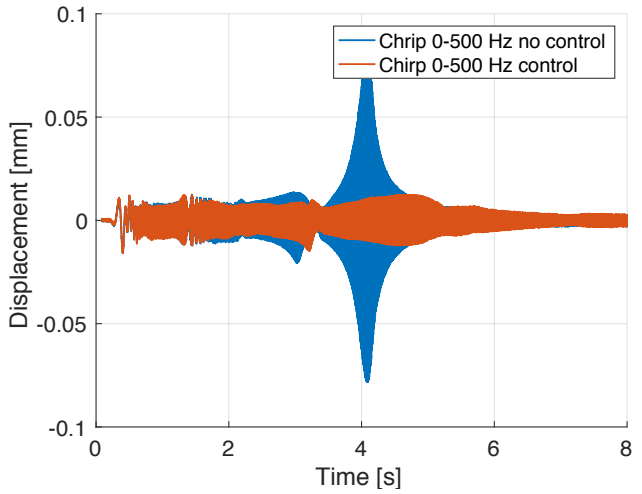

Figure 3.22: Experimental displacement in case of control on and off in case of multifrequency force applied

The same result was found in case of impulsive excitation, reproduced by impact testing with instrumented hammer (PCB 08C03) on the tool-tip and acquiring boring bar displacements by using the laser sensors.

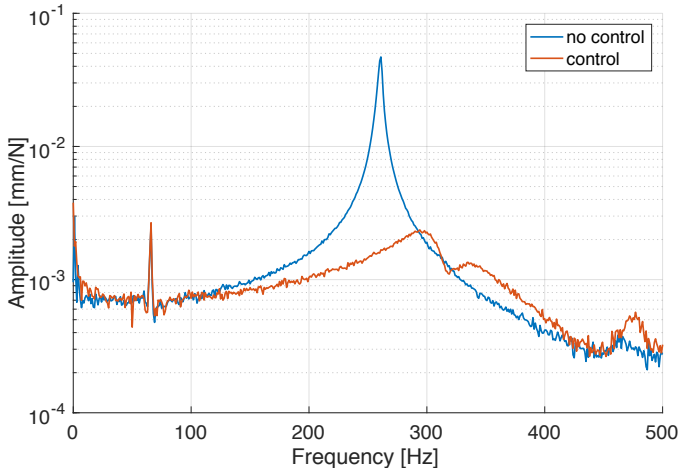

Figure 3.23: Tooltip FRF in case of control off and control on.

Frequency Response Functions highlight that active boring bar can reduce the amplitude of vibration at the natural frequency of more than 90%. As conclusion, preliminary experimental test on active boring bar, confirmed the effectiveness of the active damping system, showing a drastic reduction vibration amplitude in correspondence of the dominant mode shape.

3.3.3. Chatter test in case of control on

In order to evaluate the effectiveness of the active system on chatter, cutting tests were performed using designed active boring bar.

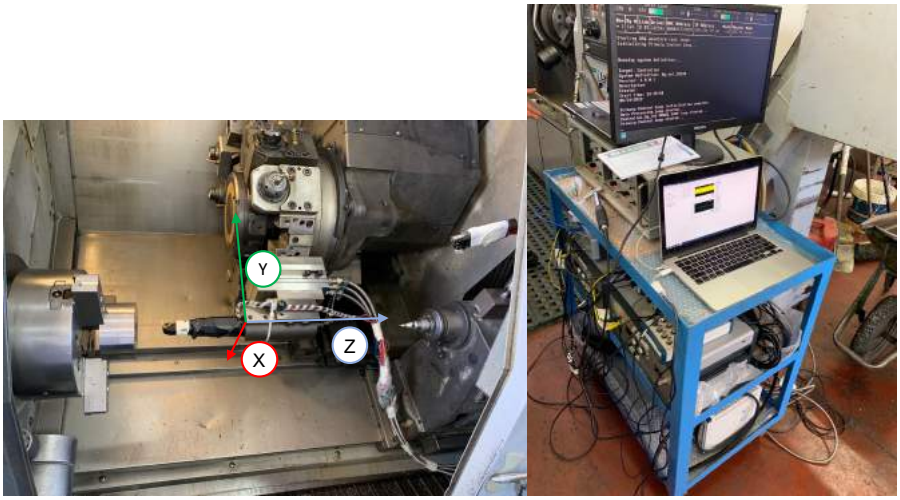

Figure 3.24: Experimental setup for cutting tests

Dynamic response of designed active boring bar in case of control off, once attached to the machine tool with 163 mm of overhang, was then compared with the standard boring bar and results are reported in Figure 3.25.

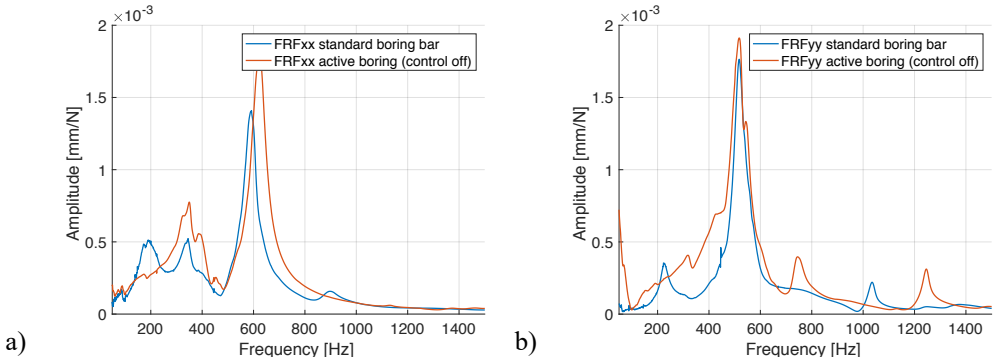

a) b)

Figure 3.25: Comparison between standard and active boring bar experimental FRF (163 mm overhang)

Results show a good accordance between dynamic behavior of standard and active boring bar, confirming the goodness of the design strategy.

In order to test the damping effect of the active system, FRFs on active boring bar, mounted with 205 mm of overhang, were measured. Comparison between the case with control on and off are reported in Figure 3.26.

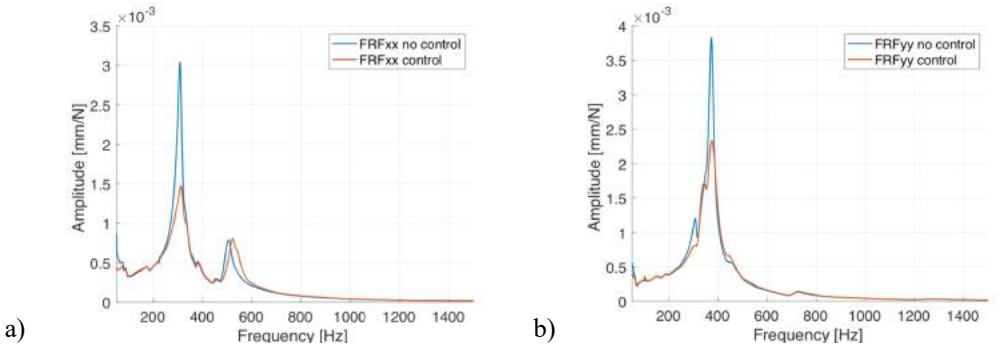

a) b)

Figure 3.26: Measured active boring bar direct FRF along x (a) and y (b) direction

Experimental results highlight a reduction, in terms of dominant peak amplitude, of around 40%, confirming the damping effect of the active system on the tool dynamics.

Chatter tests were then carried out at the same cutting velocity and feed per tooth evaluated in case of standard boring bar. Exploiting the possibility of actuate in two directions (x and y), four different configurations were evaluate in order to detect the most effective one.

By using the standard boring bar, chatter was found in correspondence of 1.4 mm of depth of cut, 0.2 mm/rev of feed per tooth and 700 rpm of spindle speed, as shown in Figure 3.27.

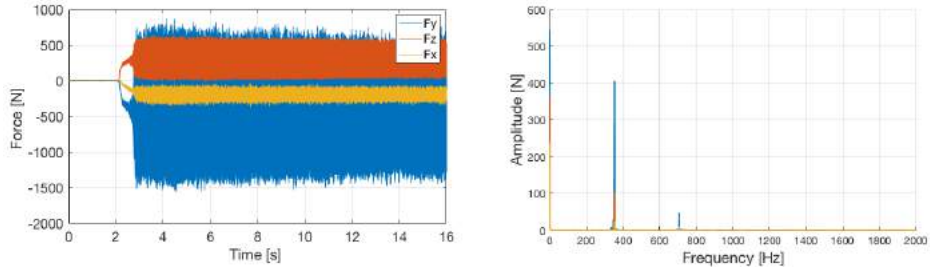

Figure 3.27: Cutting forces measured while cutting with standard boring bar (1.4 mm of depth of cut)

Cutting tests with the same cutting parameters were carried out using designed active boring bar. The use of designed prototype and of the developed control allows to work in stable conditions as demonstrated by results reported in Figure 3.28 in case of 1.4 mm of depth of cut.

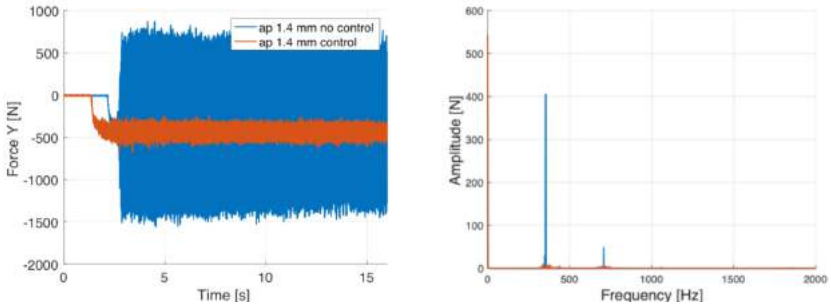

Figure 3.28: Comparison between cutting forces in case of control on and off (depth of cut 1.4 mm) in the time and frequency domain

Radial depth of cut was then increased and cutting tests were performed in case of sensor measuring along x direction and actuators acting on y direction. Results in terms of cutting forces in the time domain and in the frequency domain are showed in Figure 3.29.

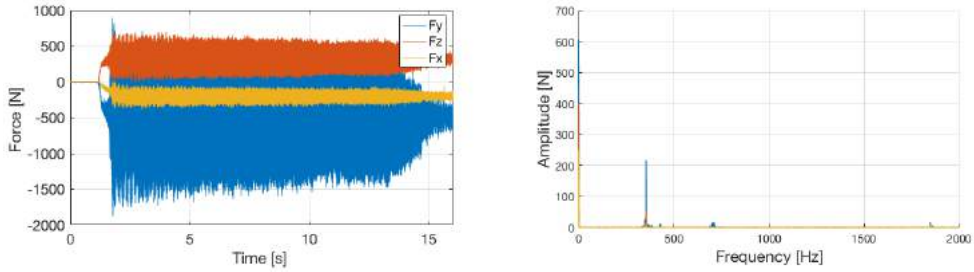

Figure 3.29: Cutting forces in case of 1.6 mm of depth of cut, sensor measuring along x and actuation along y

As clear from cutting force spectrum, the active device is not able to eliminate chatter, but acts reducing the peak amplitude in correspondence of the chatter frequency. It, indeed act, just mitigating unstable vibrations.

In order to more in depth investigate the optimal actuation direction, additional cutting tests were carried out in case of different strategies of measuring and actuation. Results in case of 1.4 mm of depth of cut are reported in Figure 3.30

a)

b)

c)

d)

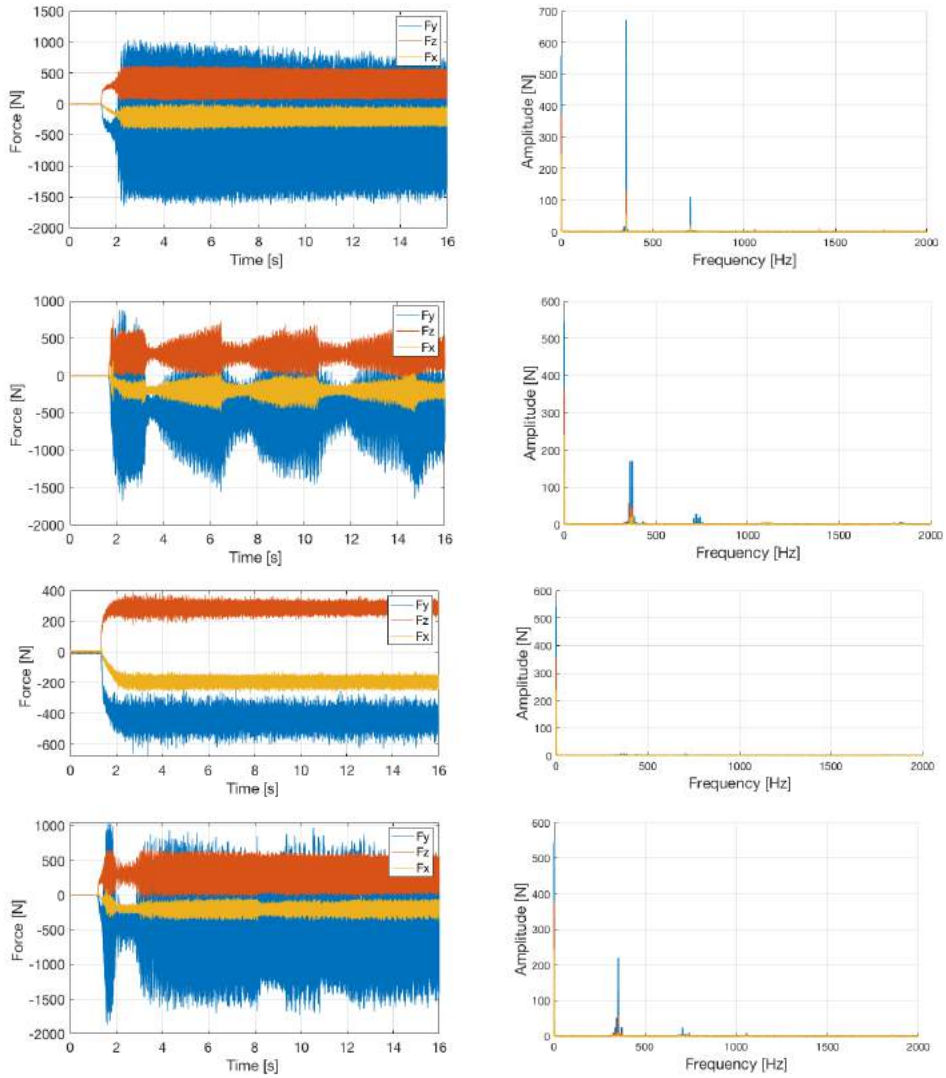

Figure 3.30: Cutting forces (depth of cut 1.4) a) sensor measuring along x, actuation along x b) sensor measuring along y, actuation along x c) sensor measuring along x, actuation along y d) sensor measuring along y, actuation along y

By measuring along x direction and actuating along y direction, cutting forces amplitude remains constant during time, as confirmed by the frequency spectrum in whom the only peak is in correspondence of a null frequency. In case b) and d), although the main contribute in the frequency spectrum is given by static force, a secondary peak is present in

correspondence. In both of cases, the control is able to disrupt the instability with a certain delay. The less effective actuation strategy is the first one, in which the sensor acquire along x direction and the actuation is along x direction. In this case the cutting force amplitude is not effectively reduced and the peak in correspondence of the chatter frequency remains the dominant one.

3.4. Conclusions

In conclusion, an active boring bar design approach tailored for DVF control was presented. The aim of the proposed approach was to provide design requirements and a structured strategy, able to support active boring bar design, considering the most significant criticalities yet unaddressed in literature. In particular, the strategy for actuators integration on the boring bar body was evaluated focusing on:

1. The most effective actuators positioning
2. Preload estimation in order to protect piezoelectric actuators from traction stress during machining
3. Preload system design
4. Protective cover design to guarantees static and dynamic equivalence between the active boring bar and the original boring bar in case of control off.

An active boring bar, designed following this approach, was realized and tested both in case of control off and of control on. Experimental tests confirm the benefits of proposed method, which allowed to:

1. Realize a dynamic equivalence in case of control off, between original and active boring bar (difference between natural frequency resulted less than 5%), confirming that the proposed approach for protective covers dimensioning is able to compensate the loss of stiffness due to removed material.
2. Provide an actuators integration design strategy able to respect size requirements and realize a significant increase of damping (around 90% of dominant mode amplitude reduction), in case of control on, confirming the effectiveness of actuators integration and placing approach.

Chatter tests using designed active boring bar were carried out to estimate the impact of the system in terms of chatter stability increases on an actual machining process. Thanks to the possibility of actuate in two different directions, cutting tests were performed in four different configurations varying sensors position and actuation direction in order to detect the most effective actuation strategy.

4. Optimization Strategy for fixturing design

The aim of this task of Ph.D. activity was to cover a lack in the scientific literature by developing a strategy able to aid supports design in order to guarantee tolerance required and stable machining for thin wall components turning. This procedure aims at find fixturing configurations that guarantee requirements starting from workpiece geometry, toolpath and tool geometry. Thanks to a black block approach, strengths are the ease of use (since it does not require specific modelling competence) and computational efficiency, that make it suitable for industrial application.

At first, a state of the art analysis was carried out in order to evaluate the most suitable approach for fixturing design to address this purpose. Then, the main framework of the algorithm was design integrating prediction models with an automatic procedure that allows to evaluate how geometrical errors and dynamic behavior varies with different support configuration. Models employed were accurately chosen and tailored in order to realize the best compromise between accuracy and computational costs. Finally, the whole algorithm was implemented and numerically verifying on a thin wall component.

4.1. Fixturing design statement and method selection

According with the definition proposed in [18], a fixture is “a mechanism used in manufacturing to hold a workpiece, position it correctly with respect to a machine tool, and support it during machining”. Fixturing design is a complex process that aims to find a suitable configuration able not only to guarantee the fixture functionality and effectiveness but also to lead to benefits for the machining process in terms of costs and final component quality.

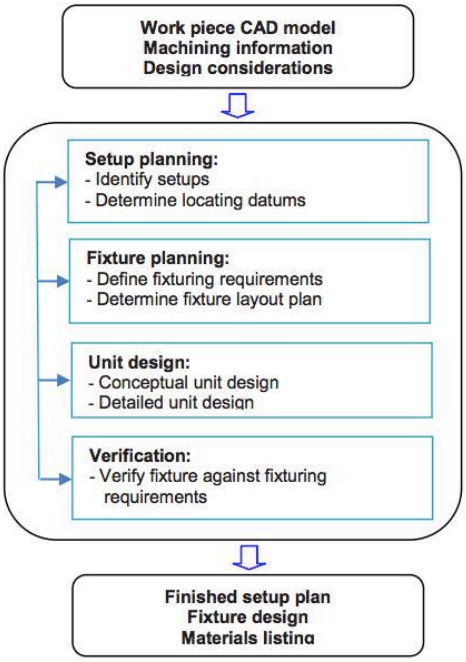

Figure 4.1. Steps for fixturing design

For this reason, several additional aspects, summarized in Table 4.1, must be taken into account while design a fixturing system.

Table 4.1. General requirements for fixturing systems

General requirements	Example of abstact sub - requirements
Tolerance	▪ The locating tolerances should meet the design tolerances requirements of the parts
Physical	▪ The fixture must be capable of physically accommodating the work-piece's weight and geometry. ▪ The fixture must allow access to the features of the work-piece that needs to be machined
Affordability	▪ Cost should not be more than the desired levels. ▪ Assembly/disassembly times should not be more than the desired levels. ▪ Operation time should not be more than the desired levels.
Constraint	▪ The fixture should guarantee the stability of the workpiece by

	ensuring that the work-piece's moment and force equilibrium are kept. ▪ The fixture should make sure that the fixture/workpiece stiffness is enough to avoid the occurrence of deformation, which could prevent the design tolerances from being reached.
Usability	▪ Weight should not be more than the desired levels. ▪ The fixture should not result in damaging the surface at the workpiece/fixture's interface. ▪ The fixture should offer tool guidance to the features of the designated workpiece. ▪ The fixture should be error-proof, i.e., the fixture should be able to avoid wrong workpiece insertions into the fixture. ▪ The fixture should assist in chip shedding by providing a way to allow the machined chips to flow away from the fixture and the work-piece.
Collision prevention	▪ The fixture should not result in collisions of the tool path-fixture. ▪ The fixture should result in work-piece fixture collisions, other than the designated clamping and locating positions. ▪ The fixture should not result in fixture-fixture collisions besides the designated points for fixture component connection.

Among these aspects, in case of thin wall component, a special attention must be paid on the necessity of guarantee the conformity to tolerances and chatter stability as discussed in Section 2.

Since several aspects must be taken into account, fixture design is often based on the designer experience and/or a trial and error approach. Nevertheless, scientific literature proposed both retrofittable intelligent fixtures and more structured methodology, developed with different aims and approaches, to improve machining process. Active fixtures are intelligent devices, mainly used for vibration mitigation [50], capable of monitoring the process in real-time and exert adequate counter-excitations. Their main advantage is that they are retrofittable to different components and, once designed, they do not require any specific modelling expertise. For this reason they represent a promising technology for industrial applications. However, due to their complexity and the necessity external power, their employment on rotating component, as in case of turning, is difficult. On the other hand, standard fixturing system, must be design according with the specific case. In order to offer an aid in fixturing design, several techniques were proposed in literature. Among these, the most common are: Rule-Based Reasoning (RBR), Case Based Reasoning (CBR) and model based procedures, often combined with Genetic Algorithms (GA).

More in detail RBR techniques are based on an experts system approach that utilizes induction rules to decide if a new problem should be further inspected or not [63].

CBR techniques [64] are based on the assumption that similar workpieces requires similar fixture and exploit the experience acquired for similar case to develop fixturing solutions. In order to improve their effectiveness, they can be combined with Neural

Network (NN) [65], interconnected networks consisting of simple components, able to develop solutions for new problems that are entered into the network.

Among all approaches, the most interesting for thin wall components turning, are the model based ones, since they allows to directly evaluate the impact of each configuration on geometrical errors and chatter stability.

This kind of approaches were largely presented in literature to achieve different aims such as minimize location error [66], minimize workpiece deformation [67] and mitigate vibration [51,68]. Their crucial aspect is the necessity to balance accuracy and computational costs. In order to achieve this goal, the most common modelling technique is FE approach [69], often interfaced with Genetic Algorithm (GA) [70–73]. These approaches usually detect an objective function that must be minimized. The values of the objective function are obtained by simulating the machining process in different fixturing configuration. Optimization algorithms allow to find the optimal solution within a limited number of simulations. In particular, GA are robust, stochastic and heuristic optimization methods extremely useful for optimizing complex systems with nonlinear functions and/or a large number of design variables. Their employment is necessary in case several configurations should be evaluated, and/or computational costs for each simulation are high, such as in case of huge FE models. Despite their effectiveness was demonstrated, almost the totality of presented approach is tailored for milling process. Fixture design in turning must also consider the necessity of an axisymmetric framework for the fixturing system in order to avoid unbalances during workpiece rotation.

4.2. Proposed approach for fixturing design

Among all requirements that a fixturing system must address, proposed approach is focused on geometrical error reduction and chatter stability that were demonstrated to be crucial for thin wall components turning. Since tolerance required and chatter stability are constraints for machining, proposed approach is designed not to provide an optimal solution but to simply detect the support configurations that guarantee these requirements, demanding the final choice to the designer. By doing this, additional aspects, like mounting easiness and costs may be evaluated in detail in a second time on a restricted solution domain.

As explained in Chapter 2 both experimental and numerical approaches may be used for geometrical error and chatter stability estimation. However, the first ones requires several tests including workpiece static and dynamic characterization, and cutting tests and results are specific for a given workpiece and tool. Moreover, in case of thin wall component, static and dynamic stiffness varies along axis position and it is influenced by material removal. For this reason, modelling techniques are preferable. To be more user friendly a black box approached was design in order to completely automate optimization procedure obtained by the integration of workpiece, cutting force and chatter prediction model. In order to globally minimize computational costs, each modelling technique was chosen as the optimal balance between accuracy, easiness of implementing and computational costs.

Then all the modelling techniques were implemented and integrated in a Matlab® environmental together with an algorithm that automatically create and run model.

The idea was then to develop a new fixturing strategy that employs a FE approach to effectively guide fixture designers, detecting a domain of solution that are able to address workpiece quality requirements. In case of large dimensional thin wall components, a vertical lathe is usually employed and the workpiece may be fixed to the workholding plate

of the turning machine by means of a flange (Figure 4.2). This solution, allowing to avoid radial that, due to low radial stiffness, may causes deformation in the workpiece is preferable compared with the use of chucks.

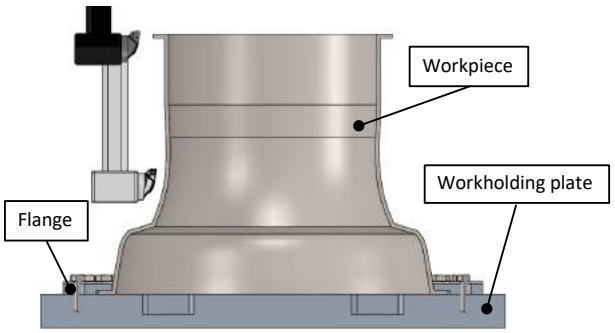

Figure 4.2. Large components holding on vertical lathes

However, this solution may not provide to the component the required support during the machining. For this reason, the use of supports may be unavoidable and needs a careful design. Since various and several aspects (i.e. functionality, cost, easiness of mounting) must be taken into account, it is difficult to develop a procedure that includes all these requirements. The proposed approach aims to aid support design by detecting a set of solutions that guarantee tolerance required and a stable machining demanding the choice of the optimal position to the designer. Indeed, once the whole solution domain is reduced, designer can decide which solution is more suitable considering all the other aspects, certain that the functional requirements are met.

An algorithm for geometrical error and chatter prediction given cutting parameters, tool and workpiece model was implemented in Matlab® (Figure 4.3). This algorithm, by interfacing with Nastran® solvers, is able to predict via FE approach workpiece static and dynamic behavior.

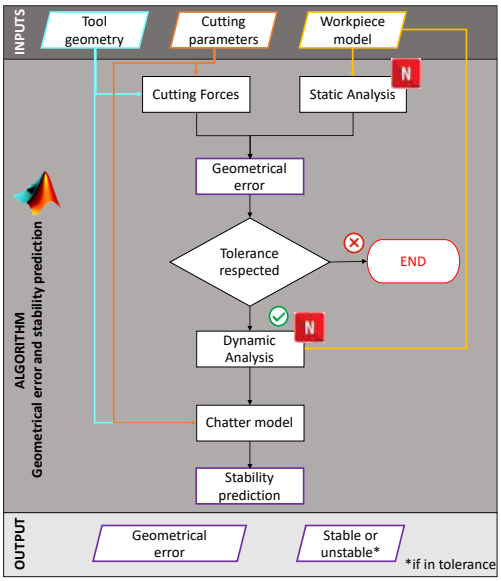

Figure 4.3. Geometrical error and Stability prediction in a given cutting point

In a given cutting point, according with prediction model, diametral error, may be estimated starting from cutting force and workpiece local stiffness. Once model is created, proposed algorithm runs a static simulation and elaborate results in order to estimate workpiece local stiffness, while cutting forces are estimated by means of a dedicated model. Machining stability may be evaluated given cutting parameters starting from relative FRF between components and tool in correspondence of the cutting point. In case of thin wall components, the main contribution is given by the workpiece dynamic response. A workpiece dynamic simulation is then carried out to estimate its FRF, that, elaborated in a chatter prediction model allows to estimate if machining is stable.

Since both tolerances and stability are required, dynamic analysis is performed only if geometrical error is less than tolerances allowing to save computational time. Moreover static analysis allows to estimate real depth of cut, that, due to displacement of workpiece surface due to the cutting force, is smaller than the nominal one. Both static and dynamic analysis are performed in each point intercepted by the toolpath, as shown in Figure 4.4, in order to take into account the stiffness variation along workpiece axis. After a tool position is evaluated, the workpiece model is updated in order to take into account the loss of stiffness due to material removal. Then the analysis is performed considering the tool in the following position.

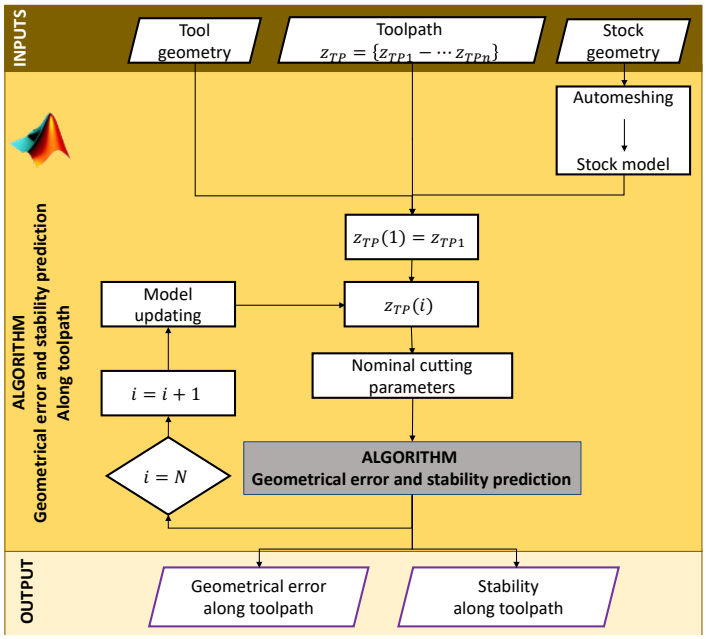

Figure 4.4. Geometrical error and stability along toolpath

At first geometrical error and stability prediction are evaluated in case of no supports added (i.e. workpiece simply hold to the lathe). In case of at least one requirement is not satisfied, the algorithm proceeds finding supports configurations that allows to address requirements.

Given toolpath, the algorithm is able to detect machined surfaces on which supports cannot be mounted. It is also possible to indicate areas in which supports may not be mounted (i.e. hard to position etc.).

In order to reduce computational time, a first evaluation is made, according with the structure showed in Figure 4.5, varying position along workpiece axis and considering all the section supported (i.e. supports are considered to be on all nodes correspondent to selected axial position).

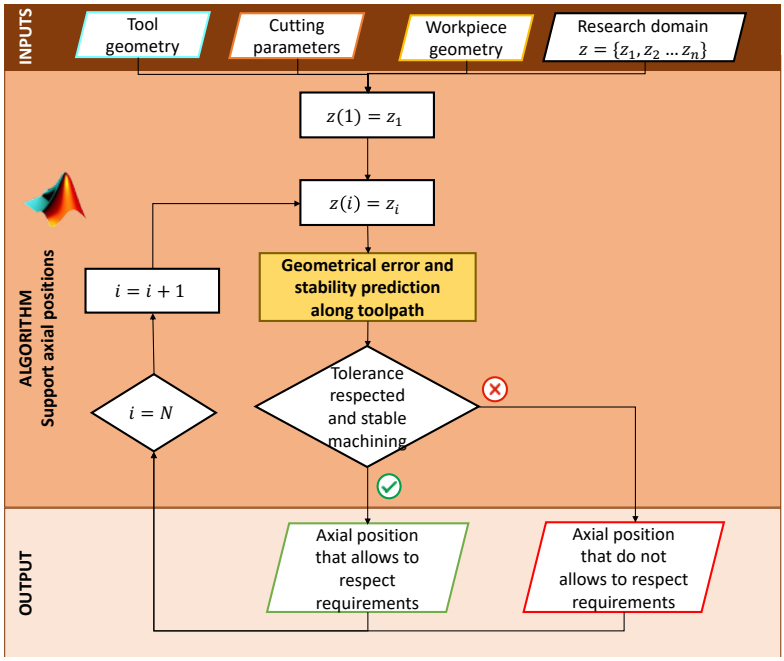

Figure 4.5. First step evaluation to find suitable axial support positions

At the end of this evaluation, solutions found to be suitable for support positioning are more in depth evaluated, gradually decreasing the number of supports, in order to find, for each axial position, minimum number of supports that guarantee requirements (Figure 4.6).

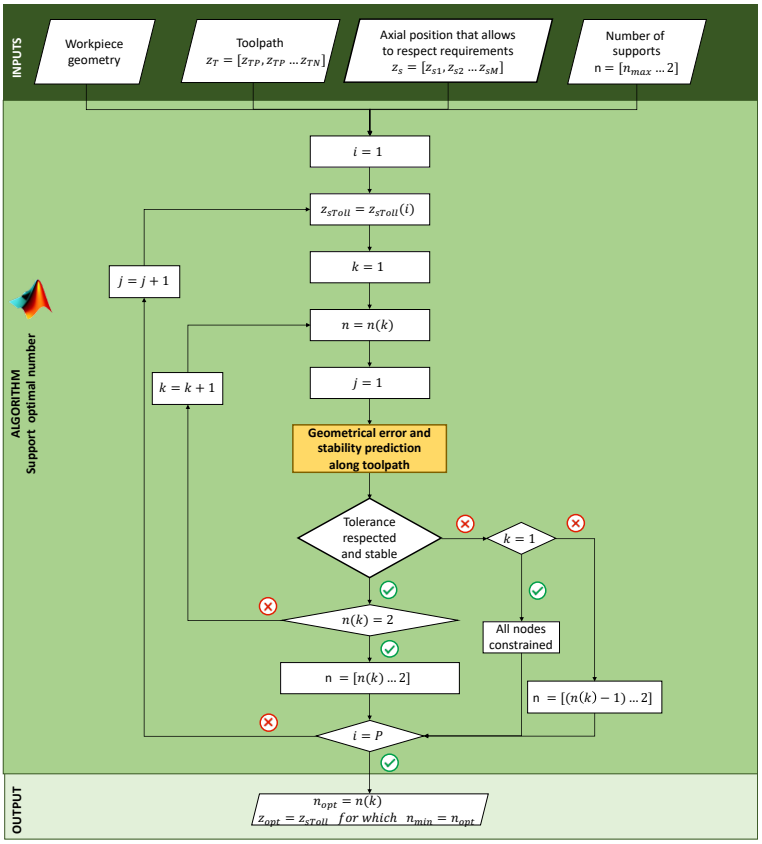

Figure 4.6. Number of supports optimization

The whole algorithm structure is shown in Figure 4.7.

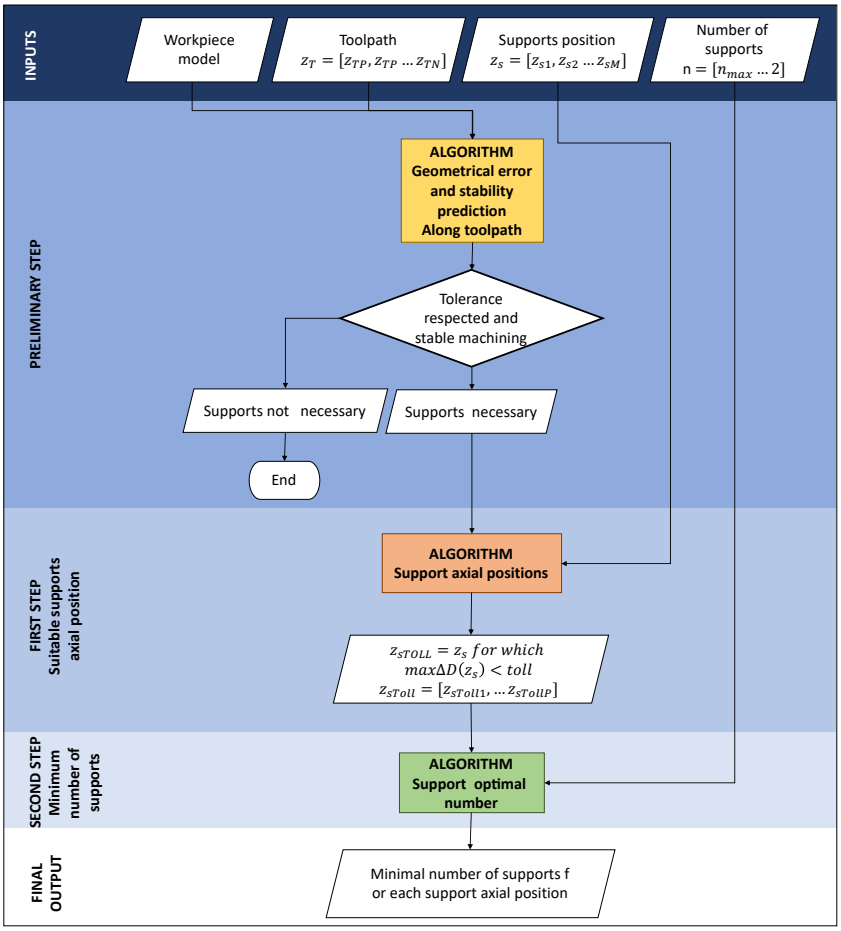

Figure 4.7. Proposed approach for support design

4.2.1. Workpiece model

Since this approach does not involve the integration with an optimization algorithm, all the possible configurations must be evaluated. Simulation computational costs are, then, the key point in order to limit computational time. The most effective technique to model thin wall components is by means of 2D elements, since stress and deformation may be considered constant along thickness. Computational cost saving, compared with 3D elements, used in case of massive components, allows to evaluated a large number of fixturing configuration in a limited time.

Moreover, thanks to the axisymmetric geometry of components turned, meshing process with 2D element may be easily automatized such as the only input required to simulate workpiece behavior is its geometry. Nastran® run models are text files in which, the key elements that describes a static and dynamic model (nodes, elements, elements property, material properties, loads and constraint) are codified. The auto - meshing algorithm is able

to create a text file in which all this information are organized according with Nastran® format.

Each element is characterized by id element, ID of nodes that detect it and properties. In case of 2D, nodes that identifies the model may be placed in correspondence of the middle surface between internal and external surface and local thickness may be assigned to each node that compose the element (nodal thickness). Starting from 2D section along the XZ axis of the component, the algorithm detect the middle surface track on XZ plane on which nodes, equally spaced at a given distance, are created. Moreover, in each node position, local thickness is calculated and assigned to correspondent node. Then for each node on the midline a given number of nodes are created by splitting nodes on the circumferential direction. Each element is then created by grouping adjacent nodes and assigning the correspondent nodal thickness.

To model fixturing condition different approaches may be used. In the proposed algoritm, the joint of the workpiece on the workholdin plate is modelled by fully constraining (blocking all degrees of freedom) the node in correspondence of the flange. However, model of the fixturing system in correspondence of the workholding may be adapted according with different clamping conditions.

For what concern supports model, since the contact is on one side (monoliteral contact), CGAP elements (Figure 4.8) were employed. These elements, indeed, in case of static analysis and linear modal analysis produces a linear stiffness matrix in which the stiffness depends on the gap state. In particular according with the gap value between two node, two stiffness, one for the open gap and one for the closed gap case, may be selected.

Figure 4.8. CGAP element coordinate system [74]

Each CGAP element is then defines by an element identification number EID, a property identification number PGAP, grid point identification number of connection points (GA and GB) and components of vector , from GA, in the displacement coordinate system at GA (X1, X2, X3). In the CGAP properties field, shown in Figure 4.9, may be selected.

Field	Definition
PID	Property identification number.
U0	Initial gap opening
F0	Preload.
KA	Axial stiffness for the closed gap (i.e. U A - U B > U0).
KB	Axial stiffness for the open gap (i.e. U A - U B < U0).
KT	Transverse stiffness when the gap is closed. It is recommended that KT ≥ (0.1 * KA).

Field	Definition
MUY	Coefficient of friction in the y transverse direction μ_y .
MUZ	Coefficient of friction in the z transverse direction μ_z .
TMAX	Maximum allowable penetration used in the adjustment of penalty values. A positive value activates the penalty value adjustment.
TRMIN	Fraction of TMAX defining the lower bound for the allowable penetration.

Figure 4.9. PGAP fields [74]

The same workpiece model is used to perform both static and dynamic analysis.

Given toolpath (i.e. tool nose center position during cutting) it is possible to find, for each cutting position, correspondent workpiece node.

In order to estimate stiffness in correspondence of each the cutting point, nominal cutting force, estimated by means of a dedicated approach (section 4.2.3), is applied in the node in correspondence of the cutting point and displacement along three direction are calculated. Since the whole FRF matrix, expressed in the lathe reference system, is required for chatter prediction, dynamic analysis is carried out considering a unitary dynamic load applied along the three direction and calculating correspondent dynamic displacements. In order to reduce the number of simulation, both in the static and dynamic analysis, the most critical position varying axial position is assumed to be in the middle position between two supports, where static and dynamic stiffness is minimum.

Once local stiffness is estimated, the algorithm is able to calculate real depth of cut (section 4.2.2), which represents the real thickness of removed material. According with this value, the model is updated in order to take into account the loss of stiffness due to material removed. The node thickness in correspondence of the cutting point is updated.

4.2.2. Geometrical error estimation

Geometrical errors are predicting evaluating the static local deformation of the component in a given cutting point under the cutting force. Cutting forces were estimated according with prediction model explained in section 4.2.3. This model, indeed, thanks to its improved accuracy compared with classical mechanistic model, allows to effectively model the presence of the tool nose radius. As result, it is suitable for cutting force estimation in finishing process where radial depth of cut are low compared with tool nose radius. Once estimated cutting force

As after mentioned, dependence of cutting forces on radial depth of cut is crucial in case of compliant parts: real depth of cut, indeed, can be significantly different from nominal one due to part deflection. Therefore, local workpiece stiffness prediction is necessary, and it should be included in cutting force prediction estimation. In order to overcome this issue, reducing in the meantime time-consuming iterations, a first estimation of the cutting forces is made considering the local stiffness: a unitary force normal to workpiece surface is applied and correspondent displacement $\bar{\delta}$ is calculated. Assuming a linear behavior, relationship between forces and displacement may be written as:

$$F = \frac{\delta}{\bar{\delta}} = k\delta \tag{4.1}$$

where k is local stiffness in correspondence of cutting point. Real depth of cut b_{real} is the one that give rise to a displacement δ_{real} for which following relation is satisfied:

$$F_r(b_{real}) = k\delta_{real} \tag{4.2}$$

A FE analysis is carried out to estimate local workpiece stiffness displacements along radial direction (x axis in lathe reference system) when cutting force, calculated for nominal depth of cut, are applied. Knowing local stiffness, is possible to establish a relation between applied force (F_a) and workpiece static deflection (δ_{real}) and then correspondent real depth of cut.

From the intersection between the curve of applied force varying the correspondent b_{real} and the curve that describes the radial cutting force varying radial depth of cut, the real depth of cut can be estimated (Figure 4.10).

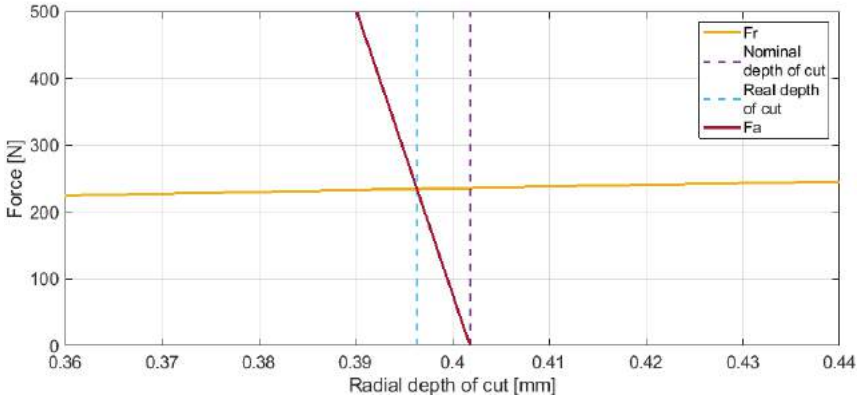

Figure 4.10: Real depth of cut estimation

In order to increase the accuracy, all the components of the cutting forces are considered while evaluating the real depth of cut (b_{real}).

4.2.3. Cutting force model

In order to develop an accurate chatter prediction model, a suitable cutting force model must be considered. In this section a discussion about the main approaches for cutting force estimation is presented in order to highlights the crucial aspects that should be taken into account while modelling cutting force.

During machining, workpiece and tools exchanges cutting forces which entity and direction can be put in relation with cutting parameters, workpiece material, tool material and tool insert geometry. In order to estimate cutting forces several approaches, with different level of accuracy were developed.

According with mechanistic models [26], it is customary to model the cutting forces in oblique cutting coordinates, i.e., tangential or cutting speed direction (F_t), chip thickness direction or perpendicular to the cutting edge (F_f), and along the cutting edge (F_r) as shown in Figure 4.11.

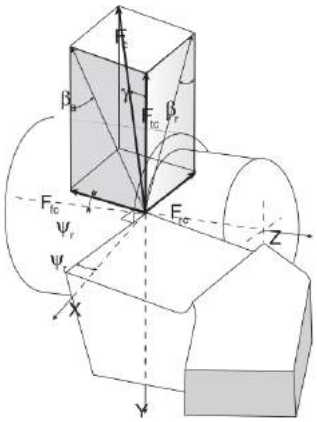

Figure 4.11: Cutting force components in turning [26]

These components may be put in relation with the estimated chip area and width of cut by means of coefficients that can be determinate experimentally or estimated starting from the cutting tool geometry and material (Eq. 4.5).

$$\begin{Bmatrix} F_{tc} \\ F_{fc} \\ F_{rc} \end{Bmatrix} = \begin{Bmatrix} K_{tc} \\ K_{fc} \\ K_{rc} \end{Bmatrix} bh + \begin{Bmatrix} K_{te} \\ K_{fe} \\ K_{re} \end{Bmatrix} b \tag{4.5}$$

Cutting forces in machine tool reference system are estimated assuming that the equivalent chord length acts as a cutting edge, and the nose radius of the tool is neglected. As result, cutting force in the machine tool reference system may be expressed as

$$\begin{Bmatrix} F_x \\ F_y \\ F_z \end{Bmatrix} = \begin{bmatrix} 0 & -\sin\psi_r & -\cos\psi_r \\ -1 & 0 & 0 \\ 0 & -\cos\psi_r & \sin\psi_r \end{bmatrix} \begin{Bmatrix} F_{tc} \\ F_f \\ F_{rc} \end{Bmatrix} \tag{4.5}$$

Despite this model is widely used for dynamic forces prediction, due to the linear relation, it does not allow to take into account non linear phenomena that are characteristic of turning process. In particular the effect of tool nose radius on cutting force direction in neglected and, as demonstrated by Eynian [37], this lead to unacceptable errors in cutting force estimation Figure 4.12.

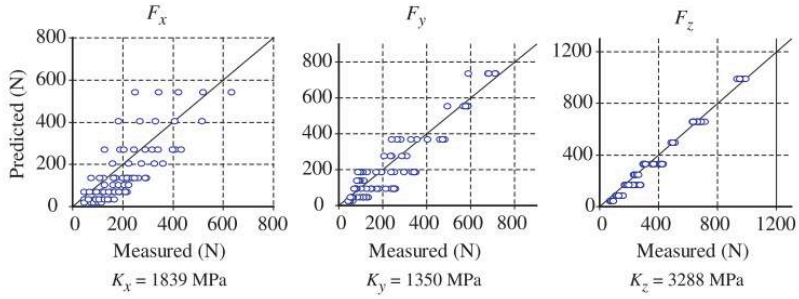

Figure 4.12. Cutting force inaccurate model [37]

The force can be more accurately modeled by dividing the chip into discrete zones or small discrete force elements [75][34].

Colwell [76] model allows to take into account tool nose radius by assuming chip flow direction perpendicular to the chord that connects intersection points of tool and workpiece. This direction is inclined of θ (chip flow angle) within feed direction (Figure 4.13).

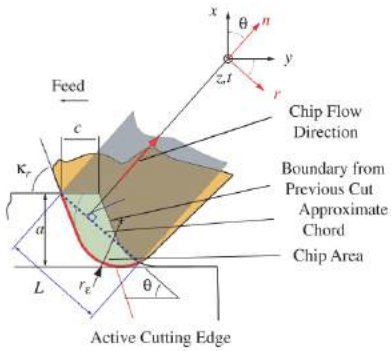

Figure 4.13. Chip flow direction according with Colwell assumption [76]

In order to estimate chip flow direction and cutting length a continuous function, able to estimate θ and L varying depth of cut and feed per tooth was implemented (equation from (4.3) to (4.5))

$$\theta = A * \text{atan}(B * b^n) \tag{4.3}$$

$$A = 2 * \psi/\pi \tag{4.4}$$

$$B = \frac{\tan\left(\frac{\pi}{4} - \frac{\pi}{4\psi} * \text{asin}\left(\frac{h}{2R}\right)\right)}{(R - R\cos\psi)^n} \tag{4.5}$$

In the proposed method, cutting force along cutting direction and in the plane xz may be expressed according with equation (4.6)

$$\begin{cases} F_c = K_{cA} * A + K_{cL} * L + K_{c0} \\ F_p = K_{pA} * A + K_{pL} * L + K_{p0} \end{cases} \tag{4.6}$$

Once F_c and F_p are known, cutting force component in the machine tool reference system may be expressed by means of chip flow angle θ.

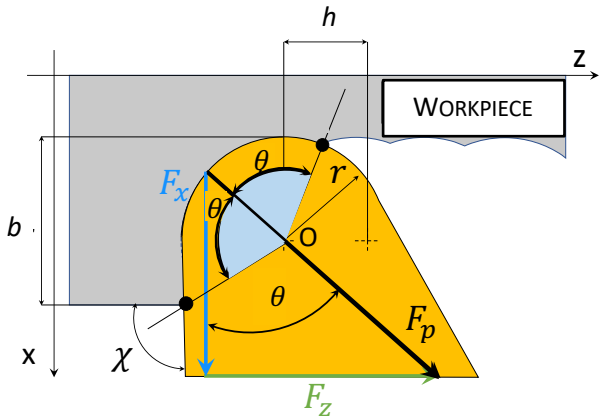

Figure 4.14: Cutting forces in xz plane

$$\begin{Bmatrix} F_x \\ F_y \\ F_z \end{Bmatrix} = \begin{bmatrix} K_{pA}\sin\theta & K_{pL}\sin\theta & K_{pA}\sin\theta \\ K_{p0}\cos\theta & K_{pL}\cos\theta & K_{pA}\cos\theta \\ K_{c0} & K_{cL} & K_{cA} \end{bmatrix} * \begin{bmatrix} 1 \\ L \\ A \end{bmatrix} \tag{4.7}$$

Experimental cutting tests were carried out in order to validate proposed method and to estimate cutting coefficients for given standard boring bar. A workpiece was mounted on the machine tool and machined on its inner surface. Cutting forces along the three directions shown in Figure 4.15 were measured by means of Kistler 9257A dynamometer.

a)

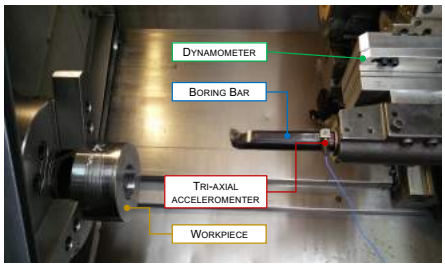

b)

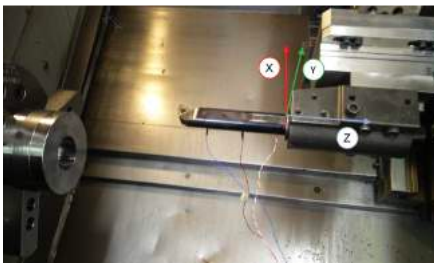

Figure 4.15: a) Experimental setup for cutting force measurement b) cutting force reference system

Forces were measured at 110 mm/min of cutting velocity, while radial depth of cut and feed per tooth are varied according with Table 4.2

Table 4.2: Cutting parameters

Radial depth of cut b [mm]	Cutting velocity v_c [mm/min]	Feed per revolution h [mm/rev]
0.1÷1	110	0.1÷0.4

Measured forces signal was elaborated in order to estimate mean cutting forces for each couple of cutting parameters. Then a bilinear optimization was carried out in order to estimate cutting coefficients.

Resultant cutting coefficients are reported in Table 4.3

Table 4.3: Estimated Cutting coefficients

K_{cA} [N/mm^2]	K_{cL} [N/mm]	K_{c0} [N]	K_{pA} [N/mm^2]	K_{pL} [N/mm]	K_{p0} [N]
2195.3	62.7	22.7	1052.5	85.4	38.7

Comparison between estimated and measured cutting forces along the three direction is shown in Figure 4.16

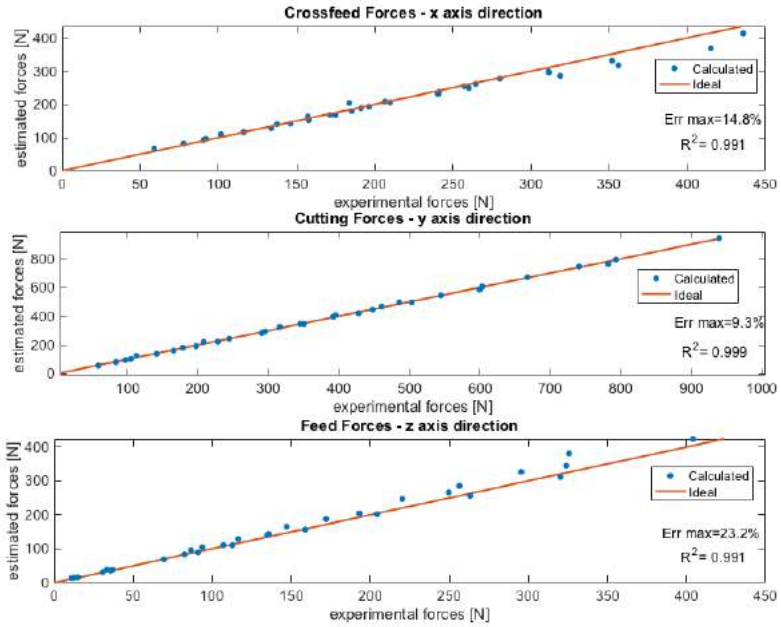

Figure 4.16: Comparison between experimental and estimated cutting forces

Comparison between estimated and experimental forces shows a good accordance. The model is able to globally reproduce the relation between forces and cutting parameters. Maximum error between experimental and numerical force is found to be on the feed force in

correspondence of the 0.1 mm of depth of cut and 0.4 mm of feed per tooth (23.2%) and in correspondence of 1.0 of depth of cut and 0.4 mm of feed per tooth. For what concern crossfeed cutting force, error is maximum in correspondence of 0.1 mm of depth of cut and 0.1 mm of feed per tooth (14.8%). For all the other cutting condition, error less than 10%.

4.2.4. Chatter prediction model

Once cutting force model was validated and cutting coefficient estimated, chatter prediction model was implemented.

Cutting force model presented in the previous paragraph highlights a relation between forces and displacements: in order to study machining stability, Eynian et al. [77] considers effects of tool displacement due to vibration on dynamic cutting forces assuming completely rigid workpiece in order to predict system stability for given cutting parameters. The same approach, adapted to the case of compliant workpiece and rigid tool was then applied. Cutting forces in machine tool reference system may be expressed as:

$$\{F_m(t)\} = [J]\{Q(t)\} + [J_\tau]\{Q(t-\tau)\} \tag{4.8}$$

Where J and J_τ are the direct and delay process gain matrices respectively (Eq. 14) while $\{Q(t)\}$ and $\{Q(t-\tau)\}$ are workpiece displacement vectors evaluated in correspondence of cutting point.

$$\left.\begin{aligned} J_{pq} &= \frac{\partial F_p}{\partial q} \\ J_{\tau_{pq}} &= \frac{\partial F_p}{\partial q_\tau} \end{aligned}\right\} \; where\; p,q = \{x,y,z\} \tag{4.9}$$

According with cutting force model presented in the previous paragraph:

$$\begin{aligned} \frac{\partial\{F_m\}}{\partial q} &= \frac{\partial}{\partial q}(rot * C_{nm} * [1 \quad L \quad A]') \\ &= rot * \frac{\partial C_{nm}}{\partial q} * [1 \quad L \quad A]' + rot * C_{nm} * \begin{bmatrix} 0 & \frac{\partial L}{\partial q} & \frac{\partial A}{\partial q} \end{bmatrix}' \end{aligned} \tag{4.10}$$

$$\frac{\partial C_{nm}}{\partial x} = \frac{\partial C_{nm}}{\partial \theta} * \frac{\partial \theta}{\partial q} = \begin{bmatrix} \cos\theta & \cos\theta & \cos\theta \\ -\sin\theta & -\sin\theta & -\sin\theta \\ 0 & 0 & 0 \end{bmatrix} * \frac{\partial \theta}{\partial q} \tag{4.11}$$

The same expression of $\partial\theta/\partial q$, $\partial A/\partial q$ and $\partial L/\partial q$ presented in [77] are considered.

Equation (4.8), that express dynamic cutting forces in the time domain, may be expressed in Laplace domain as:

$$\{F_m\} = (J + J_\tau e^{-\tau s}) * [\phi(s)] \tag{4.12}$$

And characteristic equation of the system results:

$$Ch(s) = ([I]_{3x3} + [J + J_\tau e^{-sT}]) * [\phi(s)] \tag{4.13}$$

Imaginary part of characteristic equation roots represents vibration frequency [rad/s], while real part is related to vibration damping: in particular, in case of positive real part, amplitude increases in the time domain and vibrations are unstable, while in case of negative real part vibration amplitude decreases and the machining is stable. Since the process gain

matrices (J and J_τ) and delay T are dependent on cutting parameters such as depth of cut, speed and feed, the direct stability lobes of the turning system cannot be identified by the matrix eigenvalue method of Altintas and Budak [78].

Due to the term $e^{-s\tau}$ term, characteristic equation has infinite number of roots that cannot be calculated analytically. In such cases, stability can be evaluated with Nyquist stability criterion. The presence of roots in a given domain is investigated calculating the value of the characteristic equation in all the points of a simple closed (clockwise oriented curve and containing the domain), and plotting them in the Nyquist plane.

By means of Cauchy argument (Eq. 19), is possible to correlate the number of poles P and the number of roots N in a given contour, with the number of clockwise encirclements of the origin E of the complex plot of the Nyquist diagram.

$$N = E + P \tag{4.14}$$

Since poles of characteristic equation are the poles of FRF matrix and are all stable (i.e. poles have negative real part), considering a contour that lays on the first and fourth quads, number of clockwise encirclements of the origin is the same of number of roots contained in the contour: eventual roots in such a contour have positive real part and then indicates that machining is unstable. For this reason stability can be evaluated considering a closed curve composed by a vertical line from $-j\infty$ to $+j\infty$ along imaginary axis, an half round circle with infinite radius from $+j\infty$ to $-j\infty$.

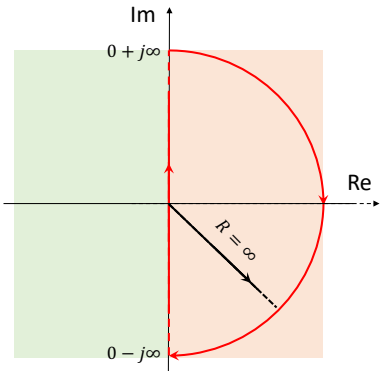

Figure 4.17: Nyquist Contour

However, in case of chatter prediction, range of interest is limited to the frequency range in which dominant mode of the structure are present[26]. For this reason, instead of evaluating the whole positive real part roots domain, the contour can be limited to (j0,+jω_{max}) interval that contains all dominant mode. In order to make the evaluation of number of encirclements easier, research of roots can be focused: for each relevant peak, a frequency range $j(\omega_i-\delta,\omega_i+\delta)$ around its frequency ω_i, is chosen and a close contour is created and mapped. δ is chosen as 0.4 of the minimum difference between two close natural frequencies, where real part is variated between 0 and 10 (that is several order higher than typical value in case of chatter). In case of instability, chatter frequency can be assumed around considered natural frequencies. An example is reported in (Figure 4.18): on the left two contours around two dominant frequencies are created: as showed the red one contains a roots. Nyquist plot of the closed curve around the lower frequency, that does not contain any roots, does not encircles the origin, while the second one, that contains a root, encircles the origin.

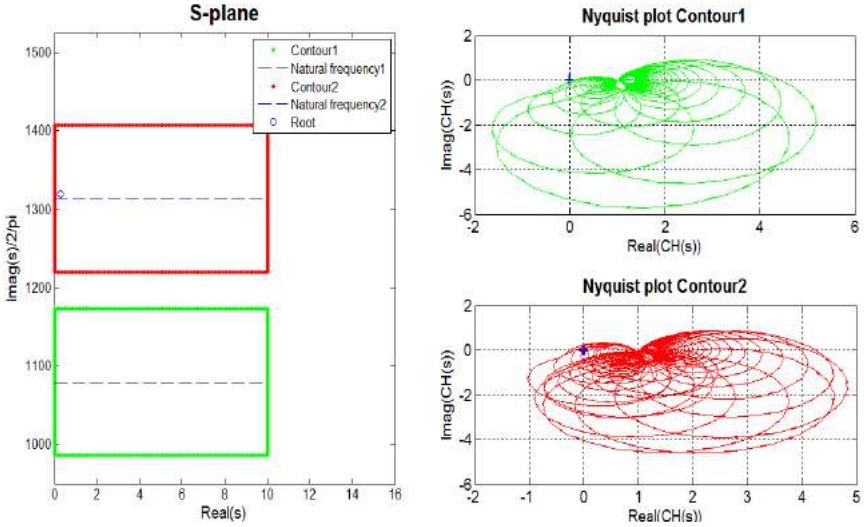

Figure 4.18: a) Modified contour considering in case of two dominant peaks b) CH Nyquist plot considering contour 1 (stable) c) CH Nyquist plot considering contour 2 (chatter)

4.3. Algorithm implementation and numerical validation

The whole algorithm, described in Section 4.2, was used to find suitable supports configurations of an Inconel 781 thin wall component (Figure 4.19) which shape is similar to the one of combustor baffle.

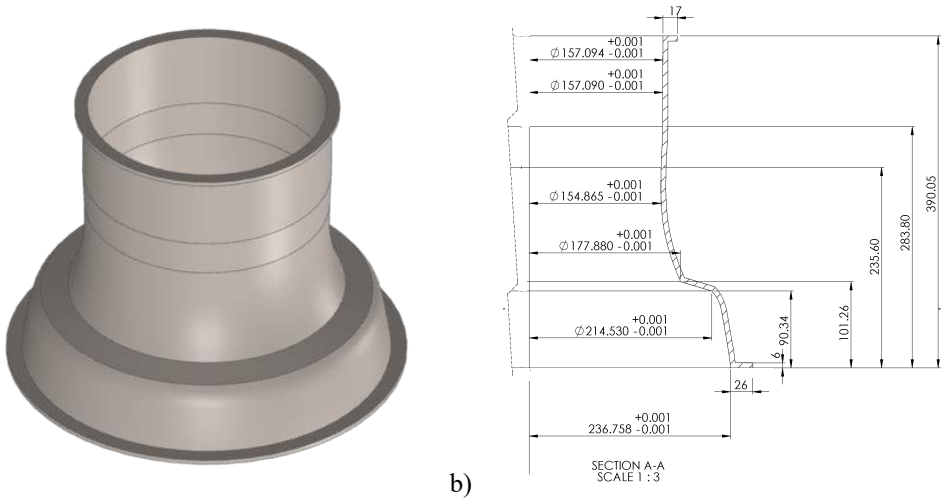

a) b)

Figure 4.19. Test case a) 3D geometry b) 2D section

Workpiece material properties are summarized in Table 4.4.

Table 4.4. Workpiece material properties

Young Modulus (MPa)	Poisson Ratio	Density (kg/m3)	Damping
2.0E5	*0.31*	*7850*	*0.03*

The workpiece is considered to be clamped by means of a flange joint to the workholding plate by means of 24 screws and supposed to be machined on the external surface according with the toolpath shown in Figure 4.20 with a CNMG 12 04 08-23 1105 tool which characteristics are summarized in Table 4.5.

Table 4.5. Cutting and insert parameters

Cutting parameters		
Cutting speed [m/min]	Depth of cut [mm]	Feed [mm/rev]
80	0.4	0.1
Insert parameters		
Tool nose radius [mm]	Rake angle [°]	Coating
0.8	-13	PVD-TiAlN

Workpiece is required to be machined guaranteeing a tolerance of 0.001 on the thickness along the whole toolpath.

Moreover supports are supposed to not be mountable out of the area indicated in Figure 4.20.

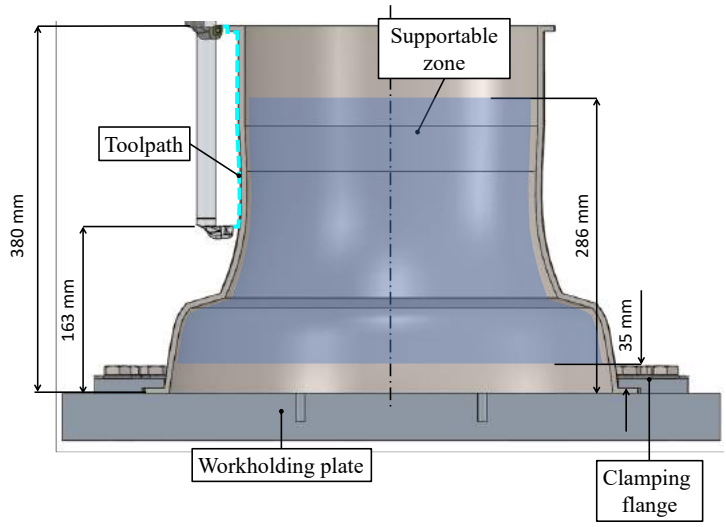

Figure 4.20. Workpiece holding and toolpath

The area in correspondence of the flange is considered to be fully constrained (all degrees of freedom blocked). In Figure 4.21 are reported all the steps for workpiece model creation. Workpiece nodes position is expressed in the machine tool reference system.

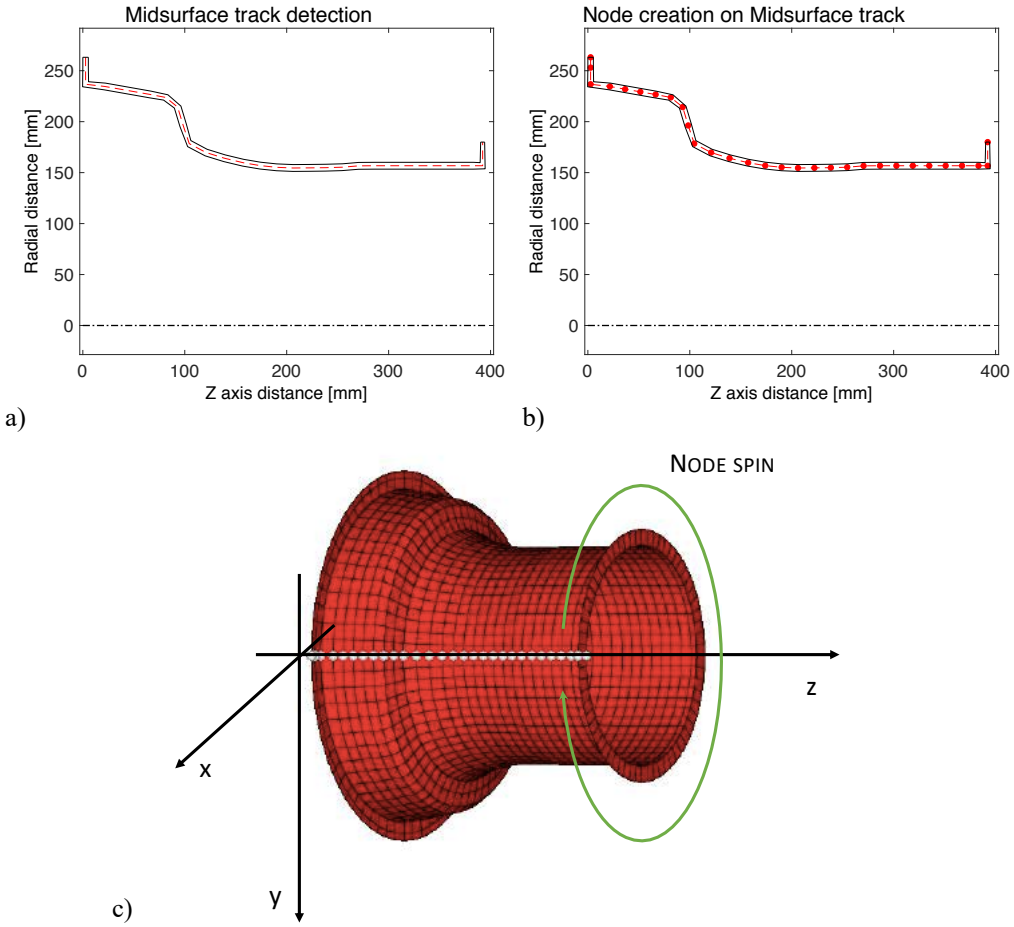

Figure 4.21. Workpiece model creation: a) midsurface track detection b) nodes on midsurface track creation c) nodes spinning and elements creation

Presented model is composed by 64 nodes in the circumferential direction and 30 in the axial direction (1920 nodes altogether).

The toolpath is acquired as a text file in which sub sequential tool position are expressed in the machine tool reference system.

Since, it was not possible to experimentally estimate cutting coefficients, measured cutting forces presented by Yao et al. [8] were considered to estimate cutting coefficients.

Table 4.6: Experimental cutting forces [8]

Cutting velocity [m/mm]	Depth of cut [mm]	Feed per revolution [mm/rev]	CrossFeed Forces (Fx) [N]	Cutting Forces (Fy) [N]	Feed Forces (Fz) [N]
40	0.2	0.1	44	101	118
40	0.4	0.15	115	251	209
40	0.6	0.2	198	440	283
40	0.8	0.25	290	675	344
50	0.2	0.15	55	124	160
50	0.4	0.1	104	171	186
50	0.6	0.25	204	496	320
50	0.8	0.2	277	558	322
60	0.2	0.2	63	151	198
60	0.4	0.25	134	333	284
60	0.6	0.1	173	243	238
60	0.8	0.15	265	439	301
70	0.2	0.25	66	166	223
70	0.4	0.2	135	274	276
70	0.6	0.15	194	319	289
70	0.8	0.1	254	321	285

Resultant coefficients were showed in Table 4.7, while comparison between experimental and estimated force is shown in Figure 4.22.

Table 4.7: Cutting coefficients for Inconel 718

K_{cA} [N/mm$_2$]	K_{cL} [N/mm]	K_{c0} [N]	K_{pA} [N/mm$_2$]	K_{pL} [N/mm]	K_{p0} [N]
2195.3	62.7	22.7	1052.5	85.4	38.7

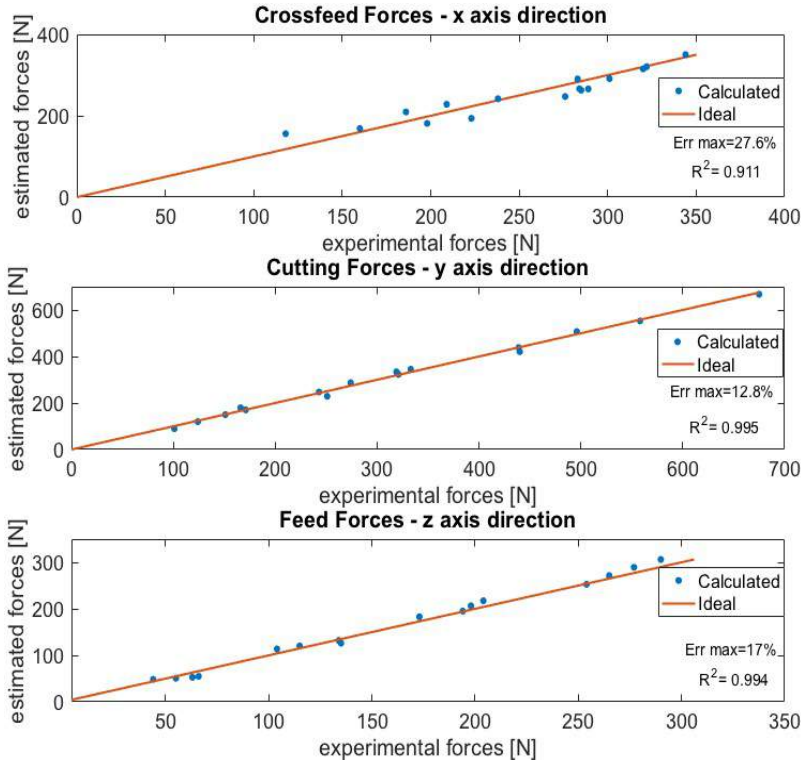

Figure 4.22 - Cutting forces: comparison between experimental data [8] **and numerical estimation**

Predicted forces along cutting velocity and along feed direction are very close to experimental one (maximum error is -13.7% and 17.3% respectively). In case of normal to feed direction forces, results appear more scattered and maximum error is slightly higher (27.6%).

Results of static and dynamic analysis in case of no additional supports highlights how the clamping system is not able to effectively support the workpiece during machining. Indeed, how shown in Figure 4.22, where local geometrical error and chatter stability is evaluated in each node intercepted by the toolpath, geometrical error exceeds tolerance in the upper part of the component. In particular, maximum error on the thickness is 0.014 mm.

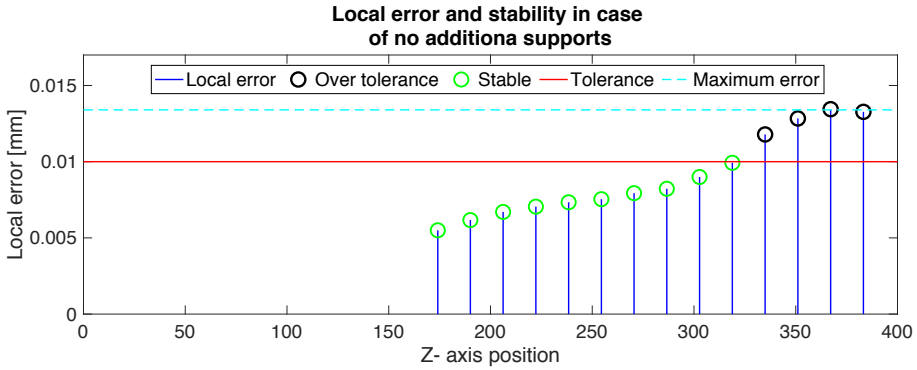

Figure 4.22. Local error and chatter stability varying tool position in case of no additional supports

According with needs to reduce computational costs, chatters stability is evaluated only in correspondence of the nodes in which geometrical error is lower than tolerance.

In order to guarantee a proper contact between supports and workpiece surface, supports and workpiece surface should be parallel. As a consequence, for each support position, contact direction is assumed parallel to the normal to the workpiece surface (Figure 4.23).

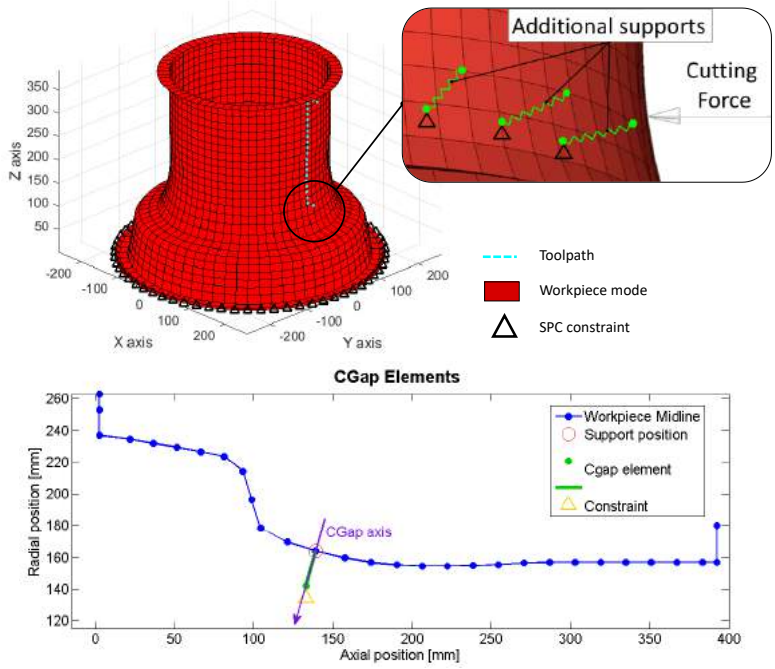

Figure 4.23. Support model

The procedure evaluated different configurations considering all the node in correspondence of each support axial position supported (i.e. one CGAP element for each node on the section). For each configuration, maximum error along the toolpath was compared with tolerance in order to detect the suitable supports positions. As shown in Figure 4.24 placing supports at a distance less than 98 mm from the workpiece holder is ineffective (red zone in Figure 4.24).

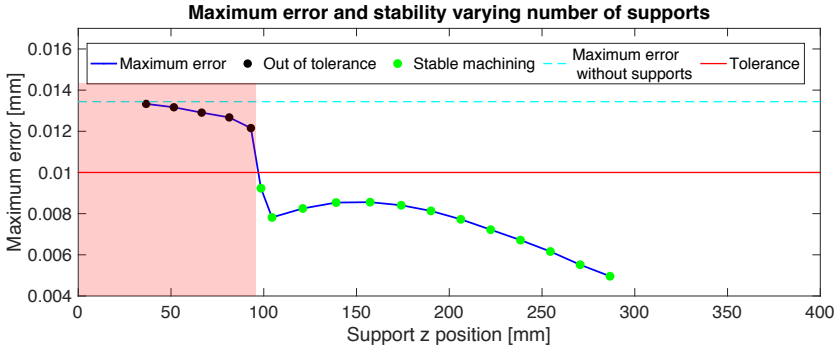

Figure 4.24. Maximum error varying support axial position

Algorithm for support minimum number detection was then implemented considering found reduced domain. In order to reduce the number of required simulations, for each configuration, workpiece static and dynamic response is evaluated in the most compliant circumferential position, that is in correspondence of the middle position between two supports Figure 4.25.

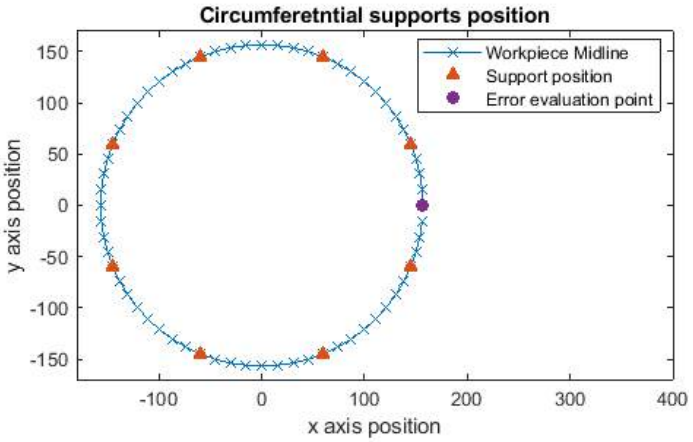

Figure 4.25: Circumferential position of nodes in correspondence of whom static and dyanamic workpiece response is evaluated

Results for each evaluated configurations are presented in Figure 4.26.

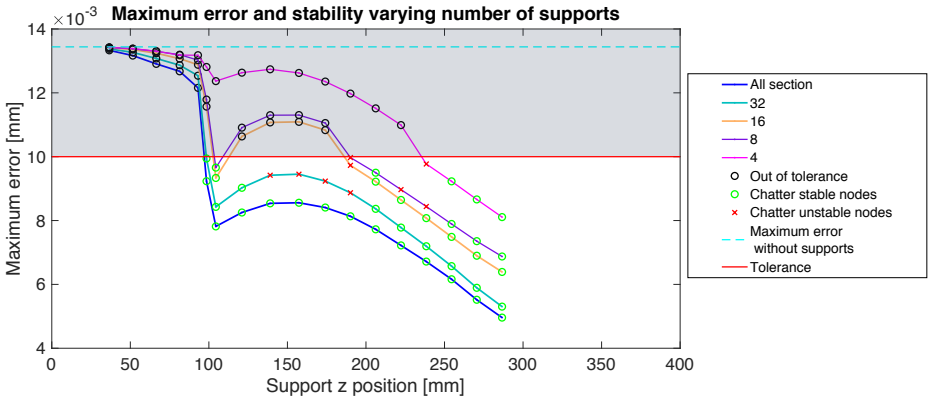

Figure 4.26. Analysis results varying supports position and number

For this application one suitable position for support positioning was to place 8 supports at a distance of around 104 mm from the workpiece holder. Indeed, this solution allows to reduce maximum geometrical error of around 32.8% by using 8 supports placed in a favorable position for mounting. A suitable configuration is presented in Figure 4.27.

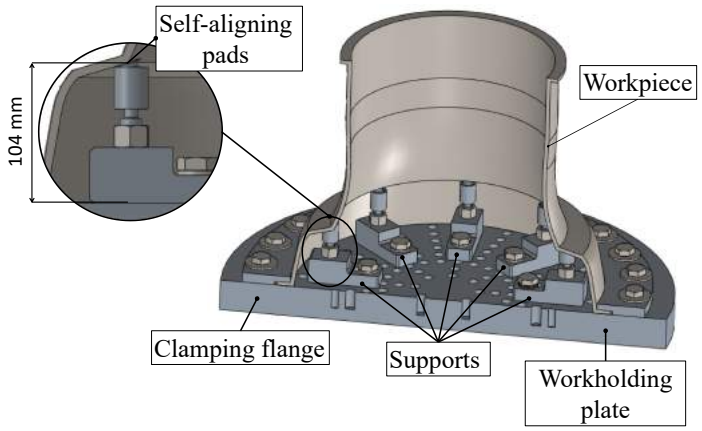

Figure 4.27. Proposed solution for supports

The paper presents a general methodology for optimal semi-finished stock geometry and supports placing in case of thin walled component turning adaptable to different workpiece geometries and cutting condition. Starting from workpiece geometry and toolpath, by means of a FE model for geometrical errors evaluation, stock allowance thickness is varied in order to reduce geometrical error and avoid chatter, guaranteeing machinability. In case of infeasibility, optimal supports configuration is found as the one that guarantees tolerance required with minimum number of supports. Proposed method was applied for a Inconel component external turning to find the configuration that guarantee a tolerance of 0.01 mm. For given stock geometry and in case of no additional supports, maximum predicted error was out of tolerance and unstable: acting on stock allowance thickness, it was possible to guarantee tolerance but machining was still unstable. Using 12 supports at a distance of 280

mm from the clamping section, maximum error is reduced of about 35%, tolerance are respected and machining is predicted to be completely stable along toolpath. The employment of this kind of method, gives an aim to supports design, avoiding time-consuming trial and error approaches. Accuracy of the proposed methodology is strictly related to workpiece and cutting force model. Experimental tests are planned to be carried out in order to validate workpiece FE model and prove the effectiveness of the entire approach.

5. Tuned Mass Damper for chatter mitigation

The second part of the Ph.D. activity was focused on the develop of solution able to increasing productivity in thin wall components turning. In particular, in this section a passive approach for chatter mitigation is presented.

Like in case of machining with slender tools, in case of thin wall component machining both active and passive techniques may be employed to improve the cutting system chatter stability. Since the most critical elements of the cutting system is the workpiece passive or active devices should be installed on the component in order to effectively change the cutting system response. However, in case of turning process, where the component rotates during machining, the employ of active devices installed on the workpiece, is complicated due to necessity to provide them energy. For this reason, the investigation on possible solution for chatter mitigation was limited to passive techniques. In particular, as discussed in Chapter 2, Tuned Mass Dampers (TMDs) were demonstrated to represent a good compromise between costs and effectiveness for chatter issues. However due to the more complicated design process and the no – retrofitability, their use in industrial field is still very limited. The aim of this activity is to develop a model strategy able to support TMD design for chatter mitigation in thin wall component turning.

Among the years several tuned mass damper typologies were proposed and used to overcome vibration issues in several field (i.e. seismic, mechanical and manufacturing).

The physical principle and the different typologies of TMDs are shown in Figure 5.1.

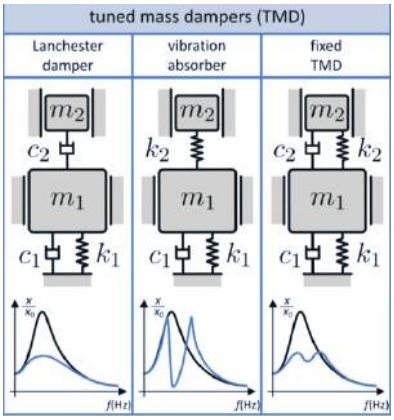

Figure 5.1. Auxiliary passive devices [38]

As shown in Figure 5.1 these devices can be schematized as 1 Dof system characterized by an inertial mass m_2, a linear spring with k_2 stiffness and a damper with c_2 damping coefficients. Once attached to a system (schematized in Figure 5.1 with a mass m_1, a spring k_1 and a damper c_1), if correctly designed, they can change component FRF in correspondence of dominant mode [79]. In particular, fixed TMDs allows to switch dominant peak into two peaks with less amplitude.

Tuning a TMDs means find the most effective TMDs geometrical and mechanical property in order to significantly shoot down the peak correspondent at the most critical component mode. Non - dimensional parameters, reported in Eq (4.1) to Eq (4.6) are usually used to characterize both tuned mass dampers and the structure on which they are installed.

$$\mu = \frac{m_2}{m_1} \tag{5.1}$$

$$\omega_1 = \sqrt{\frac{k_1}{m_1}} \tag{5.2}$$

$$\omega_2 = \sqrt{\frac{k_2}{m_2}} \tag{5.3}$$

$$f = \frac{\omega_2}{\omega_1} \tag{5.4}$$

$$\zeta_1 = \frac{c_1}{2\sqrt{k_1 m_1}} \tag{5.5}$$

$$\zeta_2 = \frac{c_2}{2\sqrt{k_2 m_2}} \tag{5.6}$$

Mass ratio μ is the ratio between TMD and structure mass, ω_1 and ω_2 are structure and TMD modal frequency respectively, ζ_1 and ζ_2 are their damping ratio and f is the ratio between TMD and structure natural frequency.

Hartog [79] proposed an analytical approach, using a 2 dofs model, to estimate f that allows to switch the amplitude peak into two equal peaks of equal magnitude in the magnitude frequency response function.

According with chatter prediction models, chatter stability limit (i.e. maximum depth of cut that gives stable machining at all spindle speeds), is inversely proportional to the maximum negative value of the real part of the FRF. Then, Sims [41] developed an analytical approach for TMD tuning in order to produce two equal peaks or troughs in the real part of the FRF. Experimental results on a milling operation highlighted how this approach was more effective than the one proposed by Hartog (Figure 5.2).

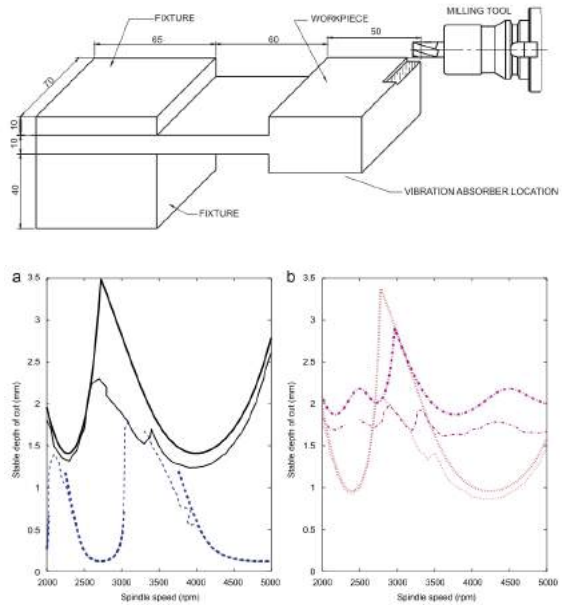

Figure 5.2. Sims [41] **experimental tests a) experimental setup b) predicted and experimental diagram stability lobes**

Although this method is demonstrated to be more effective for chatter mitigation, the main limit of this approach is the assumption that the main structure is assumed to have a single undamped mode of vibration and the effect of only a TMD is considered. According with the analysis presented in [80], the use of Multiple Tuned Mass Dampers (MTMDs) each one properly tuned to damp a specific mode, it is more effective than a single TMD having the same mass ratio. Then, Yang et al. [42] proposed design and optimization strategy extending the procedure proposed by Sims to MTMDs in order to more effectively mitigate chatter. The effectiveness of proposed method was experimentally demonstrated on a specially designed fixture of a CNC turning (Figure 5.3). In this case, tuned mass dampers are designed to effectively damp tool vibration and have different values of f and ζ_2.

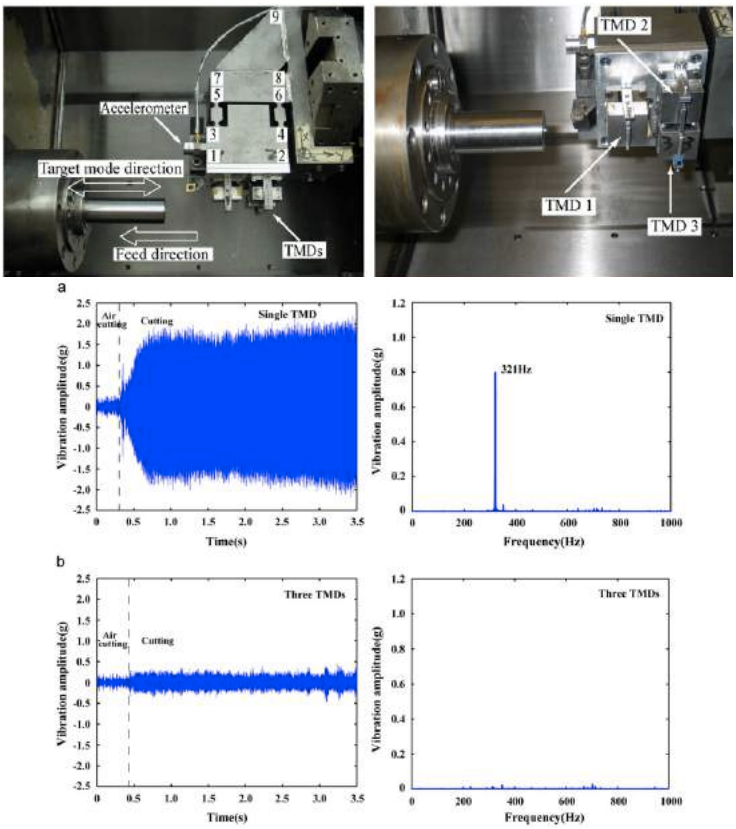

Figure 5.3. Experimental tests [42] **a) experimental setup b) results with single TMD c) results with three TMDs**

In milling, the effect of multiple dynamic absorbers mounted on the tool and having an identical mass, damping ratio, and natural frequency were investigated analytically and experimentally [44].

In the last years, the attention on TMDs optimization for chatter mitigation was focused on the improvement of models in order to more accurately predict the effect of TMDs on chatter stability and makes this approaches more general. Rubio et al. [43] proposed an optimization strategy for optimal tuning of a TMD attached at a generic section of a boring. The boring bar was modeled as an Euler–Bernoulli cantilever beam and only its first mode of vibration was taken into account. Position of TMD was chosen in correspondence of the largest displacements for the critical mode, where equivalent modal mass is lower and then required mass can be reduced for the same mass ratio.

The employ of more sophisticated techniques for component modelling, like receptance coupling, allowed to evaluate the influence of TMD position on absolute value of negative peak in real part, varying its parameters and position as presented in [45] in case of slender boring bar machining.

Despite several approaches for optimal tuning were presented in literature for tool chatter, the state of the art on TMDs applied on high compliance workpiece still presents

certain deficiencies. This lack is due to the fact that chatter frequency may significantly change during machining due to local workpiece stiffness and material removed [29].

Since the aim of this task is to develop a model based strategy for TMDs placing and tuning, the first step is the creation and validation of a suitable model able to predict the effect of TMDs on workpiece component. The standard procedure for TMDs design involves the following steps:

i) Workpiece dynamic characterization by means of experimental tests
ii) Chatter tests for chatter frequency and correspondent workpiece mode shape detection
iii) TMD positioning in correspondence of anti nodes of workpiece mode shape
iv) TMDs design and manufacturing
v) Cutting tests for asses the improvement in chatter stability

This procedure is the most robust for TMDs design, since it is based on experimental results, but, in order to consider the stiffness variation and the effect of material removal, it requires several experimental tests. On the other side the design strategies based on predictive models are not accured enough to be applied to complex workpiece geometries.

The employment of FE modelling approaches support TMDs design in phase i), ii) and in phase iii). Compared with the experimental approaches, it allows to simply taking into account the stiffness variation along workpiece axis and the effect of material removal. Moreover, workpiece model may be interfaced with a chatter prediction model in order to estimate the initial chatter stability and the improvement given by TMDs.

The challenges in doing this are related to the difficulty of creating an accurate and computational efficient model for dynamics prediction.

In the first part of the activity a standard experimental procedure for TMDs design, while in the second one a FE approach was exploited for phase i), iii) (section 4.1), and iv) (section 4.2). In the second part a suitable TMD model was developed in order to create an approach for TMDs positioning.

5.1. TMDs design experimental procedure

As a test case a cylindrical thin walled is AISI304 workpiece, which dimensions are reported in Figure 5.4 was considered.

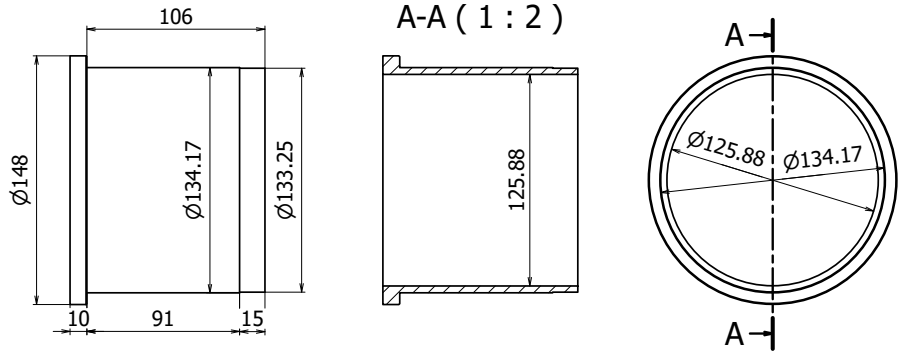

Figure 5.4. Test case geometry

In order to guarantee axisymmetric constraint and create a clamping condition that does not causes radial deformation on the workpiece, a workholding consisting on a plate and a ring assembled as shown in Figure 5.5 was designed. The plate is fixed to the machine spindle by means of four screws, while the ring is jointed to the plate tightening the workpiece by friction.

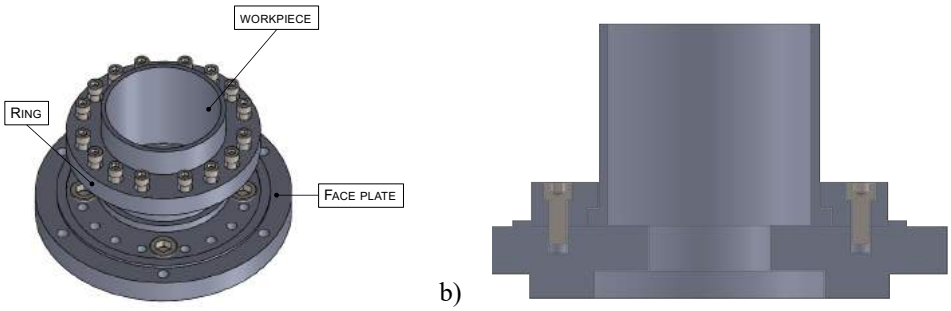

Figure 5.5. Clamping system a) elements b) clamping configuration

Workpiece dynamic characterization was carried out by means of experimental modal analysis performed via impact testing on workpiece mounted on the lathe: in order to reduce the number of experiments and sensors needed, the roving hammer technique was preferred [81]. Monoaxial accelerometer (Ono sokki, NP-2106) was placed in correspondence of point 1 in order to measure radial displacement due to impulsive radial forces applied, from time to time, in points numbered from 1 to 18 (Figure 5.6) by means of an impact hammer (PCB, 086C03).

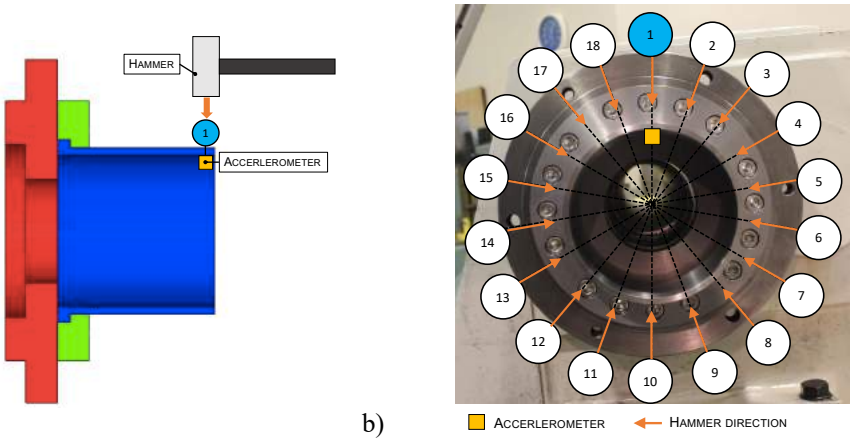

Figure 5.6. Experimental setup a) accelerometer axial position b) hammering points

Experimental results highlights a dominant trilobated mode at a frequency of 2240 Hz (Figure 5.7)

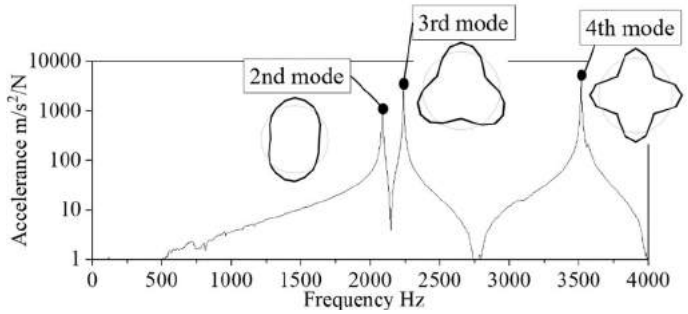

Figure 5.7. Experimental direct FRF along radial direction and correspondent mode shapes

Chatter tests were then carried out in order to detect unstable cutting parameters, chatter frequency and correspondent workpiece mode shape.

In order to measure the workpiece vibration mode in the radial direction during the chatter generation, six eddy current sensors (PU-05, Applied Electronics Corporation) were arranged at a regular pitch of 20 degrees in the radial direction of the workpiece as shown in Fig. 3(a).

a)

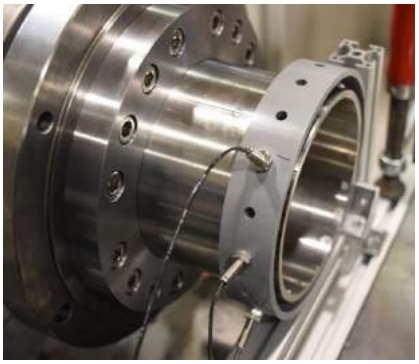

b)

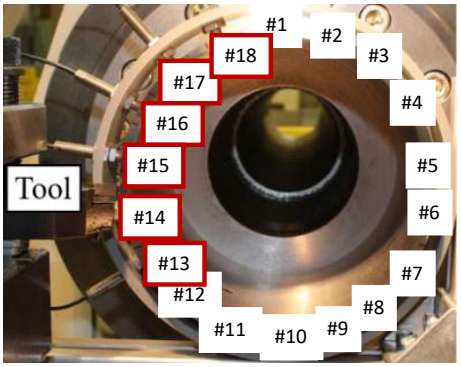

Figure 5.8: Experimental setup

The sensors were positioned 30 mm in the axial direction from the tool. The vibration displacements of measuring points from #13 to #18 in Fig. 3(b) were measured by six eddy current sensors. The vibration displacements in the points from #1 to #12 in Fig. 3(b) were predicted by interpolating considering the symmetry of the workpiece vibration mode. Fig. 3(b) shows the predicted vibration mode of the workpiece during the chatter generation.

Cutting tests were carried out considering a longitudinal turning process. Chatter onset was detected in correspondence of parameters reported Table 5.1.

Table 5.1: Selected cutting parameters

Cutting speed [m/min]	Feed rate [mm/rev]	Depth of cut [mm]

150	0.05	0.025

Chatter frequency was found to be 2230 Hz, close to the tri lobate workpiece modal shape. Vibration radial displacements of the workpiece during chatter are reported in Figure 5.9.

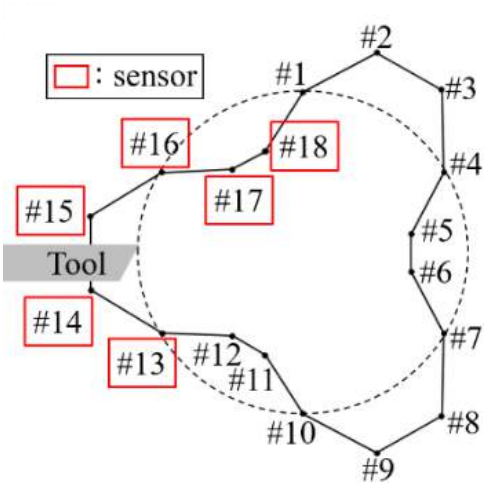

Figure 5.9: Chatter vibration mode of the workpiece

Experimental tests confirm that chatter onset due to workpiece chatter and that the most critical mode shape is the dominant one. For this reason, the aim of TMDs design was to damp workpiece vibrations, considering the chatter frequency as the target frequency. As demonstrate in [82], placing TMDs in correspondent of highest displacement for mode to be damped allows to minimize their mass. Then, TMDs were placed at the free end of the component. In this phase the damping effect was focused on a single mode and all the TMDs were considered having the same dimensions.

One of the most simple way to realize a TMD is by means of cantilever beam attached to the main structure inserting a compliant and damping material between them [83]. For selected case, a NICETACK™ double side adhesive was selected. Its dimensions and composition are reported in **Error! Reference source not found.**.

To be effective, the frequency correspond to its dominant mode once attached, should be as close as possible to the frequency of the vibration to be damped. Then the target frequency was set to 2230. Shape was selected in order to guarantee a correct contact between TMDs and workpiece that is, in case of cylindrical components, the one showed in Figure 5.21, while TMD dimensions are then variated until this condition was verified. TMD mass was fixed in order to guarantee a mass ratio of 1.5%, while length is varied until the length that guarantees the desired natural frequency is found. This procedure is usually carried out by means of analytical approaches, considering a cantilever beam constrained on one side and free on the other one. Since these approaches are not accurate in predicting the natural frequency of the beam while attached to the component by means of the double side tape, free length of the TMD is set according with experimental results.

A TMD, which dimensions are showed in Figure 5.10, was found to be the optimal compromise between mass ratio and damping effectiveness of system response.

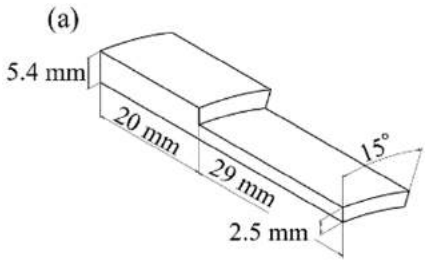

Figure 5.10: TMD dimensions

Experimental results confirm that natural frequency of the TMD is quite close the target frequency. The effect of the presence of the double side tape on the TMD FRF is highlighted on Figure 5.11

a) 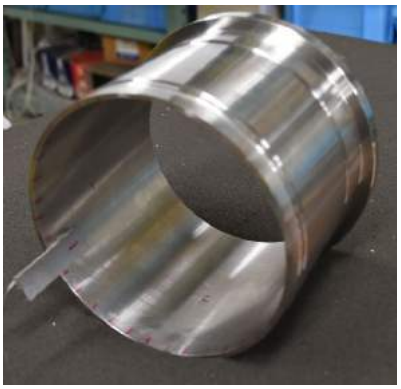 b) 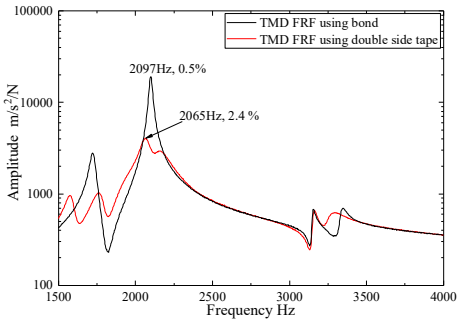

Figure 5.11: Experimental FRF of TMD once attached on the workpiece a) experimental setup b) measured FRF in case of bond (black line) and double side tape (red line)

The effect of TMDs on workpiece was validated by means of experimental modal analysis. According with [82] the most effective configuration for TMDs placing consist in placing TMDs in correspondence of the anti nodes (i.e. the position in which modal shape has the higher displacements). In case of tri-lobate modes, at least three TMDs are then necessary. The effect of the TMDs on the workpiece FRF was investigated. At first the effect of double side tape was exanimated by comparing the case of cantilever beam rigidly attached to the workpiece and the case double side tape is interposed between beam and workpiece. According with measured direct FRF showed in Figure 5.21 the effect of cantilever beam is that the dominant peaks are switched into two peaks. However the damping effect is very poor and the amplitude of the new peak is comparable with the original peak amplitude. As a consequence an additional damping effect is necessary. In case of beam attached with double side tape the damping effect drastically reduce the maximum peak amplitude of the workpiece FRF.

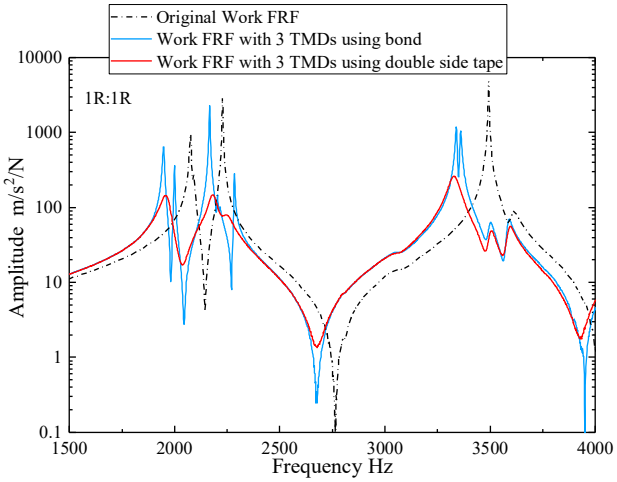

Figure 5.12: Effect of the double side tape on workpiece FRF

The effect of the number of TMDs on the workpiece response was investigated by means of experimental modal analysis starting with one TMD and increasing the number of TMDs until 4. Results in terms of radial direct FRF in correspondence of the driving point (identified by DP in Figure 5.13) are shown in inFigure 5.14.

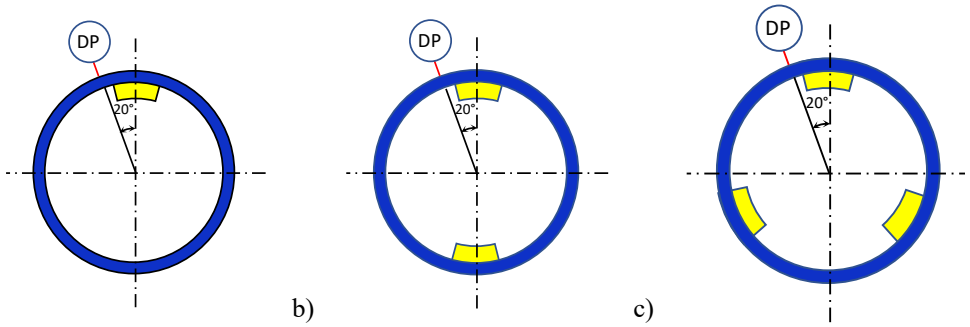

a) b) c)

Figure 5.13: Evaluated configurations

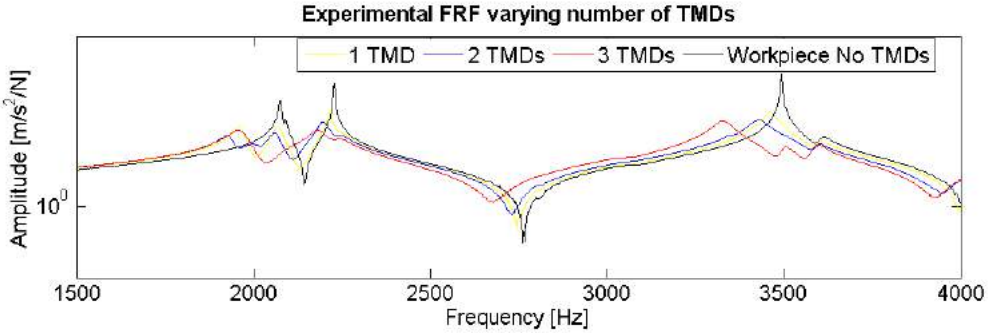

Figure 5.14: Experimental workpiece FRF varying number of TMDs

The damping effect increases with the number of TMD.

Once the configuration with three TMDs was demonstrated effectively reduce workpiece peak amplitude, cutting tests were repeated with the same cutting parameters considered in the preliminary test on the workpiece equipped with three TMDs.

In order to highlight the contribute of the TMD on machining stability, cutting tests were carried out both in case of 3 TMD attached to the workpiece and in case of three masses (with the same mass ratio of TMDs). Results in terms of workpiece displacement during cutting tests are presented in Figure 5.15.

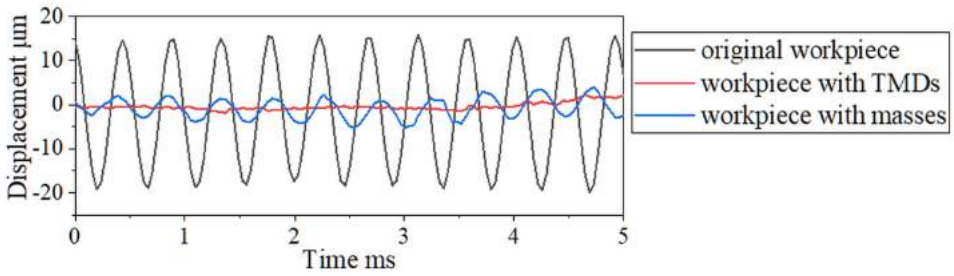

Figure 5.15: Workpiece displacement during cutting tests

In case of TMDs, the damping effect results more accentuated than in case of masses. This confirm that the damping effect is strongly influenced by TMDs dynamic behavior. Moreover, while in case of no additional TMDs, chatter onset is testified by a poor surface quality in correspondence of the cut surface (Figure 5.16), in case of three TMDs attached to the workpiece the surface has no longer has chatter marks Figure 5.16.

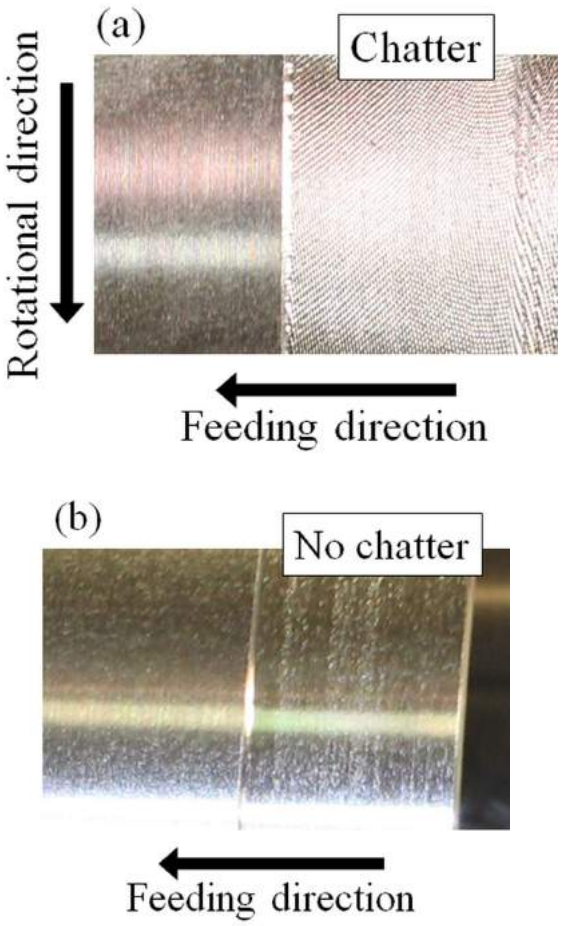

Figure 5.16: a) chatter marks in case of no TMD attached b) stable machining in case of 3 TMDs attached

In the first part of this work, the effect of the TMDs on mode coupling chatter in the turning process of a thin-walled cylindrical workpiece was experimentally investigated. It was confirmed that the chatter vibration mode of the workpiece was the circumferential vibration mode with three nodal diameters by measuring the vibration of the workpiece during the chatter generation using six eddy current sensors. According to the measured chatter vibration mode of the workpiece, three TMDs were attached to three anti-node positions of the third mode of the workpiece. A turning process test verified experimentally that mode coupling chatter was completely suppressed by the proposed TMDs. Mode coupling chatter could be suppressed even if the damping of the TMD was small and the total mass of three TMDs was less than 4.5 % of the mass of the cylindrical workpiece.

5.2. TMDs model

Since the employment of TMDs was experimentally demonstrated to be effective for chatter reduction, a modelling approach was developed in order to effectively support TMDs design. The advantages of using a modelling approach are various:

i) Component stiffness variation may be easily taken into account without requiring several experimental tests (including cutting tests)
ii) Easiness of evaluating several geometrical shapes and configuration in order to find the most effective one

In order to develop a robust model to evaluate TMD effect on workpiece dynamics and on chatter onset, the first step is create and validate workpiece model. For this purpose a FE approach, using MSC Nastran® solver, was chosen.

Workpiece material (AISI304 stainless steel) was previously characterized by means of experimental tests. Mechanical parameters are reported in Table 5.2

Table 5.2. Workpiece material parameters

Young Modulus (MPa)	Poisson Ratio	Density (kg/m3)	Structural damping
1.93E5	*0.3*	*7930*	*0.012*

Then, next step was to model the workpiece when fixed to the lathe. In order to accurately model workpiece dynamic response, the clamping system elements where included in the model

In order to accurately model the clamping system and the clamping system (Figure 5.17a), the face plate, the ring mount and the workpiece were modeled according with Figure 5.17b. The geometry of the plate and the ring was simplified, whiteout significant loss in accuracy, in order to facilitate mesh process and decrease the number of nodes. Each component is modeled using solid elements (CHEXA and CPENTA Nastran® elements).

a) 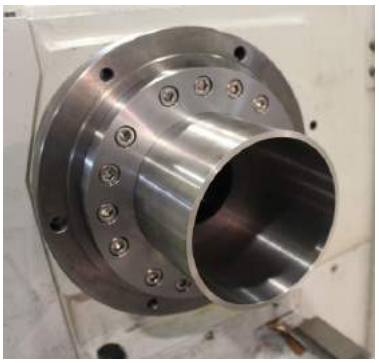

b) 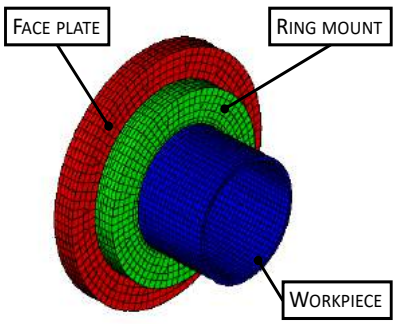

Figure 5.17. a) Workpiece fixed to the lathe b) workpiece model

The face place was supposed to be completely constrained (all dofs blocked) in correspondence of the joint screws (Figure 5.19c) in order to simulate the fixturing on the lathe spindle. The machine tool compliance is then neglected.

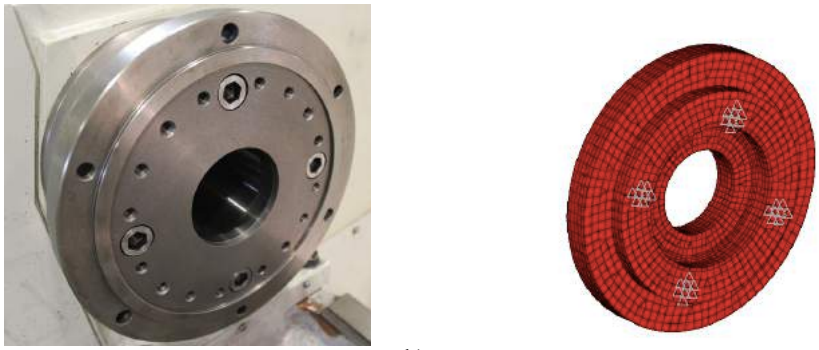

a) b)

Figure 5.18. a) Plate mounted on the lathe b) Plate model

Nodes marked with blue and yellow in Figure 5.19b are assumed to be shared between ring and plate and between ring and workpiece respectively in order to simulate the contact. This modelling techniques allows to simulate the contact between components in linear analysis.

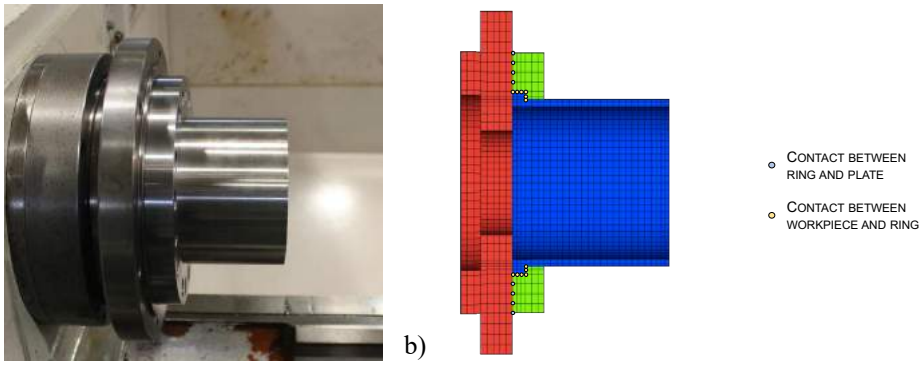

a) b)

Figure 5.19. a) Workpiece mounted on the lathe b) workpiece model

Workpiece dynamic response was then carried out by using a linear modal analysis (SOL 103 in Nastran®) for mode shape estimation and a modal frequency response (SOL 111 in Nastran®) to calculate FRF.

By means of a model updating procedure, material parameter for plate gray iron (Gray cast iron ISO185/JL/300) and ring (Carbon steel ISO C45) ring were estimated (Table 5.3: Gray iron and C45 parameters).

Table 5.3: Gray iron and C45 parameters

Gray Iron

Young Modulus (MPa)	**Poisson Ratio**	**Density (kg/m3)**	**Structural damping**
0.981E5	*0.26*	*7300*	*0.0084*
C45			
Young Modulus (MPa)	**Poisson Ratio**	**Density (kg/m3)**	**Structural damping**
2.05E5	*0.25*	*7840*	*0.002*

The correlation results after model updating (i.e. plate and ring material) are summarized in Table 5.4, while comparison between experimental and numerical direct FRF along radial direction in the driving point is shown in Figure 5.20Figure 5.20.

Table 5.4: Correlation results after FE model validation in the workpiece mounted on the lathe

Mode n°	**Natural frequency [Hz]**		**Error [%]**
	Experimental	**Numerical**	
1	2022	1891	-6.48%
2	2038	2030	-0.39%
3	2383	2397	0.59%
4	3560	3263	-8.34%
5	3895	3937	1.08%
6	4207	4134	-1.74%

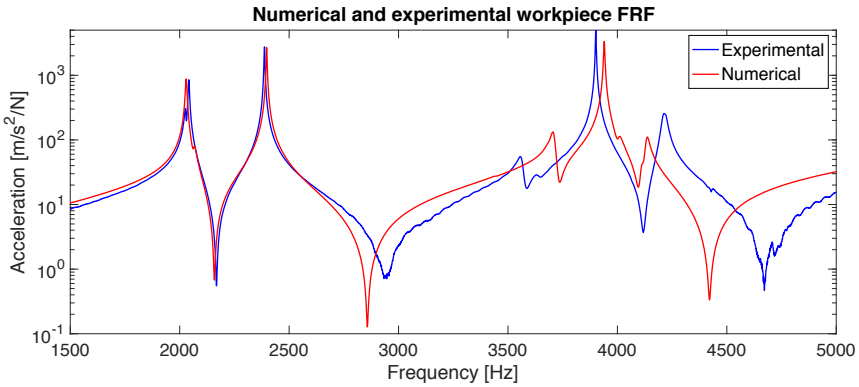

Figure 5.20: Comparison between numerical and experimental workpiece FRF

The difference, in terms of frequency of the dominant peak, is -8.34%.

The next step was to correctly model the TMDs and their effect on workpiece response.

In order to take into account the effect of both damping layer and tuned mass dampers, this two component were modeled by means of solid element (CHEXA Nastran® element) Figure 5.21. connection between TMD and double side tape was realized by node equivalence, while connection between double side tape and component was modeled by

means of glued contact feature in Nastran®. This solution was preferred due to the need of having different dimension element in the double side tape and workpiece.

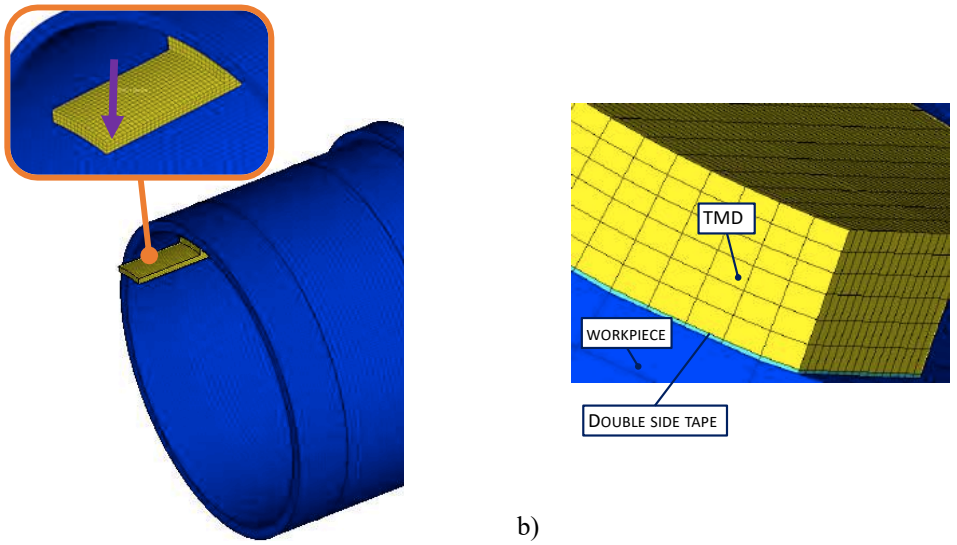

a) b)

Figure 5.21: a) FE model for TMD response prediction b) detail of beam and double side tape modelling

The same TMD used in the experimental part was considered. Both cantilever beam and double side tape material were experimentally characterized by means of model updating, exploiting the experimental results discussed in section 5.1.

Comparison between numerical and experimental FRF evaluated on the free end of a TMD attached to the workpiece in free – free conditions is showed in Figure 5.22. Material parameters for double side tape material, as result of model updating, are reported in Table 5.5.

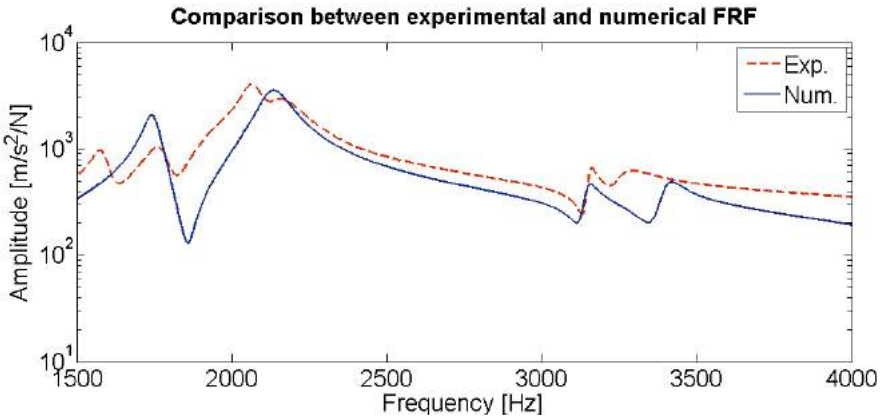

Figure 5.22: Comparison between numerical and experimental FRF of TMD once attached to the workpiece

Table 5.5: Double side tape material parameters

Cantilever Beam			
Shear Modulus (MPa)	**Poisson Ratio**	**Density (kg/m3)**	**Structural damping**
10	0.47	2070	0.9
Double side Tape			
Young Modulus (MPa)	**Poisson Ratio**	**Density (kg/m3)**	**Structural damping**
1.93E5	*0.3*	*7930*	*0.012*

Even if the model is not able to exactly reproduce the same behavior experimentally measured, the difference in terms of frequency and amplitude of the dominant mode is acceptable (+3.4% and -9.9% respectively).

Once the model of TMDs was developed and validated, the effect of different number of TMDs on the component dynamic response was investigated. Four different configurations were evaluated. In the first one only one TMD was attached to the component. The results highlights how the TMD is able to reduce peak amplitude, but the damping effect is very limited. Moreover such a configuration does not guarantee mass balance, crucial to avoid instabilities during workpiece rotation. Then number of TMD was gradually increased considering TMD equally spaced along circumference. Numerical and experimental results were then compared.

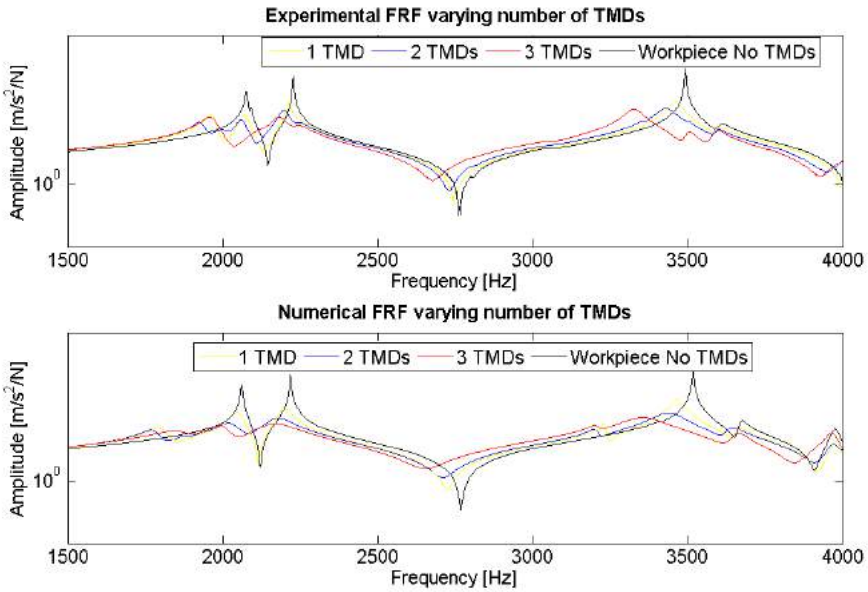

Figure 5.23: comparison between experimental (a) and numerical (b) FRF varying number of TMDs

Numerical approach is in good accordance with numerical results in terms of effect of TMDs on workpiece FRF. Increasing the number of TMDs damping effect increases. Despite the modelled response appear more damped, frequency in correspondent of the tri - lobed mode, varying the number of TMDs, is quite close to the experimental one.

This model then allows to predict effect of TMDs on workpiece response. The potentiality of this approach, compared with the one presented in section 5.1, includes the possibility of evaluate different TMDs shapes, number and position in order to select the most suitable one according with different requirements. As a future development, for example, this approach may be coupled with a chatter prediction model in order to detect the configuration that allows to optimize chatter stability field.

6. Conclusions and final remarks

The activity presented in this Ph.D. thesis deals with the development of techniques able to improve turning process accuracy, focusing on two still critic machining process: deep boring process and thin walled components turning. At first, an analysis of the state of the art was carried out in order to detect the main criticalities of these process and the related techniques presented in literature. The research was then focused on the static and dynamic issues, found to be response of geometrical errors and of workpiece surface worsening respectively. Several approaches presented in literature were analyzed in order to find the most suitable ones according with the specific case.

In particular, for what concern deep boring process, the active damping approach was found to be the most effective. The aim of the work of thesis was to design an active boring bar focusing on the integration of the actuators on the boring bar, in order to ensure a proper functioning of the actuators and a dynamics equivalent to the one of the standard boring bar. Designed active boring bar was realized and tested in order to prove the dynamic equivalence with the standard boring bar and to evaluate its effectiveness in chatter mitigation. Results confirmed the dynamic equivalence and an increment of the chatter stability field due to the active system.

Focusing on thin walled components turning, a model based strategy for supports optimal placing was developed in order to detect the most suitable configuration that guarantees tolerance and chatter stability. Thanks to the accurate choice of modelling techniques, this approach allows to evaluate different configurations with reasonable computational time. As result, it provides different solutions that are able to guarantee requirements, demanding the final choice to the operator that can then take into account several aspects (i.e. mounting easiness, costs, etc.) that are hardly formalized into an algorithm. Developed algorithm was numerically tested.

Moreover, the effectiveness of passive devices (Tuned Mass Dampers) on chatter mitigation in thin walled components turning was evaluated. For a given test case, Tuned Mass Dampers were designed following an experimental based procedure. Workpiece FRF was experimentally measured and chatter tests were performed in order to detect the target frequency and the correspondent workpiece mode shape. Then suitable TMDs were design, realized and attached to the component in order to measure the effect in terms of workpiece FRF and chatter stability. Exploiting the results experimentally obtained, a model to predict TMDs effect on the component response was developed. This model will be used to evaluate different TMDs configurations and will be coupled with a chatter prediction model in order to find the optimal TMDs configuration.

6.1. Summary of the principal achievements

In summary the main contributions of this research activity are:

- For what concerns active boring bar design
  - The formalization of requirements for a correct integration of piezo electric actuator on a boring bar
  - The detection of the most effective actuators positioning
  - The development of preload estimation model in order to protect piezoelectric actuators from traction stress during machining
  - A model based preload system design
  - A model based approach for protective cover design able to guarantees static and dynamic equivalence between the active boring bar and the original boring bar in case of control off.
- For what concerns the support optimization strategy
  - A suitable FE modelling approach for workpiece static and dynamic response prediction was selected to optimally balance accuracy and computational efficiency
  - A cutting force model and a chatter prediction model were developed in order to take into account the influence of the tool radius on cutting force direction
  - A model based approach was developed and implemented in order to find all the support configurations able to guarantee tolerance required and stable machining, starting from workpiece geometry, tool geometry and toolpath
- Regarding TMDs application for thin walled components turning
  - Effect of TMDs on workpiece response and chatter was experimentally proved
  - A model to predict the effect of TMDs on workpiece response was developed and experimentally tested

6.2. Industrial applicability of the developed solution

The employment of developed active devices in the industrial field is very promising. Designed active boring bar was demonstrated to be effective in chatter mitigation while not requiring to the turning operator any specific competence in chatter modelling. Moreover, its design make this devices adaptable to different tool configurations (i.e. overhangs) without compromising its effectiveness.

Additional fixturing structures, have been already used to support workpiece in thin walled components turning. Proposed approach allows to overcomes the limits of the experience based approach by aiding fixturing designers in detecting the configurations that guarantees tolerances required and a stable machining. Although presented approach exploits results of the process model, the integration of each modelling techniques and the automatization of the workpiece model removes the need to modelling skills. Indeed, unlike others CAFD techniques, the inputs required (workpiece geometry, tool geometry and toolpath) are the basics information that defines a turning process.

Unlike the first two approaches, the develop on TMDs is not yet mature for the industrial field. However, proposed modelling technique to estimate TMDs influence on

workpiece dynamic response, may support and aid TMDs design allowing to simulate several TMDs geometries in order to detect the most effective one.

6.3. Potential future developments

Some future developments are already under consideration with the purpose of improving the achieved results and extending the investigation to different applications. The foreseen future developments of the proposed research can be summarized as follows:

- Developed active boring bar may be used to further investigate the optimal actuation direction
- Developed optimization strategy for supports placing will be the experimental validation of its effectiveness by means of cutting tests and chatter tests.
- As a future development the effect of additional damping elements (i.e. damping materials or TMDs) interposed between the component and the supports, in order to further improve chatter stability, may be evaluated by including damping elements in the model.
- Presented model for TMDs may be coupled with a chatter prediction model in order to detect the optimal TMDs shape in order to to maximize chatter stability
- Presented model for TMDs may be coupled with a chatter prediction model and implemented in an algorithm, that similarly to the one proposed for fixturing optimization, can aid the choice of the optimal TMDs number and position in order to maximize chatter stability

Acknowledgements

Foremost, I would like to express my sincere gratitude to all the people working in this Department, starting from my supervisors Prof. Gianni Campatelli. I owe to them a big part of my professional and personal growth and I am very grateful for how they encouraged me, supporting my motivation for the research topic and allowing me plenty of autonomy in conducting my research, although keeping a constant and valuable supervision on it. Thanks to them I had the opportunity of study come in depth of a topic that, more than any other, piqued my interest. Thanks to this experience I also had the opportunity of work with a research group composed by extraordinary people that contributed to my professional and personal growth. In particular I would like to thank Dr. Eng. Antonio Scippa, Dr. Eng. Niccolò Grossi, Dr. Eng. Lorenzo Sallese and Dr. Eng. Filippo Montevecchi who often supported for offering me their expertise and for giving me precious tips and suggestions.

I am grateful also to Prof. Yutaka Nakano of the Tokyo Institute of Technology firstly for having shared his knowledge on passive damping techniques and for the opportunity of work with him. Moreover, I would like to thank him for guesting me at the Tokyo Institute of Technology and for the opportunity of working in such a prestigious university.

Last but definitely not least, I owe a huge thank to my whole family and all my friends that never stopped encouraging me and believing in me, way more than I would have done myself. Among them I want to include my husband, Simone that supported me in the most difficult moments during my Ph.D. activity.

.

Bibliography

1. Ramesh, R.; Mannan, M.A.; Poo, A.N. Error compensation in machine tools - a review. Part I: Geometric, cutting-force induced and fixture-dependent errors. *Int. J. Mach. Tools Manuf.* **2000**, *40*, 1235–1256.
2. Tobias, A. *Machine tools vibration (Vibraciones en Maquinas-Herramientas)*; URMO: Spain, 1961;
3. Malluck, J.A.; Melkote, S.N. Modeling of Deformation of Ring Shaped Workpieces Due to Chucking and Cutting Forces. *J. Manuf. Sci. Eng.* **2004**, *126*, 141.
4. Walter, M.F.; Ståhl, J.E. Machining of ring shaped work pieces. *J. Mater. Process. Tech.* **1995**, *48*, 239–245.
5. Benardos, P.G.; Mosialos, S.; Vosniakos, G.C. Prediction of workpiece elastic deflections under cutting forces in turning. *Robot. Comput. Integr. Manuf.* **2006**, *22*, 505–514.
6. Cui, B.; Guo, J. Modeling of dimensional errors in slender bar turning process using artificial neural networks. *Appl. Mech. Mater.* **2009**, *16–19*, 549–553.
7. Kaymakci, M.; Kilic, Z.M.; Altintas, Y. Unified cutting force model for turning, boring, drilling and milling operations. *Int. J. Mach. Tools Manuf.* **2012**, *54–55*, 34–45.
8. Yao, C.; Zhou, Z.; Zhang, J.; Wu, D.; Tan, L. Experimental study on cutting force of face-turning Inconel718 with ceramic tools and carbide tools. *Adv. Mech. Eng.* **2017**, *9*, 1–9.
9. Zhang, G.; Guo, C. Modeling of Cutting Force Distribution on Tool Edge in Turning Process. *Procedia Manuf.* **2015**, *1*, 454–465.
10. Carrino, L.; Giorleo, G.; Polini, W.; Prisco, U. Dimensional errors in longitudinal turning based on the unified generalized mechanics of cutting approach. Part I: Three-dimensional theory. *Int. J. Mach. Tools Manuf.* **2002**, *42*, 1509–1515.
11. Carrino, L.; Giorleo, G.; Polini, W.; Prisco, U. Dimensional errors in longitudinal turning based on the unified generalized mechanics of cutting approach. Part I: Three-dimensional theory. *Int. J. Mach. Tools Manuf.* **2002**, *42*, 1509–1515.
12. Kops, L.; Gould, M.; Mizrach, M. Improved analysis of the workpiece accuracy in turning, based on the emerging diameter. *J. Manuf. Sci. Eng. Trans. ASME* **1993**, *115*, 253–257.
13. Qiang, L.Z. Finite difference calculations of the deformations of multi-diameter workpieces during turning. *J. Mater. Process. Technol.* **2000**, *98*, 310–316.
14. Yang, S.; Yuan, J.; Ni, J. Real-time cutting force induced error compensation on a turning center. *Int. J. Mach. Tools Manuf.* **1997**, *37*, 1597–1610.
15. Mayer, J.R.R.; Phan, A.V.; Cloutier, G. Prediction of diameter errors in bar turning:

A computationally effective model. *Appl. Math. Model.* **2000**, *24*, 943–956.
16. Phan, A. V.; Cloutier, G.; Mayer, J.R.R. A finite-element model with closed-form solutions to workpiece deflections in turning. *Int. J. Prod. Res.* **1999**, *37*, 4039–4051.
17. Estrems, M.; Arizmendi, M.; Zabaleta, A.J.; Gil, A. Numerical Method to Calculate the Deformation of Thin Rings during Turning Operation and its Influence on the Roundness Tolerance. *Procedia Eng.* **2015**, *132*, 872–879.
18. Zhu, S.; Ding, G.; Qin, S.; Lei, J.; Zhuang, L.; Yan, K. Integrated geometric error modeling, identification and compensation of CNC machine tools. *Int. J. Mach. Tools Manuf.* **2012**, *52*, 24–29.
19. Topal, E.S.; Çoğun, C. A cutting force induced error elimination method for turning operations. *J. Mater. Process. Technol.* **2005**, *170*, 192–203.
20. Kurnadi, M.S.; Morehouse, J.; Melkote, S.N. A workholding optimization model for turning of ring-shaped parts. *Int. J. Adv. Manuf. Technol.* **2007**, *32*, 656–665.
21. Wang, H.; Rong, Y.; Li, H.; Shaun, P. Computer aided fixture design: Recent research and trends. *CAD Comput. Aided Des.* **2010**, *42*, 1085–1094.
22. Merritt, H.E. Theory of Self-Excited Machine-Tool Chatter: Contribution to Machine-Tool Chatter Research. *J. Eng. Ind.* **1965**, *87*, 447–454.
23. Jafarzadeh, E.; Movahhedy, M.R. Numerical simulation of interaction of mode-coupling and regenerative chatter in machining. *J. Manuf. Process.* **2017**, *27*, 252–260.
24. Gasparetto, A. A System Theory Approach to Mode Coupling Chatter in Machining State Equations for the Heat Exchanger Edited by Foxit Reader Kx Xj. *J. Dyn. Syst. Meas. Control* **1998**, *120*, 545–547.
25. Quintana, G.; Ciurana, J. Chatter in machining processes: A review. *Int. J. Mach. Tools Manuf.* **2011**, *51*, 363–376.
26. Altintans, Y. *Manufacturing automation*; Second Edi.; ISBN 9780521172479.
27. Urbikain, G.; Fernández, A.; López de Lacalle, L.N.; Gutiérrez, M.E. Stability lobes for general turning operations with slender tools in the tangential direction. *Int. J. Mach. Tools Manuf.* **2013**, *67*, 35–44.
28. Chiou, R.Y.; Liang, S.Y. Chatter stability of a slender cutting tool in turning with tool wear effect. *Int. J. Mach. Tools Manuf.* **1998**, *38*, 315–327.
29. Gerasimenko, A.; Guskov, M.; Duchemin, J.; Lorong, P.; Gouskov, A. Variable compliance-related aspects of chatter in turning thin-walled tubular parts. *Procedia CIRP* **2015**, *31*, 58–63.
30. Mehdi, K.; Rigal, J.F.; Play, D. Dynamic behavior of a thin-walled cylindrical workpiece during the turning process, Part 1: Cutting process simulation. *J. Manuf. Sci. Eng. Trans. ASME* **2002**, *124*, 562–568.
31. Tobias, S.; Fishwick, W. Theory of regenerative machine tool chatter. *Engineering* **1958**, *205*, 199–203.
32. Eynian, M. Prediction of vibration frequencies in milling using modified Nyquist method. *CIRP J. Manuf. Sci. Technol.* **2015**, *11*, 73–81.
33. Berglind, L.; Ziegert, J. Analytical time-domain turning model with multiple modes. *CIRP Ann. - Manuf. Technol.* **2015**, *64*, 137–140.
34. Lazoglu, I.; Atabey, F.; Altintas, Y. Dynamics of boring processes: Part III-time domain modeling. *Int. J. Mach. Tools Manuf.* **2002**, *42*, 1567–1576.
35. Altintas, Y.; Weck, M. Chatter stability of metal cutting and grinding. *CIRP Ann. - Manuf. Technol.* **2004**, *53*, 619–642.
36. Urbikain, G.; Olvera, D.; de Lacalle, L.N.L.; Elías-Zúñiga, A. Spindle speed

variation technique in turning operations: Modeling and real implementation. *J. Sound Vib.* **2016**, *383*, 384–396.
37. Eynian, M. Chatter stability of turning and milling with process damping. **2010**.
38. Munoa, J.; Beudaert, X.; Dombovari, Z.; Altintas, Y.; Budak, E.; Brecher, C.; Stepan, G. Chatter suppression techniques in metal cutting. *CIRP Ann. - Manuf. Technol.* **2016**, *65*, 785–808.
39. Marui, E.; Ema, S.; Hashimoto, M.; Wakasawa, Y. Plate insertion as a means to improve the damping capacity of a cutting tool system. **1998**, *38*, 1209–1220.
40. Edhi, E.; Hoshi, T. Stabilization of high frequency chatter vibration in fine boring by friction damper. **2001**, *25*, 224–234.
41. Ã, N.D.S. ARTICLE IN PRESS Vibration absorbers for chatter suppression : A new analytical tuning methodology. **2007**, *301*, 592–607.
42. Yang, Y.; Muñoa, J.; Altintas, Y. Optimization of multiple tuned mass dampers to suppress machine tool chatter. *Int. J. Mach. Tools Manuf.* **2010**, *50*, 834–842.
43. Rubio, L.; Loya, J.A.; Miguélez, M.H.; Fernández-sáez, J. Optimization of passive vibration absorbers to reduce chatter in boring. *Mech. Syst. Signal Process.* **2013**, *41*, 691–704.
44. Nakano, Y.; Takahara, H.; Kondo, E. Countermeasure against chatter in end milling operations using multiple dynamic absorbers. *J. Sound Vib.* **2013**, *332*, 1626–1638.
45. Bansal, A.; Law, M. A receptance coupling approach to optimally tune and place absorbers on boring bars for chatter suppression. *Procedia CIRP* **2018**, *77*, 167–170.
46. Venter, G.S.; Silva, L.M. do P.; Carneiro, M.B.; da Silva, M.M. Passive and active strategies using embedded piezoelectric layers to improve the stability limit in turning/boring operations. *Int. J. Adv. Manuf. Technol.* **2017**, *89*, 2789–2801.
47. Tewani, S.G.; Rouch, K.E.; Walcott, B.L. A study of cutting process stability of a boring bar with active dynamic absorber. *Int. J. Mach. Tools Manuf.* **1995**, *35*, 91–108.
48. Tanaka, H.; Obata, F.; Matsubara, T.; Mizumoto, H. Active Chatter Suppression of Slender Boring Bar Using Piezoelectric Actuators. *JSME Int. journal. Ser. C, Dyn. Control. Robot. Des. Manuf.* **2012**, *37*, 601–606.
49. Silva, M.M. Da; Cervelin, J.E.; Calero, D.P.; Coelho, R.T. Availability study on regenerative chatter avoidance in turning operations through passive and active damping. *Int. J. Mechatronics Manuf. Syst.* **2014**, *6*, 455.
50. Sallese, L.; Innocenti, G.; Grossi, N.; Scippa, A.; Flores, R.; Basso, M.; Campatelli, G. Mitigation of chatter instabilities in milling using an active fixture with a novel control strategy. *Int. J. Adv. Manuf. Technol.* **2017**, *89*, 2771–2787.
51. Zeng, S.; Wan, X.; Li, W.; Yin, Z.; Xiong, Y. A novel approach to fixture design on suppressing machining vibration of flexible workpiece. *Int. J. Mach. Tools Manuf.* **2012**, *58*, 29–43.
52. Wan, X.J.; Zhang, Y. A novel approach to fixture layout optimization on maximizing dynamic machinability. *Int. J. Mach. Tools Manuf.* **2013**, *70*, 32–44.
53. Gouskov, A.M.; Voronov, S.A.; Novikov, V. V.; Ivanov, I.I. Chatter suppression in boring with tool position feedback control. *J. Vibroengineering* **2017**, *19*, 3512–3521.
54. Ganguli, A.; Deraemaeker, A.; Horodinca, M.; Preumont, A. Active damping of chatter in machine tools - Demonstration with a “hardware-in-the-loop” simulator. *Proc. Inst. Mech. Eng. Part I J. Syst. Control Eng.* **2005**, *219*, 359–369.
55. Mancisidor, I.; Munoa, J.; Barcena, R. Optimal control laws for chatter suppression

using inertial actuator in milling processes. *11th Int. Conf. High Speed Mach. Sep 2014, Prague, Czech Repub.* **2014**.
56. Bilbao-Guillerna, A.; Barrios, A.; Mancisidor, I.; Loix, N.; Muñoa, J. Control laws for chatter suppression in milling using an inertial actuator. *Isma 2010* **2010**, 265–278.
57. Pratt, J.R.; Nayfeh, A.H. Design and modeling for chatter control. *Nonlinear Dyn.* **1999**, *19*, 49–69.
58. Chen, F.; Hanifzadegan, M.; Altintas, Y.; Lu, X. Active damping of boring bar vibration with a magnetic actuator. *IEEE/ASME Trans. Mechatronics* **2015**, *20*, 2783–2794.
59. Harms, A.; Denkena, B.; Lhermet, N.; Tools, M. Tool adaptor for active vibration control in turning operations. *Proc. 9th Int. Conf. New Actuators, ACTUATOR 2004* **2004**, 694–697.
60. Smirnova, T.; Åkesson, H.; Håkansson, L.; Lars, H. *Modeling of an Active Boring Bar*; Blekinge Institute of Technology Research report; 2007;
61. Andrén, L.; Håkansson, L. Active Vibration Control of Boring Bar Vibrations - Algoritmi. *Res. Rep. No 200407* **2004**.
62. Yong, Y.K. Preloading Piezoelectric Stack Actuators in High-Speed Nanopositioning Systems. *Front. Mech. Eng.* **2016**, *2*, 1–9.
63. Peng, G.; Chen, G.; Wu, C.; Xin, H.; Jiang, Y. Applying RBR and CBR to develop a VR based integrated system for machining fixture design. *Expert Syst. Appl.* **2011**, *38*, 26–38.
64. Kolodner, J.L. An introduction to case-based reasoning. *Artif. Intell. Rev.* **1992**, *6*, 3–34.
65. Lin, Z.C.; Huang, J.C. The application of neural networks in fixture planning by pattern classification. *J. Intell. Manuf.* **1997**, *8*, 307–322.
66. Li, B.; Melkote, S.N. Improved workpiece location accuracy through fixture layout optimization. *Int. J. Mach. Tools Manuf.* **1999**, *39*, 871–883.
67. Kulankara, K.; Satyanarayana, S.; Melkote, S.N. Iterative fixture layout and clamping force optimization using the genetic algorithm. *J. Manuf. Sci. Eng. Trans. ASME* **2002**, *124*, 119–125.
68. Liu, C.; Li, Y.; Shen, W. A real time machining error compensation method based on dynamic features for cutting force induced elastic deformation in flank milling. *Mach. Sci. Technol.* **2018**, *22*, 766–786.
69. Ratchev, S.; Phuah, K.; Liu, S. FEA-based methodology for the prediction of part-fixture behaviour and its applications. *J. Mater. Process. Technol.* **2007**, *191*, 260–264.
70. Kashyap, S.; DeVries, W.R. Finite element analysis and optimization in fixture design. *Struct. Optim.* **1999**, *18*, 193–201.
71. Krishnakumar, K.; Melkote, S.N. Machining fixture layout optimization using the genetic algorithm. *Int. J. Mach. Tools Manuf.* **2000**, *40*, 579–598.
72. Wang, Y.; Chen, X.; Liu, Q.; Gindy, N. Optimisation of machining fixture layout under multi-constraints. *Int. J. Mach. Tools Manuf.* **2006**, *46*, 1291–1300.
73. Selvakumar, S.; Arulshri, K.P.; Padmanaban, K.P.; Sasikumar, K.S.K. Design and optimization of machining fixture layout using ANN and DOE. *Int. J. Adv. Manuf. Technol.* **2013**, *65*, 1573–1586.
74. MSC Software MSC Nastran Quick Reference Guide 2014. **2014**.
75. Reddy, R.G.; Ozdoganlar, O.B.; Kapoor, S.G.; DeVor, R.E.; Liu, X. A stability

solution for the axial contour-turning process. *J. Manuf. Sci. Eng. Trans. ASME* **2002**, *124*, 581–587.
76. Colwell, L.V. Predicting the Angle of Chip Flow for Single Point Cutting Tools. *Trans. ASME* **1956**, *76*, 199–204.
77. Eynian, M.; Altintas, Y. Chatter Stability of General Turning Operations With Process Damping. *J. Manuf. Sci. Eng.* **2009**, *131*, 041005.
78. Altintaş, Y.; Budak, E. Analytical Prediction of Stability Lobes in Milling. *CIRP Ann. - Manuf. Technol.* **1995**, *44*, 357–362.
79. Den Hartog, J.P. *Mechanical Vibrations*; McGraw-Hill, Ed.; Forth edit.; 1956;
80. Joshi, A.S.; Jangid, R.S. Optimum parameters of multiple tuned mass dampers for base-excited damped systems. *J. Sound Vib.* **1997**, *202*, 657–667.
81. Ewins, D.J. Modal Testing: Theory and Practice (Mechanical engineering research studies). *Res. Stud. Press Ltd.* 1984.
82. Ewins, D. *Modal Testing, Theory, Practice, & Application*; Wiley, Hoboken, U., Ed.; 2nd editio.; 2000;
83. Nakano, Y.; Takahara, H.; Kondo, E. Countermeasure against chatter in end milling operations using multiple dynamic absorbers. *J. Sound Vib.* **2013**, *332*, 1626–1638.